

https://dspace.org/

Investigation of the potential use of concentrating solar thermal technology for essential oil extraction and techno-economical comparison of renewable and conventional energy sources

Manyako, Khutsang Erence

2021

https://hdl.handle.net/10539/32949

Downloaded from a DSpace repository. https://dspace.org/



INVESTIGATION OF THE POTENTIAL USE OF CONCENTRATING SOLAR THERMAL TECHNOLOGY FOR ESSENTIAL OIL EXTRACTION AND TECHNO-ECONOMICAL COMPARISON OF RENEWABLE AND CONVENTIONAL ENERGY SOURCES

Prepared by

Khutsang Erence Manyako

Submitted to

School of Chemical and Metallurgical Engineering, Faculty of Engineering and the Built Environment, University of the Witwatersrand, Johannesburg, South Africa

Supervisors: Prof Mulopo and Dr Chiyanzu

October 2021

DECLARATION

I, Khutsang Erence Manyako, declare that this dissertation is my own unaided work. It is being submitted to the University of the Witwatersrand, Johannesburg, for the degree of Master of Science in Engineering. It has not been submitted elsewhere for any examination or qualification.

Signature: 

12 th day of October 2021

ABSTRACT

Distillation of essential oils is one of the processes that demand significant amounts of saturated steam. Majority of distillation processes are carried out using conventional energy sources requiring significant quantities of electrical energy. In addition, conventional steam distillation contributes significantly to the carbon dioxide emissions, thus harming the environment. The challenges mentioned can be resolved by concentrating solar thermal (CST) technologies in medium temperature level (80-240 ℃) since wide range of agro-based processes operate well within this temperature range. Most of the industrial solar plants in South Africa use the flat plate and evacuated tube collectors with temperature below 100^{o}C, which is ideal for only low temperature process applications. Therefore, CST technologies would be vital for the survival of the already cost-burdened agro-based industries. There are several CST technologies, however, the suitable ones for industrial process heat are parabolic trough collector (PTC), linear fresnel collector (LFC) and parabolic dish collector (PDC). Although CST technologies have a great potential, there are only few realized projects. In terms of the research conducted, particularly on the use of CST technology for steam distillation of essential oils, only few studies can be located. Therefore, this research seeks to investigate further about the potential use of CST technology for essential oil steam distillation.

The PTC was selected for this research, due to its maturity and long record of successful operation. The components of PTC were specified and sourced according to energy requirements of an existing gas-powered steam distillation and installed for steam distillation of citrus peels. For comparative analysis, conventional gas-powered steam distillation and laboratory steam distillation were conducted. The results showed that PTC can compete with fuel gas, and in some cases, the yields of essential oil were comparable with that of laboratory experiments, thus rendering the PTC sufficient for deployment in agro-based industrial applications. In the case of gas-powered steam distillation, the essential oil yields were 0.65, 0.44 and 1.17 % for orange, lemon and mandarin, respectively. For PTC, the yields were 0.67, 0.53 and 1.09 %, which showed to be in the expected ranges. Gas Chromatography results for PTC experiment showed the presence of key components (e.g. 90% limonene) in the essential oils. The PTC achieved an overall system efficiency of 54.99 %, which is significant, given the fact that some parts of the system were not thermally insulated, thus adding to other efficiency problems that the system had. Having considered a techno-economic review, it has been proven that PTC can economically be used for steam distillation of essential oils.

ACKNOWLEDGEMENT

I would like to sincerely acknowledge and thank my supervisor, Prof. Mulopo for his continued support in this research. I thank him for his valuable suggestions, constructive criticisms, comments and commending. His numerous comments and suggestions helped me to improve the quality of my work.

I would like to thank my co-supervisor Dr Chiyanzu for being present in every aspect of the research project and playing a key role in assisting to coordinate the resources required for the research. I thank him for his passion for research, which led him to share numerous suggestions.

My sincere appreciations goes to my sponsor, Agricultural Research Council-Agricultural Engineering (ARC-AE), which played a pivotal role in providing funding for my tuition fees, research equipment and research consumables.

I thank the University of the Witwatersrand and ARC-Animal Production for offering analytical services required for my experimental work.

Finally, I would like to express my great appreciation to my wife Nomfundo Manyako and my daughter Bontle, parents, sisters and brothers for their unfailing love, support, patience and understanding during the course of the research project.

TABLE OF CONTENTS

Page

CHAPTER 1: INTRODUCTION 1

1.1 Background 1

1.2 Motivation 2

1.3 Aims and Objectives 4

1.4 Structure of the Dissertation 5

CHAPTER 2: LITERATURE REVIEW 6

2.1 A Historical Overview of Essential Oils 6

2.2 Sources of Essential Oils 6

2.3 Essential Oils Compositions 6

2.4 Application of Essential Oils 7

2.5 Factors that Affect the Yield and Quality of Essential Oils 8

2.6 Conventional Essential Oil Extraction Techniques 9

2.6.1 Solvent extraction 9

2.6.2 Enfleurage 9

2.6.4 Distillation 10

2.6.5 Cohobation 11

2.6.6 Hydrodiffusion 12

2.6.7 Expression or Cold pressing 12

2.7 Current Innovative Essential Oil Extraction Techniques 12

2.7.1 Ultrasound-assisted extraction of essential oils 12
2.7.2 Super-critical fluid extraction of essential oils 13
2.7.3 Accelerated solvent extraction 14
2.7.4 Sub-critical water extraction 14
2.7.5 Microwave-assisted extraction 14
2.8 Sources of Energy for Essential's Oils Production 15
2.8.1 Conventional energy sources 15
2.8.2 Non-conventional energy sources 16
2.9 Concentrating Solar Thermal Technologies for Industrial Process Heat 17
2.9.1 Small sized parabolic trough collector system 17
2.9.2 Compound parabolic collector 18
2.9.3 Parabolic dish collector system 19
2.10 Current Use of CST technologies for Agro-Based Processing 20
2.10.1 Solar cookers 20
2.10.2 Desalination 24
2.10.3 Baking with solar energy 25
2.11 Research on Essential Oil Steam Distillation With CST Technology 26
2.12 Concentrating Solar Thermal System Components 27
2.12.1 Mirrors 27
2.12.2 Receivers 29
2.12.3 Thermal energy storage 31

2.12.4 Chemical storage....33
2.13 Heat Transfer Fluids....33
2.14 Solar Tracking....34
2.15 Solar Thermal Steam Generating Systems....35
2.15.1 Steam flash concept....35
2.15.2 Direct steam generation (DSG)....36
2.15.3 Unfired boiler concept....37
2.16 South African Solar Resource....38
2.17 Conclusions....43
CHAPTER 3: MATERIALS AND METHODS....45
3.1 Laboratory Steam Distillation of essential oils....45
3.1.1 Description of steam distillation laboratory apparatus....45
3.1.2 Laboratory methodological approach used for steam distillation....49
3.2 Gas-powered Essential Oil Steam Distillation....50
3.2.1 Description of gas-powered essential oil steam distillation....50
3.2.2 Methodological approach used for gas-powered essential oil steam distillation unit....51
3.3 Selection of the Concentrating Solar Thermal Technology for Steam Distillation of Essential Oils....52
3.4 PTC-Powered Essential Oil Steam Distillation....54
3.4.1 Description of PTC-powered essential oil steam distillation....54
3.4.2 Parabolic trough collector....55

3.4.3 Heat collecting element (Receiver tube) 56

3.4.4 Single axis tracking system 56

3.4.5 Water, steam and synthetic oil pipe network 57

3.4.6 Distillation tank 60

3.4.7 Methodological approach used for PTC-powered essential oil steam distillation unit. 60

CHAPTER 4: RESULTS AND DISCUSSIONS 63

4.1 Characterization: Proximate Analysis 63

4.1.1 Dry matter, ash, total solids, moisture contents of fresh citrus peels 63

4.1.2 Protein, fat and carbohydrates 64

4.2 Laboratory Experiments 65

4.2.1 Yields of orange, lemon and mandarin peels 65

4.2.2 Energy consumption analysis in a laboratory scale 68

4.2.3 Average instantaneous power supply into the system 70

4.3 Field Experiments 70

4.3.1 Gas-powered field experiment 70

4.3.2 Comparative analysis of results (Laboratory and gas-powered field experiment) 73

4.3.3 PTC-powered field experiment 74

4.3.4 Comparative analysis of gas-powered laboratory and field experiments 76

4.4 Gas Chromatography Results 85

4.5 Techno-Economical Analysis 89

4.5.1 Techno-economic review 89

CHAPTER 5: CONCLUSIONS AND RECOMMENDATIONS 93

5.1 CONCLUSIONS 93

5.2 RECOMMENDATIONS 94

CHAPTER 6: REFERENCES 97

APPENDIX A.1: Thermal analysis of the PTC 113

APPENDIX A.2: Thermal analysis of a distillation tank 116

APPENDIX A.3: Thermal energy modelling 121

APPENDIX B.1: Sizing procedure.....124

APPENDIX C.1: Estimation of DNI and selection of a suitable PTC 127

APPENDIX D.1: Data sheet for therminol 66 132

APPENDIX E.1: Geometric properties of air 134

APPENDIX F.1: Proximate analysis data.....135

APPENDIX G.1: Laboratory steam distillation of orange samples 139

APPENDIX G.2: Laboratory steam distillation of lemon samples 140

APPENDIX G.3: Laboratory steam distillation of orange samples 141

APPENDIX H.1: Citrus peels's moisture content (laboratory experiments).....143

APPENDIX H.2: Citrus peels's moisture content (Gas-powered).....143

APPENDIX H.3: Citrus peel's moisture content (PTC-powered) 144

APPENDIX I.1: Gas-powered steam distillation 146

APPENDIX I.2: Energy consumption (Gas-powered experiments) 147

APPENDIX I.3: Heat losses (Gas-powered experiments).....147

APPENDIX J.1: PTC-powered Steam distillation 149

APPENDIX J.2: Energy consumption (PTC-powered experiment) 150

APPENDIX J.3: Heat losses (PTC-powered experiment).....152

LIST OF FIGURES

Figure 2.1. Comparison of solar collector efficiencies (Kalogirou, 2003) 18

Figure 2.2 Schematic diagram of a box cooker (Panwar *et al*., 2012) 21

Figure 2.3. Parabolic dish solar cooker (Panwar *et al*., 2012) 23

Figure 2.4. Scheffler dish system (Panwar *et al*., 2012) 23

Figure 2.5 Schematic diagram of a flash boiler steam generation concept (Modified from Kalogirou, 2004) 36

Figure 2.6. Schematic diagram of a direct steam generation concept (Modified from Kalogirou, 2004) 37

Figure 2.7. Schematic Diagram of an Unfired Boiler Concept (Modified from Kalogirou, 2004) 38

Figure 2.8 Global distribution of GHI(Top) and DNI(Bottom)(Meyer *et al*., 2012 40

Figure 2.9. Long term average DNI for South Africa (Solargis, 2017) 41

Figure 3.1. Glassware Apparatus: (1) heating mantle, (2) flask, (3) extraction vessel, (4) stand and clamp, (5) spiral condenser, (6) adaptor, (7) separation funnel (8) funnel, (9) florentine (Modified from Shakir and Salih, 2015) 46

Figure 3.2. Laboratory steam distillation system glassware 47

Figure 3.3. Essential oil separation 48

Figure 3.4. Collected essential oil 48

Figure 3.5. LPG-powered essential oil steam distillation unit 50

Figure 3.6. Gas-powered essential oil steam distillation unit in operation 51

Figure 3.7. Schematic diagram of the PTC-powered essential oil steam distillation 54

Figure 3.8. Parabolic trough (PT20) installed at ARC-AE premises.....55

Figure 3.9 Image of True North-South aligned PTC as captured from the Satellite at Agricultural Research Council (-25°43'46", 28°16'34").....57

Figure 3.10. Schematic diagram of fluid flow of the PTC-powered essential oil steam distillation unit apparatus (South East Isometric View).....59

Figure 3.11 Steam production during system test.....60

Figure 3.12 Steam distillation unit set-up.....61

Figure 3.13 Essential oil and hydrosol separation.....62

Figure 4.1: Yield and temperature.....67

Figure 4.2 : Energy consumption per 100 gram of plant material.....68

Figure 4.3 Energy consumption per one gram of oil produced.....69

Figure 4.4 Energy consumption per 100 g of plant material.....71

Figure 4.5 Energy consumption per gram of essential oil.....72

Figure 4.6 Energy consumption per 100 g of plant material.....75

Figure 4.7 Energy consumption per gram of essential oil.....75

Figure 4.8 Comparison of essential oil yields (%).....77

Figure 4.9 Energy consumed per 100 gram of essential oil produced in laboratory and field experiments.....78

Figure 4.10 Comparison of energy consumed per one gram of essential oil produced in laboratory and field experiments.....79

LIST OF TABLES

Table 2.1 Chemical compounds of essential oils (Modified from Tongnuanchan and Benjakul, 2014).....7

Table 2.2 Essential oil plants and their extraction methods (Modified from Tongnuanchan and Benjakul, 2014).....8

Table 2.3. Sizes of areas with CSP potential in South Africa (Modified from Hermann *et al*., 2014).....42

Table 2.4. Suitability classes (Modified from Hermann *et al*., 2014).....42

Table 3.1. Parameters of the selected parabolic trough Collector (PT-20) 56

Table 3.2. Thermo-physical properties of therminol 66.....58

Table 4.1. Dry matter, ash, total solids, moisture contents of fresh citrus peels 63

Table 4.2. Dry matter, ash, total solids, moisture contents of fresh citrus peels after distillation.....63

Table 4.3.**Composition before distillation**.....65

Table 4.4. **Composition after distillation** 65

Table 4.5. Yields of orange, lemon and mandarin peels.....67

Table 4.6. Yields and energy consumed.....69

Table 4.7. Distillation temperature 71

Table 4.8. Yields of orange, lemon and mandarin peels.....71

Table 4.9 Essential oil extracted per unit plant dry matter 72

Table 4.10. Laboratory and field experiments 73

Table 4.11 Yields of orange, lemon and mandarin peels.....74

Table 4.12 Essential oil extracted per unit plant dry matter 76

Table 4.13 Percentage decrease of energy consumption 80

Table 4.14 Comparison of CO_2 emissions 80

Table 4.15 Total CO_2 emissions emitted during steam distillation of orange, lemon and mandarin 81

Table 4.16 Orange peels chemical compositions 85

Table 4.17 Lemon peels chemical compositions 87

Table 4.18 Mandarin peels chemical compositions 88

LIST OF SYMBOLS

$	Dollar
wb	wet basis
%	Percentage
¢	cent
€	Euro
A	Ampere
CO_2	Carbon Dioxide
DC	Direct Current
g	gram
GHz	GigaHertz
h	hour
kg	kilogram
kW	kilowatt
kWh	kilowatt hours
m	meter
m^2	square meter
mb	millibar
MHz	MegaHertZ
ml	Millilitre

MPa	Megapascal
MWh	Megawatt hours
nm	nanometer
^{o}C	Degree Celsius
PWh	Petawatt hours
RPM	Revolution Per Minute
V	Voltage
W	Watt
µm	micrometre

NOMENCLATURE

ADF	Acid Detergent Fibre
ADL	Acid Detergent Lignin
ARC-AE	Agricultural Research Council-Institute for Agricultural Engineering
ASE	Accelerated Solvent Extraction
CFD	Computational Fluid Dynamics
CPC	Compound Parabolic Collector
CSP	Concentrating Solar Power
CST	Concentrating Solar Thermal
CTC	Cylindrical Trough Collector
d.m	dry matter
DNI	Direct Normal Irradiation
DSG	Direct Steam Generation
ED	Electrodialysis
ETC	Evacuated Tube Collector
FPC	Flat Plate Collector
GC	Gas Chromatography
GHI	Global Horizontal Insolation
HDH	Humidification-Dehumidification
HFC	Heliostat Field Collector

HFO	Heavy Fuel Oil
HTF	Heat Transfer Fluid
IPH	Industrial Process Heat
IRR	Internal Rate of Return
IST	Industrial Solar Technology
LCOE	Levilized Cost of Electricity
LCOH	Levilized Cost of Heat
LFC	Linear Fresnel Collector
LHTES	Latent Heat Thermal Energy Storage
LPG	Liquefied Petroleum Gas
MAE	Microwave-Assisted Extraction
MD	Membrane distillation
MED	Multi-Effect Distillation
MSF	Multi-Stage Flash
NDF	Neutral Detergent Fibre
N.m	Newton meter
NPV	Net Present Value
PCM	Phase Change Materials
PDC	Parabolic Dish Collector
PDSC	Parabolic Dish Solar Cooker
PHE	Plate Heat Exchanger

PTC	Parabolic Trough Collector
PV	Photovoltaic
REIPPP	Renewable Energy Independent Power Producer Procurement Programme
RO	Reverse Osmosis
SFE	Super-Critical Fluid Extraction
SHP	Solar Heat and Power
SHTES	Sensible Heat Thermal Energy Storage
TES	Thermal Energy Storage
UAE	Ultrasound-Assisted Extraction

CHAPTER 1: INTRODUCTION

1.1 Background

The world's energy demand is skyrocketing as a result of population growth and industrial revolutions (Kanaan and Vakeesan, 2016). Furthermore, due to the greenhouse gas emissions, energy production and consumption, especially in the manufacturing sector, are unsustainable (Farjana *et al*, 2018). It is worth noting that the world's population has increased by 2 billion in a single generation, with developing countries bearing a disproportionate share of the burden (Kannan and Vakeesan, 2016). It is expected that the global population will continue to grow by more than one billion people, reaching 8.5 billion by 2030 and 9.7 billion by 2050. Africa contributes the highest population growth rates of 2.55 % (Shahsavari and Akbari, 2018). On the other hand, the combustion of fossil fuels (oil, coal, natural gas, and so on) accounts for at least 70% of carbon dioxide (CO_2) emissions (Sardeshpande and Pillai, 2012). According to Kalogirou (2014), global CO_2 emissions are expected to be reduced to 75% of 1985 levels by 2050 if energy efficiency and renewable energy sources are widely adopted. Wind, hydro, geothermal, solar, and other renewable energy sources abound. However, because of the desirable environmental and safety aspects, it is widely believed that solar energy should be used instead of other alternative energy forms because it can be supplied in a sustainable manner without harming the environment (Kalogirou, 2014).

Heating accounts for 44 percent of total final energy demand in South Africa. Energy usage for industrial purposes accounts for 67% of total energy demand, followed by the residential sector at 25%, and the commercial and agricultural sectors at 8 and 0.5 %, respectively (Joubert *et al.*, 2016). Several industrial sectors have been identified as having favorable conditions for solar energy application. Sterilization, pasteurization, drying, hydrolyzing, distillation and evaporation, washing and cleaning, and polymerization are the most important industrial processes that use heat at a medium temperature level (Kalogirou, 2014). A significant portion of the heat used by industrial processes is at temperatures that solar thermal technologies can meet. Solar thermal technologies are classified into two types: non-concentrating and concentrating. Non-concentrating solar thermal technologies use the same area for both intercepting and absorbing solar radiation, whereas sun-tracking concentrating solar thermal (CST) technologies typically have concave reflecting surfaces to intercept and focus the sun's beam radiation to a smaller receiving area, increasing the radiation flux (Kalogirou, 2014). Generally, temperatures above 80°C necessitate the use of CST technologies (Sardeshpande

and Pillai, 2012). The four main CST technologies used to generate solar thermal energy are HFC, PDC, LFC, and PTC), although the only ones suitable for industrial process heat are PTC, PDC and LFC (Häberle, 2012). Among these three solar collectors, PTC is the most mature system capable of achieving temperature of up to 400 °C (Kalagirou, 2014).

1.2 Motivation

Many industries can benefit from solar thermal technologies. Agro-processes for example is one of the industries, which can have its share of benefit from solar thermal energy. This is critical because agriculture contributes significantly to CO_2 emissions. Agricultural emissions from developing countries, for example, have been reported to be significantly higher than those from developed countries. In 2005, developing countries contributed 74% of global agricultural emissions, while developed countries contributed only 26% of global agricultural emissions (Bundschuh *et al*., 2017). Furthermore, the agro-food chain absorbs roughly one-third of global energy production, with crop production accounting for about 12% and manufacturing, distribution, retail, preparation, and cooking accounting for nearly 80%. When it comes to resolving the energy crisis and reducing agricultural emissions, it is clear that the agricultural sector in developing countries must become a part of the solution (Bundschuh *et al*., 2017),. Solar energy has been used for food processing since ancient times, when food processing and preservation were important in nutritional and aesthetic applications (Barba *et al*., 2019). Solar energy is still used in applications such as water pumping, solar cooking, brackish water distillation, and so on (Bundschuh *et al*., 2017).

One of the important uses of solar energy is in the extraction of essential oils. Essential oils are liquids containing volatile aroma compounds derived from plant materials that have found industrial applications in the production of perfumes, cosmetics, soap, shampoos, and cleaning gels. Another important application of essential oils is in the agro-food industry, where they are used to make beverages and flavor foods (Rios, 2016). Because of their fragrance, anti-oxidant, and anti-microbial properties, essential oils derived from aromatic plants and spices are highly valued in the pharmaceutical, food and cosmetic industries (Valderrama and Ruiz, 2018). The yield of essential oils from essential oil bearing plants is typically between 0.005 and 10%. (Chemat and Boutekedjiret, 2015). Because yields are low and the commercially accepted traditional extraction method, namely distillation, is energy intensive (Neumann *et al*., 2010; Afzal *et al*., 2017), and essential oils are high-value products (Valderrama and Ruiz, 2018), energy efficiency and sustainable energy sources, such as CST technologies, have the potential

to support and improve the extraction process while reducing the carbon footprint. Although, the CST technologies have a great potential in the agro-processes and industrial sector as a whole, they have not yet been deployed extensively as compared to other applications of solar thermal collectors for replacing fossil fuel and reducing carbon footprint (Häberle, 2012).

Steam distillation of essential oils, a type of distillation and one of the agro-based processes involving a separation process for temperature sensitive natural aromatic compounds, is still important in the extraction of essential oils, although it is energy intensive. In medium temperature applications, concentrated solar collectors can generate significant amounts of saturated steam suitable for steam distillation. The majority of distillation processes use conventional energy sources that require significant amounts of fossil fuels. Solar energy can meet these massive energy demands in essential oil processing and related agro-based processes (Afzal *et al*., 2017). The majority of existing solar thermal plants use flat plate collectors (FPC) and evacuated tube collector (ETC) systems with maximum temperatures of less than 100°C, which are only suitable for low temperature process applications (Greentrust, 2017). As a result, the use of CST technologies to convert solar energy to thermal energy at medium to high temperatures would be critical for the survival of already-costly agro-based industries (including the essential oil's Industry). Steam distillation remain the most commonly used method for extraction (Masango, 2005). As a result, several solar thermal technologies that produce or supply saturated steam to extraction equipment can be used to extract essential oil.

Essential oil crops thrive in temperate, mediterranean, and subtropical climates, and the majority of them thrive in many parts of South Africa. The majority of South Africa's essential oil crops are grown in KwaZulu-Natal, Eastern Cape, Western Cape, and the Lowveld regions of Mpumalanga and Limpopo provinces. These crops are also grown in the cooler, higher-elevation areas of Gauteng and Free State provinces (South Africa, Department of Agriculture, Forestry and Fisheries, 2012). South Africa has a diverse range of producers who grow essential oil crops. Commercial and emerging farmers, farmers looking for alternative crops, co-operative farmers and community projects, as well as the cottage industry, produce essential oils. However, these community farmers encounter financial burden of operating the conventional steam distillation units. The technologies for extracting essential oils are available and user-friendly (Macaskill, 2017). However, these technologies rely heavily on traditional energy sources, which are expensive, particularly for small-scale farmers. In addition to the high cost of conventional technologies, the centralized nature of these technologies make the

distillation processes unmanageable for small-scale farmers (Munir and Hensel, 2010). In response to the problems mentioned earlier, this study aims to integrate a PTC into an agro-based process (Steam distillation of essential oils), with an intention to fulfil the following aims and objectives.

1.3 Aims and Objectives

The study's main aim is to determine the suitability of solar thermal generated steam for essential oil extraction by comparing extraction capacity, oil yield, and quality to that of a conventional essential oil steam distillation technology, as well as to investigate the possibilities of their use in agriculture, resulting in:

- Promoting the deployment and adoption of renewable and sustainable energy sources.
- Particularly, development of localized or mobile steam distillation unit.

The basic goals to accomplish the above aim are as follows:

- Integrate solar energy, especially in the form of thermal energy, into an agro-based process namely; the essential oil steam distillation.
- Investigate the conditions necessary for the optimal performance of the solar-powered essential oil distillation process.
- Conduct a comparative study of the optimal conditions for solar-powered essential oil distillation and those of fossil-powered essential oil distillation unit.
- Assess economic and technical feasibility of solar-powered essential oil distillation process in South Africa.

1.4 Structure of the Dissertation

Chapter 1 is an introductory chapter, which sets a scene for the reader. Necessary background on the research topic, motivation and aims of the research (including short term and long terms objectives) are outlined.

Chapter 2 is a literature on the research topic. Firstly, a background on essential oil's history, sources of essential oils, chemical compositions, applications, and factors that affect the quality and yield of essential oils are detailed, followed by a review of different traditional essential oil extraction methods, innovative extraction techniques and sources of energy for essential oil's production (including both conventional and non-conventional energy sources). The rest of the chapter is dedicated on exploring:

- The potential of solar energy (particularly CST technologies for industrial process heat).
- Current application of CST technologies in agro-based processes.
- Current research and development on essential oil's steam distillation with CST technologies.
- CST system components.
- Solar steam generating components.
- South African Solar Resource (Suitability of South Africa for CST technologies).

Chapter 3 is a methodology chapter outlining the experimental procedure followed to complete the research. Experimental procedures used for laboratory and field steam distillations are explained in detail. This includes a full description of the material (PTC system, laboratory essential oil steam distillation apparatus and field essential oil steam distillation unit) used.

Chapter 4 is a presentation and summary of experimental results (proximate analysis of the feedstock, energy consumption data, essential oil yield and quality) and discussions including the techno-economic review of CST systems.

Chapter 5 outlines the concluding remarks, together with recommendations of further work resulting from this research.

CHAPTER 2: LITERATURE REVIEW

2.1 A Historical Overview of Essential Oils

Throughout centuries, people have viewed essential oils with great interest, although most of their applications have disappeared with time. It is commonly known that the extraction of essential oils from aromatic plants dates back from the beginning of humankind. Essential oils have a wide range of applications including their use for cooking to enrich the flavor and health benefits of food. Their applications are also in the production of perfumes and cosmetics. In ancient Egypt, essential oils were used for pharmaceutical purposes, perfumery, and in the art of embalming and preparing bodies for burial (Rios, 2016). Numerous civilizations throughout history have used essential oils and fragrances for different applications, including religious ceremonies and therapeutic agents against infectious diseases. The Romans, Jews, Phoenicians, the Greeks, Mayas and Aztecs in Americas as well as other cultures located around the Mediterranean basin possessed a fragrance culture of great refinement (Rios, 2016).

2.2 Sources of Essential Oils

Essential oils are volatile odoriferous oil and aromatic oily liquids derived from different parts of the plant, such as flowers (e.g. rosemary and lavender), leaves (e.g. lemongrass and jamrosa), leaves and stems (e.g. geranium and patchouli), peels (e.g. cinnamon and cassia), wood (e.g. cedar and pine), roots (e.g. vetiver and valerian), seeds (e.g fennel and coriander), fruits (orange and lemon), rhizomes (e.g. ginger and orris) and gums or oleoresin exudations (e.g. balsam of Peru, and balsam of Tolu) (Handa, 2008; Tongnuanchan and Benjakul, 2014). They are formed in vesinogenou layer of cell wall or in the chloroplast of the leaf (Hamid *et al*., 2011). In some cases, they are not formed in the plant itself, but they are produced through the hydrolysis of certain glycosides, as it is the case with valeriana or garlic (Hamid *et al*., 2011; Rios, 2016).

2.3 Essential Oils Compositions

The main components of essential oils are oxygenated compounds (alcohols, esters, aldehydes, ketones, and phenols), hydrocarbons, terpenes, lactones, and acids. Among these, the oxygenated compounds are the principal source of odour. They are more resistant to oxidizing and resinifying influences as compared to other components. Unlike the oxygenated compounds, the unsaturated constituents (monoterpenes and sesquiterpenes) are inclined to oxidize or resinify when exposed to air and light. During the development of essential extraction

technologies, it is critical to have the precise knowledge of individual components of oxygenated compounds, and their physical characteristics, such as thermal stability, vapor-pressure relationship and thermal stability (Handa, 2008). Table 2.1 shows some of the chemical compounds of essential oil bearing plants.

Table 2.1 Chemical compounds of essential oils (Modified from Tongnuanchan and Benjakul, 2014)

Oregano	Chemical Compounds
Mandarin	Sabinene, cis-Limonene oxide, Linalool, α-Pinene, di-Limonene
Lemongrass	Camphene, β-Citral, α-Citral, α-Pinene, 3-Carene
Orange	Decanal, Linalool, Citronellol, Myrcene, cis-Limonene oxide
Lemon	Citronellal, α-Citral, α-Pinene, Limonene, Terpniol

2.4 Application of Essential Oils

Essential oils are used in a wide variety of consumer goods such as pharmaceuticals, confectionery, food products, soft drinks, distilled alcoholic beverages, insecticides, detergents, soaps, toilet products, cosmetics and perfumery. Essential oils are used in pharmaceutics for their potential as medicinal agents. They have been found to possess a diversity of pharmacological properties (Herman *et al*., 2019). Pharmacological actions of essential oils include anti-bacterial, anti-fungal, anti-viral, anti-inflammatory, anti-lice, anti-tumor, anti-dandruff and anti-oxidant properties (Ali *et al*., 2015). Insecticidal, nematocidal, anti-microbial, anti-viral, anti-fungal properties of the essential oils also play an important role in the agro-food industry. Food products such as confectionery sodas, soft drinks, and distilled alcoholic beverages use essential oils (Naeem *et al*.**,** 2018). Due to the presence of anti-microbial and anti-oxidant properties, essential oils can act as additives. The use of essential oils for agro-food industry may be limited because of the unique smell of the essential oil compounds which may alter the smell and flavour of foods (Tongnuanchan and Benjakul, 2014). The use of essential oils for cosmetics, soap, detergent, and perfume industry is of great interest from an economic perspective. Globally, the essential oil's production of perfumes has increased, with special groups of aromatic plants being highly preferred in the market. For example, lavender, and thyme are prized highly for manufacturing of fine and novel perfumes (Rios, 2016).

2.5 Factors that Affect the Yield and Quality of Essential Oils

Various factors are responsible for the quality and yield of essential oils. These factors include agronomy factors, namely: climate, drought, soil type, water stress and stresses induced by pests and micro-organisms, cultivation practices and propagation (seed or clones). Other factors include harvest timing, extraction method, storage, and preparation of the plant material before essential oil extraction and precisely knowing where oil cells in the plant are located and which part of the plant material contains essential oils (Schmidt, 2010). For example, in the case of preparation of plant material, it was found that plant material with small particle size yielded higher initial extraction rates when the study was conducted with super-critical fluid extraction (Masango, 2001). On the other hand, the quality and yield are dependent on extraction techniques (Hamid *et al.*, 2011).These techniques used to extract essential oils include different types of distillation methods (water distillation, water and steam distillation, steam distillation), cohobation, maceration and enfleurage and so on(Handa, 2008). Table 2.2 shows some of the essential oils bearing plants and their methods of extraction.

Table 2.2 Essential oil plants and their extraction methods (Modified from Tongnuanchan and Benjakul, 2014)

Extraction technique	Essential oil plants
Solvent extraction - Solvent	sage (Salvia officinalis), apiaceae (Ptychotis verticillata), chasteberry (Vitexagnuscastus L)
Super-critical CO2	rosemary (Rosmarinus officinalis), fennel (Foeniculum vulgare), patchouli (Pogostemon cablin)), lavender (Lavandula angustifolia Mill), coriander (Coriandrum sativum L)
Subcritical water	olive (Olea europaea), fructus amomi, marjoram (Origanum majorana), coriander seeds (Coriandrum sativum L)
Distillation - Steam	clove (Eugenia caryophyllata), orange (Citrus sinensis), rose-scented geranium (Pelargonium sp), lavender (Lavandula dentata L.), eucalyptus (Eucalyptus citriodora)
Water distillation	rosemary (Rosmarinus officinalis), rose-scented geranium (Pelargonium sp), lavender (Lavandula angustifolia Mill), rosemary (Rosmarinus officinalis), oregano (Origanum vulgare L)
Hydrodiffusion	orange (Citrus sinensis), rosemary leaves (Rosmarinus officinalis)

2.6 Conventional Essential Oil Extraction Techniques

2.6.1 Solvent extraction

Solvent extraction technique is used for the extraction of essential oils that are thermosensitive. It is used in the production of perfumes and vegetable oil or biodiesel (Aziz *et al*., 2018), and suitable for expensive, fragile and thermosensitive plant materials like hyacinth, jasmine and tuberose (Khaled *et al*., 2015). Generally, the mixture of the plant material and solvent is mildly heated, followed by filtration. Subsequently, the solvent is evaporated in order to concentrate the filtrate (Aziz *et al*., 2018). In order to complete the extraction process, the concentrate is mixed with pure alcohol and allowed to undergo distillation at low temperatures. Solvents that are used for the extraction include acetone, hexane, petroleum ether, methanol, or ethanol. This essential oil extraction is complicated, time-consuming and costly as compared to other extraction methods (Tongnuanchan and Benjakul, 2014).

2.6.2 Enfleurage

Enfleurage is one of the oldest extraction methods of producing essential oils. It has been in use, primarily for the production of essential oils from flowers (e.g. jasmine). A refined odourless cold fat is spread on the plant material (e.g. flowers). The odours from the flowers are released and dissolved in the fat as a result. The process is repeated until the cold fat is saturated, with the old flowers being replaced by new flowers. After that, the fat is collected, and the oil is extracted using alcohol (Stratakos and Koidis, 2016). Despite the introduction of the modern process of extraction with volatile solvents, enfleurage still plays an important role (Singh, 2008), although according to today's standard, it is costly, time consuming and labour intensive (Stratakos and Koidis, 2016).

2.6.3 Maceration

Maceration is appropriate for use in cases where the oil yields from conventional distillation methods are low (Khaled *et al*., 2015). In maceration, the oil cells of the fragrant flowers are submerged in either hot fat or oil where they undergo rupturing. The fat or oil extracts the essential oils. Fat is removed from spent flowers and recycled for absorption of essential oils from new batch of fragrant flowers. The hydraulic press is used to further recover the retained fat from the flowers. The resulting perfumed pornade is marketed as it is but it is frequently extracted with strong alcohol to yield extracts (Jain and Ravikumar, 2010).

2.6.4 Distillation

Distillation is considered the most common and cost-effective method for production of essential oils throughout the world. This process separates the oil by vaporizing the oils from the plants, then cooling the vapour mixture to separate the oil from the water on the basis of immiscibility and density of essential oil and water (Tandon, 2008). The main advantage of the distillation systems is that they can be conducted with simple equipment and can be located close to the production site. Even in remote locations, large quantities of plant material can be extracted in short period of time. Distillation is not labour intensive and requires a lower labour skill (United Nations Industrial Development Organization and Food and Agriculture Organization of the United Nation, 2005). There are three common distillation methods for essential oils bearing plants, namely: water distillation, water and steam distillation, and steam distillation.

(a) Water Distillation

The essential oil plant material is packed in a distillation tank containing water in order to extract essential oils plants. The two are allowed to reach boiling point, and the essential oil is released from the plant material due to the effect of steam. The indirect cooling with water from the condenser causes the water vapour mixture to condense. Because of the different densities and immiscibility of oil and water, the distillate from the distillation tank flows from a condenser into a separator, where oil is separated naturally from hydrosol (Handa, 2008). The advantage of using this approach is that water distillation units are relatively cheap. However, required products are degraded during hydrolysis or polymerization of sensitive components because of prolonged heat exposure. Water distillation consumes a lot of fuel, thus making the distillation uneconomical. The method is used if it is unpractical to use the other two distillation methods (Handa, 2008).

(b) Water and Steam Distillation

In water and steam distillation method, the design is similar to that of water distillation method. The plant material is positioned above a grill or perforated plate. The grill or perforated plate is placed above the boiling water in a distillation tank. However, this set-up reduces the capacity of the tank volume but a high packing density may recompense this because the plant material is not immersed in water. This method has some advantages over water distillation method, namely: higher oil yield, faster extraction rates, energy efficiency and minimal changes of oil

component due to wetness and thermal conductivity of the tank from the heat source (United Nations Industrial Development Organization and Food and Agriculture Organization of the United Nation, 2005).

(c) Direct Steam Distillation

In Steam distillation, steam is directed from outside, usually from a stand-alone boiler, to a distillation tank (Handa, 2008). This method is one of the most widely used for extracting essential oils from plants (Tandon, 2008). Although different methods of production have developed over time, steam distillation still hold a bigger proportion in terms of its use in the essential oil industry. According to Masango (2005), 93% of essential oils plants are extracted through the use of a steam distillation system, while 7% is extracted through other methods. In direct steam distillation, controlling of the quantity and the quality of steam can be achieved (Handa, 2008). Due to the ability to control the steam quantity and quality, the risk of thermal degradation is reduced, as temperatures are below 100 °C. However, the capital cost of steam distillation process is high, with payback period of more than ten years (United Nations Industrial Development Organization and Food and Agriculture Organization of the United Nation, 2005). The amount of essential oil produced is determined by four key factors: distillation time, temperature, operating pressure, and plant material consistency (Chemat and Boutekedjiret, 2015). Direct steam distillation outperforms the other two distillation methods: water distillation, and water and steam distillation (Handa, 2008).

2.6.5 Cohobation

Cohobation is a method that is applied only during either, a water distillation or water and steam distillation (Handa, 2008). According to Schmidt (2010), in all cases of water distillation, this method is applied. When the water or water and steam distillation is completed and essential oil separated, the distillate water is returned to the distillation tank and boiled again to recover essential oil (Handa, 2008). Any essential oil constituents that are dissolved or emulsified in the water are separated from the water, and resulting in increased essential oil yield (Schmidt ,2010). The motive behind this method is to reduce the losses of oxygenated components, especially phenols which dissolve in distillate water. In most of the essential oils, the essential oil loss through water is below 0.2%. However, for phenol-rich essential oils the quantity of oil in the distillate water is ranging from 0.2% to 0.7%. Cohobation is suitable for temperatures of

less than 100° C, and anything beyond 100° C will degrade oxygenated constituents in the distillate (Handa, 2008).

2.6.6 Hydrodiffusion

Hydrodiffusion extraction method is similar to a steam distillation method. The main difference between the two methods is that in hydrodiffusion method, the steam is supplied from the top of the distillation tank (Ranjitha and Vijiyalakshmi, 2014). This method applies to only dry plant materials, which can be damaged at boiling temperature (Aziz *et al.*, 2018). The essential oil is condensed from the area in which the plant materials is supported by the grill or perforated plate. The condensed oil is separated through a separation funnel. This method is used for extraction of essential oil plants such as jasmine, pandanus, marigold, and rose. Less quantity of steam, shorter extraction time and higher oil yield can be achieved as compared to other methods (Ranjitha and Vijiyalakshmi, 2014).

2.6.7 Expression or Cold pressing

Expression or cold pressing is the oldest extraction method and is used almost exclusively for the production of citrus peel essential oils (Stratakos and Koidis, 2016). This is because the chemical composition of the oil is thermosensitive (Schmidt, 2010). Thermal instability of the aldehydes will result in compromised quality of oil if expression is not used. There is, however, one exception. Commercial lime oil may be cold pressed or allowed to undergo steam distillation. The two essential oils resulting from these two methods will have different odours, and subsequently vary markedly. Normally, the expressed citrus peel is treated with hot steam to recover any essential oil that has remained in it. This process's by-products, mostly limonene, are used in the solvent industry. Cattle feed is made from the remaining peel and fruit flesh pulp (Schmidt, 2010).

2.7 Current Innovative Essential Oil Extraction Techniques

2.7.1 Ultrasound-assisted extraction of essential oils

In ultrasound-assisted extraction (UAE), the ultrasound frequencies ranging from 20 kHz to 2000 kHz are applied to a raw plant material (Handa, 2008). The raw plant material is immersed in either water or methanol or ethanol or any suitable solvent, after which the plant material and solvent or water are subjected to the effects of the ultrasound (Hesham *et al.*, 2016). The ultrasound effects are due to the cavitation, which comes from the production and breakdown

of microbubbles. When the microbubbles grow in size they eventually collapse powerfully. It is this powerful collapse that forms mechanical forces which damage the cell membrane of the plant material, thus producing high yields of extracted essential oils in a shorter extraction time (Stratakos and Koidis, 2016). The UAE method has been used for the production of many essential oils such as those originating from the flowers, seeds or leaves (Hesham *et al*., 2016). The UAE method has already demonstrated improvements on the yield, extraction time, energy consumption, selectivity and preservation of thermosensitive compounds (Khaled *et al*., 2015). Although there are many more advantages, including that of the extraction of rauwolfia root, the high capital costs have limited the large-scale application of the UAE technique (Handa, 2008).

2.7.2 Super-critical fluid extraction of essential oils

Super-critical fluid extraction (SFE) uses the super-critical state of CO_2. This super-critical state is attained through compressing and heating CO_2. Then, super-critical CO_2 is allowed to pass through plant material to extract volatile compounds. Two separators are then used to separate CO_2 and essential oils (Aziz *et al*., 2018). Supercritical fluids have been used as solvents for a wide variety of applications such as essential oil and metal cation extraction. In practice, more than 90% of all analytical SFE is performed with carbon dioxide (CO_2) for several practical reasons (Hesham *at al*., 2016). Besides having attributes such as low critical pressure of 74 bars and temperature of 32°C, CO_2 is relatively low cost, non-toxic, non-flammable, non-corrosive, safe to handle, and accessible in high purity, and is easy to remove from the extract. However, the main disadvantage of CO_2 is the fact that it is a non-polar fluid with no permanent dipole moment. Thus, its ability to dissolve polar or high molecular weight analytes is limited (Khaled *et al*., 2015). Sometimes organic solvents such as ethanol or methanol are used to modify carbon dioxide (Handa, 2008; Hesham *at al.*, 2016). These organic solvents improve the mobile-phase polarity, thus enabling separations of more polar analytes (Kubeczka, 2010). Carbon dioxide is sometimes replaced by argon because it is more cost-effective and more inert (Handa, 2008). Super-critical extracts proved to be of higher quality, with better functional and biological activities. The other advantage of this method is that where steam distillation fails to extract many essential oils, SFE can be used successfully. This method is still very costly and not easily handled. (Hesham *at al*., 2016). However, it is reported that SFE is more economically feasible when compared to the steam distillation, the reason is because of the low yields and high energy

consumption associated with the steam distillation technique (Tongnuanchan and Benjakul, 2014).

2.7.3 Accelerated solvent extraction

Accelerated solvent extraction (ASE) is a solid-liquid extraction technique that is conducted at high temperature and pressure. Temperatures range is between 50° and 200°C, whereas pressures range is between 10 and 15 MPa. The role of the increased temperature is to accelerate the extraction kinetics while the increased pressure keeps the solvent in the liquid state, thus achieving safe and rapid extraction. ASE usually uses organic solvents. However, pressurized hot water can be used in the place of a solvent and in such a case, the extraction process is called sub-critical water extraction (Tandon and Rane, 2008).

2.7.4 Sub-critical water extraction

The application of ASE with subcritical water as the extractant carries a great potential because water is non-toxic, cheap and environmentally friendly (Khaled *et al.*, 2015). In sub-critical water extraction, temperatures are maintained between 100 and 374 °C, whereas pressure is maintained up to 10 bar to keep the liquid phase of water (Tongnuanchan and Benjakul, 2014; Khaled *et al*, 2015). This technique has advantages over conventional extraction methods in terms of extraction time and cost savings. For example, the time taken to run an extraction process is 15 minutes as opposed to 3 hours taken by conventional extraction methods. When essential oils with more valuable properties are extracted, for example those with higher amount of oxygenated components and with no significant presence of terpenes, significant cost saving in energy and plant materials can be recognized (Aziz *et al*., 2018).

2.7.5 Microwave-assisted extraction

Microwave-assisted extraction (MAE) is different from the conventional heating methods which usually depend on the thermal processes of convection and conduction, which eventually lose energy to the surroundings. With MAE techniques, the heating takes place in such a way that there is no heat lost to the surrounding as the heating is in a closed system. Shorter extraction times of less than 30 minutes can be achieved with MAE (Khaled *et al*., 2015). In terms of the ease of use and operational cost, this extraction technique performs better than SFE. However, under normal conditions MAE utilizes high quantity of solvents, which renders it less environmentally friendly as compared to SFE (Stratakos and Koidis, 2016). MAE has

been successfully used in laboratory scale, although its use at the industrial-scale is still remaining low. Capacity of 3 t/h MAE is available (Pangarkar, 2008).

2.8 Sources of Energy for Essential's Oils Production

2.8.1 Conventional energy sources

Wood, Coal and Biomass

Wood, coal and biomass are the traditional fuels for distillation. The biomass used can be dried or extracted biomass (Schmidt, 2010). In distillation systems that use wood, coal or biomass, the fuel used can be fed either manually or automatically, depending on the size of the distillation system (Essential Distillation Equipment South Africa, 2017). The disadvantage associated with this energy source is that the heating surface area limits the steam production, thus resulting in extended distillation time and sometimes lower production of essential oil. As compared to a modern steam distillation unit with external boiler, firewood consumption may be up to to 2.5-times greater. However, this may not be critical where there is an abundance of low cost fuel. In many developing countries, fuel supplies are getting scarce and costly and low thermal efficiency can directly affect the cost of production (Tandon, 2008). Wood, coal and biomass-fired boilers require regular cleaning and not all of them require inspections from the government, depending on the size and type, low pressure or high pressure (Essential Distillation Equipment South Africa, 2017).

Fuel Oil or Gas

According to Schmidt (2010), oil and gas are commonly used fuels for steam distillation. The ones commonly used for the purpose of distillation are diesel and Liquefied Petroleum Gas (LPG)**.** Diesel or gas boiler installations are regulated by the laws and require inspections by government officials. They are not easy to clean and maintain and require certain water types to operate (Essential Distillation Equipment South Africa, 2017). The drawback with fuel oil and gas is the fact that, they are limited and the prediction is that in the next 40 to 50 years, they will be depleted (Saidur *et al*., 2011).

Electric Boilers

Electric boilers do not necessarily fall under conventional heating systems. They are classified as steam generators when they are set to operate at atmospheric pressure. Due to their operation at atmospheric conditions, they are not regulated by the governing laws. However, these boilers can be modified to produce pressurized steam and in such a case, they are classified as boilers or modern boilers. Unlike fuel oil and gas boilers, electric boilers are easy to clean and maintain (Essential Distillation Equipment South Africa, 2017). As explained in chapter one, steam distillations draw more electricity, and therefore the use of electricity, particularly when it is generated from coal-fired power stations, may not be practical and economical.

2.8.2 Non-conventional energy sources

The non-conventional energy sources include the advanced extraction techniques discussed in section 2.7, they are UAE, MAE, sub-critical water and SFE extraction (Giacometti *et al.*, 2018). They are based on a six principles of green extraction, namely: (1) use of renewable plant resources, (2) use of alternative solvents such as water or agro-solvents, (3) reduced energy consumption, (4) production of co-products instead of waste, (5) shorter extraction times, and (6) recovery of natural extracts without contaminants (Chemat *et al*., 2012). According to Giacometti *et al*. (2018), It has been reported that on the industrial scale, these principles have shown to promote the sustainable production with decreased application of water and solvents, elimination of production of wastewater and hazardous substances, and elimination of the usage of fossil energy.

2.9 Concentrating Solar Thermal Technologies for Industrial Process Heat

Industrial process heat temperatures are not only lower than those usually used for electricity generation, but the power spectrum is also narrower. The systems have a peak thermal capacity in the range of kWs and hardly reach several MW (Häberle, 2012). The annual energy gains for these systems are ranging from 550 to 1100 kWh/m^2 (Kalogirou, 2003). Solar thermal technologies are categorized as stationary (non-tracking, single axis, and double axis) or mobile (tracking, single axis, and double axis). Flat plate collectors (FPC), evacuated tube collectors (ETC), and compound parabolic collectors (CPC) are examples of stationary collectors . LFC, PTC, and cylindrical trough collector (CTC) are single axis collectors, while PDC and HFC are double axis collectors (Kalogirou, 2003). It is important to note that not all of these solar collectors are suitable for industrial process heat because some of them (especially PDC and HFC) operate at very high temperatures that are suitable for electricity generation; however, the double axis can be adjusted for industrial process heat in some cases. Stationary collectors (FPC, ETC, and CPC) and single axis PTC are two types of solar collectors that are ideal for industrial process heat. Low temperature applications (below 80°C) are possible with FPC and ETC. CPC is the only stationary collector on the market that uses concentrating technology to provide operating temperatures of up to 240°C (Kalogirou, 2003). The following parts go into industrial process heat concentrating solar technologies.

2.9.1 Small sized parabolic trough collector system

Large PTCs for large solar thermal power plants were the subject of research and development in the late twentieth and early twenty-first centuries. New smaller PTCs, on the other hand, have been produced for process heat applications at temperatures below 300°C. These collectors may provide industrial process heat (IPH) to a number of applications, enabling them to eliminate the use of fossil fuels (Zarza-Moya, 2012). Sterilization, pasteurization, drying, hydrolyzing, distillation and evaporation, washing and cleaning, and polymerization are all processes that can benefit from the use of small PTCs. Process heat collectors are usually smaller than those used in concentrating solar power (CSP) applications for electricity production. Aperture widths usually range from 1 to 3 meters, collector total lengths between 2 and 10 meters, and geometrical concentrating ratios between 15 and 20 meters (Fernandez-Garca *et al.*, 2010). The structure of small PTCs is lighter. Many companies began producing small PTCs capable of working in temperatures ranging from 50 to 300°C as early as the 1980s. One of the first companies to create PTCs was Industrial Solar Technology (IST) Corporation

(Kalogirou, 2003). The IST-PT1, PTC-1800 collector, and PolyTrough-1200 are examples of small PTCs specifically designed for IPH. These collectors can reach temperatures of 288°C, 200°C, and 230°C, respectively (Zarza-Moya, 2012). PTCs are a well-established technology that can withstand high temperatures while maintaining high performance (Kalogirou, 2003).The research that led to these conclusions was carried out in a mediterranean environment with different solar radiation levels between 500 and 1000 w/m^2 (Kalogirou, 2003). Figure 2.1 shows that as the amount of solar radiation increases, the efficiency rises. As seen on the graph, PTC and CPC show to have high efficiencies.

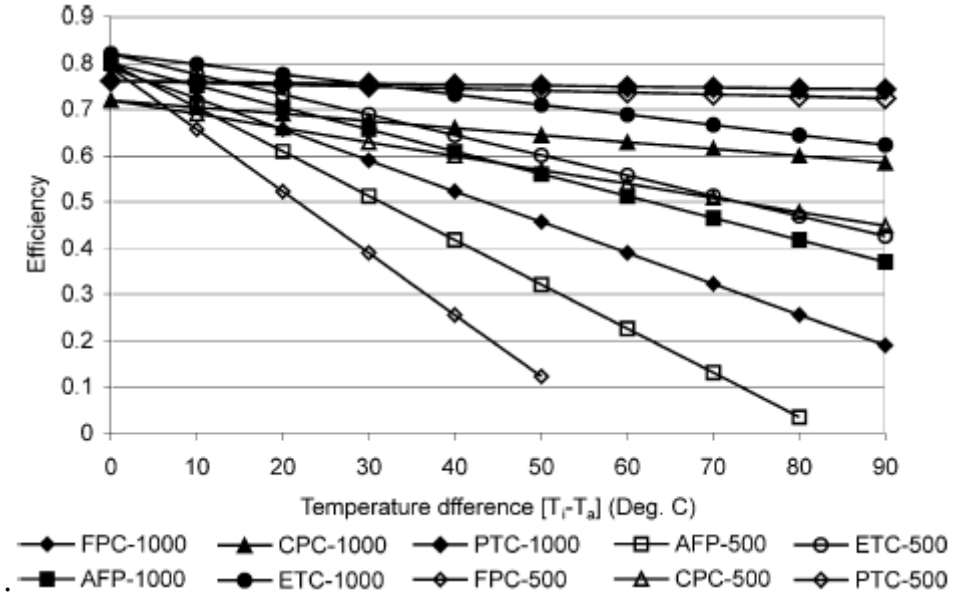


Figure 2.1. Comparison of solar collector efficiencies (Kalogirou, 2003)

2.9.2 Compound parabolic collector

CPC consists of two parabolas, one placed on the right hand side of the receiver and the other one placed on the left side of the receiver. The receiver is situated at the bottom. CPC has multiple reflections of radiations which are caused by larger angular spread (Barone *et al.*, 2019). Due to the fact that they are stationery collectors, solar radiations can only be received when the sun is within the collector's acceptance angle (Kalogirou, 2003). However, in certain application where high temperatures are required, CPCs can be enhanced to track the sun. The concentration ratios of CPCs are low, hence rough or intermittent tracking system can be used to track the sun (Barone *et al.*, 2019). CPCs are capable of collecting some of the diffuse radiation, and can operate up to 300°C, CPCs can be cheap than PTCs, because they usually do not require tracking (Pranesh *et al.*, 2019).

2.9.3 Parabolic dish collector system

As mentioned earlier in section 2.9, point focus systems are not suitable for IPH as they operate at high temperatures, which are undesirable for IPH. However, a point focus systems like PDC can be modified for the supply of IPH. Two modified PDCs, which are commonly used in India are Schefler Dish and ARUN.

(a) Schefler dish

There are a number of dish systems called scheffler dishes, which were popularized in India, mostly for large-scale solar cooking installations. They use a fixed focus to concentrate radiations and because of that, they can be classified as heliostats. An interesting feature about the scheffler dish is its adaptation of the reflector's shape to the yearly change of the solar altitude. This allows for the use of a relatively simple polar axis mechanism for the daily tracking. The overall concentration ratios achieved are small when compared to the ordinary PDC dish, and similar to linear concentrators (Häberle, 2012). The main advantage of the Scheffler dish lies in the fixed focus of the system, which reduces structural complexity and enables direct steam generation. However, the system has low concentration ratios and because of that, low temperatures of up to 150℃ can be acieved. Although the maximum temperature for scheffler dishes is 150℃, they are mostly operated at a temperature of 120 ℃, and any temperature more than 120 ℃ will comprise the system efficiency (Sardeshpande and Pillai, 2012).

(b) ARUN

An example of another dish system is ARUN. ARUN is the brand name of the first PDC System to be developed for medium temperature applications. It was developed by Clique Developments PVT LTD., Mumbai. ARUN-160 and ARUN-70 are the two parabolic dishes developed by Clique Developments PVT LTD., Mumbai and they have apertures areas of 160 and 70 m^2, respectively. There are ARUN dish systems of different sizes, for example ARUN 100, ARUN 30. ARUN-160 weighs about 20 tonnes and has a steam output of 100 to 120 kg per hour, with thermal output of 80 to 100 kW (International Renewable Energy Agency and The Energy Technology Systems Analysis Programme, 2015). According to Kedare *et al.* (2006), ARUN has potential to save 25 to 100% of the energy used for process heat in industrial units depending on temperatures and load cycles of the process. Other advantages of this PDC System are (Sardeshpande and Pillai, 2012):

- High concentration ratios.
- High operating temperatures.
- Double axis tracking and control system for ease of operation and safety.

Some of the disadvantages are high installation time (two to three months to fabricate PDC) and high weight of the system, thus making installations on the roof tops not practical (Sardeshpande and Pillai, 2012). In addition, PDCs can reach stagnant temperatures of up to 1500 °C, thus making the system not suitable for the case of medium temperature applications (Mishra *et al*., 2019).

2.10 Current Use of CST technologies for Agro-Based Processing

Heating water, buildings and swimming pools are currently the most popular applications for solar thermal energy. The majority of collectors used are flat-plate collectors that are fixed in place (Kalogirou, 2003). Other solar thermal energy applications have not been generally recognized, necessitating further studies. Solar energy is used for baking, cooking, pasteurization, drying, solar assisted distillation of brackish water, and solar distillation of aromatic plants, to name a few applications.

2.10.1 Solar cookers

The first known person to build a box to solar cook food was Horace de Saussure. Horace de Saussure was a Swiss naturalist and the grandfather of solar cooking. He cooked fruits in a primitive solar box cooker that reached temperatures of 88 ◦C. Present design of solar cooker started evolving in the 1950s. Different aspects of solar cooking designs were studied by researchers and it was concluded that properly constructed solar cookers not only cooked food thoroughly and nutritiously, but were simple to make and use (Panwar *et al*., 2012). In spite of the many advantages of solar cookers, they are not widely used, especially for household cooking. However, in developing countries with abundant annual solar radiation, deployment of solar cookers has recently increased. About million solar cookers have been installed globally and are used by more than 11 million people. These cookers are mainly in use in Africa and South Asia (Aramesh *et al*., 2019).

Solar cookers are usually divided into two types: concentrating type and box type cookers. The concentrating solar cookers use reflectors to concentrate solar energy on the cooking vessel, while the box solar cookers use greenhouse effects in conjunction with solar concentration

(Sansaniwal *et al*., 2018). Concentrating solar cookers can be categorized in different ways based on their characteristics. They can be direct type or indirect type depending on the method of heat transfer to the cooking pot. Solar radiation concentrates directly onto the cooking pot in direct solar cookers, while in indirect solar cookers, solar energy is first used to create high temperature and pressure steam, which is then transferred to the kitchen (Indora and Kandpal, 2019). Solar cookers and concentrating type solar cookers are discussed below.

(a) Box type

These types of cookers are simple in design, cost effective and widely used in cooking rice, vegetables, meat and other items (Refer to Figure 2.2). However, the cooking time required is high (1-2.5 h) and they are unable to perform satisfactorily in winter and at heavy cooking load conditions. According to Barba *et al*. (2019), solar cookers should also contain fresnel lenses or two booster mirrors to maximize the solar radiation.



Figure 2.2 Schematic diagram of a box cooker (Panwar *et al*., 2012)

(b) Concentrator type

Solar concentrating cookers have been widely used, but they are not as popular as the box type (Aramesh, 2019). Concentrating solar cookers are efficient, however frequent adjustment is required to maintain point focus. These type of cookers either work on one or two axes of tracking with a concentration ratio up to 50 and temperature up to 200 ℃, which is suitable for water boiling and cooking (Panwar *et al*., 2012). Solar concentrating cookers take short time to cook and is faster even with high moisture content food (Sansaniwal, 2019). According to Panwar *et al*.(2012), concentrating solar cookers are expected to demonstrate high performance because of the large collection area employed. However, the net amount of heat used is still low. Introducing the oven type concept as an alternative approach for collecting the concentrated solar energy would boost the overall efficiency (Panwar *et al*., 2012). The common solar concentrating cookers are parabolic dish solar cooker (PDSC) and Scheffler Dish.

Parabolic dish solar cooker has a steel support structure that holds the pot in a focal position and tracks the sun along with a pot (Refer to Figure 2.3). PDSC system consists of PDC, structural support, and a solar-based double axis tracker. A typical example of a PDSC is SK-14 solar cooker, it has aperture area of 1.54 m^2 and a focal length of 0.28 m. The SK-14 can use approximately 15 minutes to boil water when the direct normal irradiation (DNI) is 600 W/m^2. The PDSC can be used for up to 10 to15 persons. For small to medium applications PDSC, 1 to 10 m^2 area can be considered and such PDSC can cater for many persons (Indora and Kandpal, 2018). Other PDSCs, which are commercially available, are (Indora and Kandpal, 2018):

- SK-23 which has an aperture area of 4.15 m^2, and operating temperatures of 250-400℃ at its focal length. This PDSC system can serve 15-20 persons and save 15-20 liquefied petroleum gas (LPG) cylinder of 14.2 kg.
- SK-30 with an aperture area of 7 m^2, and operating temperatures of 250-400℃ at its focal length. This PDSC system can serve 40-50 persons and can save 25-30 LPG cylinder of 14.2 kg.
- PRINCE-15 with an aperture area of 1.5 m^2, and operating temperatures of 250-400℃ at its focal length. It can serve 8-10 persons and can save 8-10 LPG cylinder of 14.2 kg.

- PRINCE-40 has an aperture area 4 m^2, and operating temperatures of 250-400°C at its focal length. This PDSC system can serve 40-50 persons and can save 25-30 LPG cylinder of 14.2 kg.

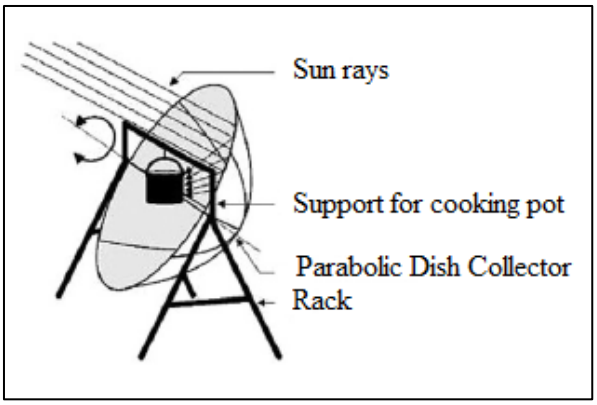


Figure 2.3. Parabolic dish solar cooker (Panwar *et al*., 2012)

In **scheffler dish system** as shown on Figure 2.4, the direct normal irradiance (DNI) is first reflected from the scheffler dish, which is a primary reflector, and then to the secondary reflector, which then channels energy to the pot. These cooking systems are common in India. A typical scheffler dish with an aperture area of 16 m^2 occupies 35 m^2 on the ground and is capable of generating an energy output of 5.5 kW on a clear sunny day. A small scheffler dish, which is suitable for a family can cook 1.2 litre within 10 minutes, whereas a community size scheffler dish of 10 m^2 aperture area can boil 4.5 litre of water in 10 minutes when the DNI is 700 W/m^2 (Panwar *et al*., 2012).

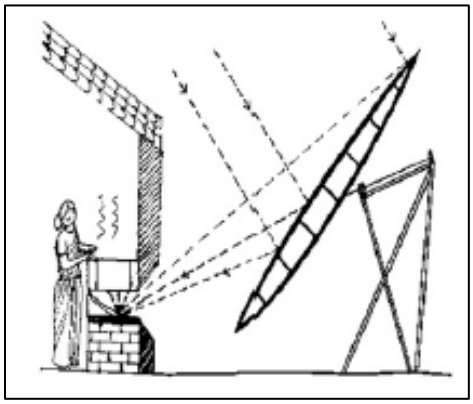


Figure 2.4. Scheffler dish system (Panwar *et al*., 2012)

ARUN 160 is one of the products for Clique Solar. The installed ARUN of 160 m^2 area was reported to have a capability of operating 270 days and saving 27000 litre of furnace oil per year which is equivalent to savings of 100 to 115 litre of furnace oil pear clear sunny day. ARUN100 was reported of having being able to generate 60kg/h of steam in a clear sunny day at 6 bars. The ARUN100 can prepare meals for up to 3500 persons and save 30 to 40 kg of LPG. This solar system is water saving since the same steam that carries energy is condensed back for re-use into the solar system (Indora and Kandpal, 2018). The peak efficiency of ARUN has been reported to be 65% whereas the annual efficiency is from 50 to 60% (Indora and Kandpal, 2018).

Parabolic trough cooker also have a potential for solar cooking. One such example was demonstrated by Kumaresana *et al*. (2016), whereby concentrating cookers consisted of a PTC, Thermal energy storage in the form of phase change materials (D-Mannitol), and a tava port. Therminol 55 was selected as a heat transfer fluid (HTF). During the day, the PTC solar cooker was run to collect energy and the system attained a temperature of 175 °C. The system was set up to release energy to the tava pot at night, therefore, it was allowed to discharge energy to the pot at night. During the discharging process, the PTC had to be by-passed to prevent energy from dissipating to the PTC. Olive oil with known properties was poured into the pot before the discharging of energy takes place. The aim of the experiment was to investigate the performance of the system, and to study the characteristic behaviour of the discharging process. The tava pot was capable of receiving heat from the thermal energy storage (TES tank) at a constant rate, though there were considerable amount of energy lost during the process. Piping circuit, TES tank and and tava cooker all had losses of 54.3, 25.3 and 4.1%, respectively. An effort to reduce these losses can improve performance significantly (Kumaresana *et al*., 2016).

2.10.2 Desalination

Solar energy can be used indirectly in the form of thermal, mechanical or electrical energy. Examples of indirect solar desalination include membrane distillation (MD), reverse osmosis (RO), humidification-dehumidification(HDH), multi-effect distillation (MED), multi-stage flash(MSF) and electrodialysis (ED). According to Ahmed *et al*. (2019), RO is seen as the most suitable technology for large-scale solar-powered desalination systems. Employment of CSP technology to drive desalination systems has been considered as a highly viable option to sustainably supply the required energy. CSP plants generate high temperature heat that can be utilized to produce electricity via power cycles to meet the heat requirements for different

applications such as water desalination systems (Mohammadi *et al.*, 2019). One axis-tracking solar collectors, linear Fresnel concentrators or parabolic troughs are the most efficient technologies to drive an organic rankine cycle (ORC) in order to produce the energy required for an RO system (Pouyfaucona and García-Rodríguez, 2018).

ROs are complex processes, involving highly skilled technical personnel and often used in large-scale operation. However, there is still a potential for rather simple promising techniques to desalinate brackish water and can possibly be used at a small-scale level. A typical example of that, is the use of PDC to desalinate brackish water. In the experiment documented by Tiwari and Sahota (2017), the system consisted of PDC, double Plate Heat Exchanger(PHE), pumps for brackish water circulation, and a PV-powered two axis tracker. The PDC had a reflective surface of 3.142 m^2 and an absorber area of 0.031 m^2. A part of the absorber was insulated with a rock wool while the other part was left bare for the purpose of concentrating DNI. A PDC had a focal length of 0.693 m. The two PHEs worked separately; one was used to condense brackish water vapours from the absorber, which is then collected, while the other one was used to preheat brackish water before it is channelled to the absorber. With this system absorber temperature of 150.7℃ was reached at a DNI of 626.8 W/m^2. A water yield of 5.12 kg/day was reached. The average efficiency of the system was found to be 34.69 %, with a maximum yield of 1.2 kg/h(Tiwari and Sahota, 2017).

2.10.3 Baking with solar energy

An experiment on baking with solar energy was done, where a solar, parabolic trough collector bakery consisted of a duratherm 600 HTM which circulated between the PTC and the coils of the oven. The coils of the oven contained the duratherm 600 HTM, which was responsible for transferring heat to the oven. To keep the heat evenly, a fan was used to blow air inside an oven. The PTC bakery system yielded 1248 W of energy, which was not adequate for a complete bakery (Mishra *et al.*, 2019). Mishra *et al*. (2019) then concluded that to reach the desired temperatures (220-240 ℃) required to completely bake the bread using the same DNI, the heat loss coefficient from inside surface walls of the oven must be decreased by applying an appropriate insulation material. The other possible alternative is to increase the aperture area of the PTC, and for this alternative, computations were done using computational fluid dynamics (CFD) analysis, and found out that the aperture area should be increased to 5 m^2, given the heat loss coefficient does not change (Mishra *et al.*, 2019).

Another study was done by Ayub *et al*. (2018), whereby the scheffler reflector was used. The bakery system consisted of the scheffler reflector, which is a primary reflector, a small reflector mounted on the bottom of the oven, an 80 W, DC fan for air circulation, and the oven. In the system, DNI was reflected from the primary reflector to the secondary reflector, which in turn, focused energy towards the oven. The system was set up to perform the thermal analysis (Energy- and exergy-based thermal analyses) of a solar concentrated technology for baking. After running the experiment, the average temperature was found to be 180 ℃. Energy utilization was found to be 0.01–0.07 kW, energy utilization ratio of 25–75%, exergy losses of 0.19–1.08 and exergy efficiency of 6.62–56.46%. The overall exergy efficiency was 59.26 %. According to Ayub *et al.* (2018), the system yielded good results and the system can be optimized by taking control of baking conditions. Other important suggestions are that the receiver size, air-flow rate, number of food samples and moisture content should be considered in order to maximise the amount of energy while reducing the losses of energy (Ayub *et al*., 2018).

2.11 Research on Essential Oil Steam Distillation With CST Technology

Research and development in the use of CST technologies for essential oil steam distillation is uncommon. However, a few notable studies on powering essential oil steam distillation process are that of Munir (2010), Kulturel and Tarhan (2016). Munir (2010) used an 8 m^2 schefler dish to reflect solar radiation onto a 0.434 m^2 secondary mirror, which guided the radiation to a distillation pot made of 2 mm thick food-grade stainless steel. The stainless steel pot had a diameter of 400 mm and a height of 1210 mm. Clove, fennel, cumin, patchouli, cassia, and orange peel essential oils were extracted using a schefler dish. The power consumed in extracting these essential oil bearing plants was found to be 0.133 for clove, 0.503 for fennel, 0.574 for cumin, 2.716 for cassia, and 2.807 kWh for orange peel. The overall system efficiency rate was found to be 43%. Kulturel and Tarhan (2016), on the other hand, used 3.4 m^2 x 7 CPCs to power a cylindrical distillation pot with a diameter of 300 mm and a height of 530 mm. The distillation pot was built from a 2 mm thick sheet of 304 stainless steel. To extract 28.2 ml of essential oils from 9.1 kg of peppermint leaves, the system used 3.18 kWh of thermal energy. The total efficiencies were then calculated to be between 27.9 and 34.3 %. Efficiencies for these two Schefler Dish and CPCs can be increased by considering various modifications. In the case of CPC, Kulturel and Tarhan (2016) indicated that automating the various system components would boost the overall performance of the system.

2.12 Concentrating Solar Thermal System Components

2.12.1 Mirrors

Solar mirrors are the most significant part of CST technology because they absorb and reflect solar radiation first. They must have a highly reflective surface in the solar spectrum of 250-2500 nm, which is a widely recognized solar spectrum that solar mirrors can use. With the spectral range of sunlight of 250-2500nm, silver and aluminum have suitable reflective properties. Highly reflective metals like silver or aluminium or metal coatings on substrates are used as solar collectors. Glass, plastics, and polymers can all be used as substrates. The configurations of solar mirrors may be used to identify them (Fernandez-Garcıa *et al.*, 2017). As an example, the solar mirror is classified as second surface form if it has a transparent layer in front, such as glass, methacrylate, or polycarbonate, and the reflective surface is at the back. The reflecting surface is at the front of the solar mirror if it has an opaque substrate, and the solar mirror is referred to as a first reflector. Protective films must be applied to solar mirrors to avoid corrosion and oxidation. Transparent coatings cover first-surface mirrors, while coatings or layers of substrates protect second-surface mirrors from the rear (Fernandez-Garcıa *et al.*, 2017).

(a) Second surface mirrors

Most of the mirrors used in CSP technologies are glass mirrors. They are second surface mirrors since the reflective material is at the back of a glass layer (Fernandez-Garcıa *et al.*, 2017). This section will discuss three different types of second surface mirrors, namely: silvered thick-glass mirrors, silvered thin-glass mirrors and laminated silvered glass mirrors.

Silvered thick-glass mirrors consists of a thick layer of glass of 3 or 4 mm that is coated in front of the silver layer. The silver layer can easily undergo corrosion and other forms of degradations, and therefore, it is further protected on the backside by layers of copper and two or three protective paints. The type of glass used must be clear white or low iron glass. For the silvered thick-glass mirrors to be environmentally free, the lead contents in paints must be low and the copper protective layer replaced by cation-ion based solution. This implies that the new silvered thick-glass mirrors without the elements lead and copper must be able to perform better than silvered thick-glass mirrors with lead and copper as protective layers against the corrosion (Fernandez-Garcıa *et al.*, 2017).

Silvered thin-glass mirrors have the same composition and durability as the silvered thick-glass mirrors but the glass thickness is 1 mm. A 1 mm glass thickness contributes in reducing the weight of the solar collector, hence the silvered thin-glass mirrors are cost effective when compared to the silvered thick-glass mirrors. Due to the thickness being small as opposed to 4 mm thickness, the reflective properties have improved (Fernandez-Garcıa *et al*., 2017). Examples of the use of silvered thin-glass mirrors is found in small PDC, PTCs and secondary concentrators. There are already silvered thin-glass mirrors operating commercially and achieving a solar-weighted hemispherical reflectance of 95.7%. The trend is already headed towards this type of mirrors because of their excellent reflective properties, durability and associated low cost. Prototype designs of silvered thin-glass mirrors with a glass layer of 100 mm ultra-thin, have been tested and found to achieve solar-weighted hemispherical reflectance of 97.7% (Fernandez-Garcıa *et al*., 2017).

Laminated silvered glass mirrors are covered by glass on both sides of the silver layer. The thickness of the mirror is the same as that of silvered thick-glass mirrors. Due to the covering of glass to both sides of the silver layer, the mirror is expected to be durable. The solar-weighted hemispherical reflectance is as high as the silvered thick-glass mirrors because of a thin layer (about 1-2mm) of glass. Laminated silvered glass mirrors are used commercially, though they are expensive than thick glass mirrors (Fernandez-Garcıa *et al*., 2017).

(b) First Surface Mirrors

In first surface mirrors a reflective layer is covered with a very thin layer of transparent coating of less 5 μm to enhance durability (Fernandez-Garcıa *et al*., 2017). The following section is a description of aluminium and polymeric mirrors.

Aluminium reflector consists of a pure aluminium deposited on a polished aluminium substrate with protective layers of aluminium oxide in between and a transparent coating. Other aluminium reflectors are made of organic or anodized aluminium top coatings. Aluminium mirrors can withstand high wind loads and are cheap when compared to glass mirrors. When they are subjected to the environment or air, they develop a passive layer which is used to further protect the aluminium mirror against corrosion. Aluminium mirrors durability reduces significantly when exposed to industrialized polluted areas, however, this can be resolved by putting a glass cover on the aperture plane of the collector. They are less durable than glass

mirrors. They are suitable for medium temperature applications because of their low solar-weighted hemispherical reflectance (Fernandez-Garcıa *et al*., 2017).

Silvered polymer film has several layers of polymers deposited on top of the silver layer, the polymers are sometimes deposited on the back side of the silver. Silvered polymer film are flexible which enables them to be constructed to any shape**.** Research is still underway to improve the durability of the mirrors (Fernandez-Garcıa *et al*., 2017).

2.12.2 Receivers

(a) Receivers tubes for PTCs

PTC receiver tubes are usually made up of two concentric pipes: an outer glass envelope and an inner steel pipe through which an HTF fluid flows. A glass envelope is normally made of low borosilicate glass to increase solar radiation transmittance, while a steel pipe is made of steel and covered with a selective coating with an optically selective surface. The solar absorptance of the optically selective surface is high, while the emittance of thermally produced infrared radiation is low. To increase solar transmittance, the glass envelope is typically coated with anti-reflective material (Zarza-Moya, 2012). Receivers are either evacuated or non-evacuated tubes.

Evacuated tubes contain a vacuum between the steel pipe (absorber) and the glass envelope. The vacuum of 10^{-5} mb, for example in evacuated tube receivers is used to minimize the thermal loss along the receivers. Evacuated tube receivers are expensive and therefore, commonly used where the operating temperatures of the PTC system exceeds 300℃, and where the use of such receivers are justified by a high thermal efficiency and a high thermal output. Evacuated tube receivers can significantly improve performance of the PTC system. For example, in PTC system with receiver length of 150 m, aperture area of 828 m^2, and at a fluid temperature of 375℃, thermal losses can be decreased to 35 kW. A PTC system receiving a beam solar insolation of 925 W/m^2 and at an incidence angle of 15º generates 450 kW at an ambient temperature of 25℃ (Zarza-Moya, 2012). The high optical quality reflectors that are used in large, commercial, high temperature PTCs, together with high degree of accuracy in the assembly process of PTC system components result in high peak optical efficiency in the range of 0.74-0.79. As a result of the excellent optical efficiency and the reduction of thermal losses due to the use of evacuated tube receivers, the overall thermal efficiency of about 70% for an HTF temperature of 375℃ can be achieved. For many high temperature commercial PTC

systems, similar results of high peak optical efficiency and overall thermal efficiency are achieved due to the similar assembly tolerances, high optical reflectors, and evacuated tube receivers (Zarza-Moya, 2012).

Non-evacuated tube receivers are used in industrial process heat applications. PTCs for process heat use non-evacuated tube receivers and polished aluminium metallic reflectors which are of optical quality lower than that of high temperature PTCs and because of that, overall efficiencies are reduced to 0.5-0.65. According to Zarza-Moya (2012), non-evacuating receiver tubes are suitable for operating temperatures below 300°C since thermal losses experienced in non-evacuating tubes are not so critical. Non-evacuating tube receivers are composed of an outer glass envelope and an inner steel pipe which carries an HTF, though there is no vacuum between concentric pipes. The selective coatings that are used for non-evacuating tubes are not as complex as those ones for evacuated tube receivers. They are normally either black nickel or black chrome because they are not expensive. For both evacuating tube and non-evacuating tube receivers, the length of a receiver tube is less than 5 m, this is because of the limitations caused by manufacturing constraints. For non-evacuated receiver tubes, receivers' tubes are connected together by threaded joints, whereas for evacuated tubes, receiver tubes are connected through welding (Zarza-Moya, 2012). A further technical aspect that distinguishes the evacuated tube receivers from the non-evacuated tube receivers is the use of bellows that are found in evacuated tube receivers. Bellows maintain the airtight conditions between the steel pipe and the glass (Pernpeintner, 2017).

(b) Receivers for LFC

Receivers for LFC can be either evacuated tube receivers or absorber tube embedded in a cavity which serves as a secondary reflector (Pernpeintner, 2017). Evacuated tube receivers are not commonly used for LFC systems (Platzer and Hildebrandt, 2012). Cavity receiver serves as a secondary reflector. This receiver is constructed such that, the solar radiations that are not directed to the absorber tube are reflected to the absorber tube, thus increasing the efficiency of the system. Because this absorber tubes are not evacuated receiver tubes, a cover is used to prevent convective heat losses due to winds. The cover is made of glass material (Pernpeintner, 2017). Another use of cavity receivers, also known as trapezoidal receiver, is when multiple tubes are placed below the cavity. It was designed by solar heat and power (SHP) Company. The reason to design this type of a receiver was to eliminate the optical efficiencies losses in the secondary mirrors, but also to reduce the degradation of the mirrors due to high heat loading

on the surfaces of mirrors. The trapezoidal receiver was found to be optically efficient and utilized low cost receiver tubes with small diameters, positioned in a horizontal plane to enhance the efficiency of the trapezoidal receiver (Mills, 2012).

(c) Receivers for point focus systems

Receivers for point focus systems, namely PDC and HFC have high temperature and high concentration ratios than linear systems and causes the production of an absorber to be a complex process. In point focus systems, a loss of 1% is equivalent to a significantly higher loss in energy. For example, a 1% or 0.01 loss in a system that has 600℃ and 1000 concentration ratio will result in energy loss of 10 kW/m^2, requiring a reduction of thermal emittance by 30% in order to break even or compensate for the loss. Similarly, a 1% or 0.01 loss in a system that has 800℃ and 3000 concentration ratio will result in energy loss of 30 kW/m^2, requiring a reduction of thermal emittance by 40%. Practically, only the non-selective absorbers are used for receivers (Platzer and Hildebrandt, 2012). Two treatments exist for point focus systems, either the receiver is painted black or it is uncoated. For uncoated receivers, the receivers are subjected to an oxidation layer when exposed to the atmosphere, however, this oxidation layer is advantageous as it has good absorptive characteristics which further enhances absorption of solar radiation. In many applications, once this thin, passive layer has covered the receiver, there is no any need for further treatment of the receiver surface in order to increase its absorptive characteristics (Pernpeintner, 2017).

2.12.3 Thermal energy storage

Since sunlight is not available at night or on cloudy days, it is important to maintain a steady supply of energy even when the weather is not optimal. One of the options is solar thermal energy storage (TES). TES is used in CSP systems to provide energy at night or on cloudy days. HTFs and storage materials are used in TES systems. Direct or indirect TES systems are available. The HTF used to transfer energy from the solar collector field is used to store heat in tanks in direct systems. The need for a second HTF for storage, as well as a heat exchanger between the storage tank and the HTF, is removed in direct systems. A heat exchanger binds the TES system to the HTF in indirect systems. The indirect method, in which a thermal oil such as Therminol is used as an HTF and isolated from the TES by a heat exchanger, is the most common technique in PTC systems (Batuecas *et al*., 2017). In PTCs, where synthetic oil is used as an HTF, the use of a molten-salt two-tank indirect system is popular. Molten salt is

used to store energy in 80% of TES systems (Fernandez-Garcıa *et al*.,2019). Sensible heat thermal energy storage (SHTES) and latent heat thermal energy storage (LHTES) are two types of TES systems.

(a) SHTES system

SHTES system is a well-established technology that is currently being used in CSP. Thermal oils, earth materials (i.e. rocks), metals, salts, and water are widely used for sensible heat thermal energy storage (SHTES). Low melting points, a broad operating temperature range, high thermal conductivity, thermal stability, low vapour pressures, and corrosion resistance are all desirable properties for SHTES (Batuecas *et al*., 2017). With the exception of liquid metals and thermal oils, sensible heat storage materials are inexpensive. The main drawback of sensible heat storage materials is their low temperature stability during discharge. During the discharge process, the HTF's outlet temperature steadily decreases (Alva *et al*., 2018). The most commonly used sensible TES materials are thermal oils or synthetic oils.

(b) LHTES system

LHTES system is still at a research and development stage. The main reason why the research and development has not yet been popularized is the current challenges associated with encapsulating of phase change materials (PCM) and enhancing the heat transfer process (Xu *et al*., 2015). PCMs store heat in the form of latent heat during a constant temperature process like phase change. Usually solid to liquid phase change is used. Solid to solid phase changes are also applicable but the latent heat stored is small. However, the advantages of solid to solid phase change is no leakages are found and there is no need for encapsulation (Alva *et al*., 2018). The TES system using PCMs involves two processes. One is the charging process, whereby the TES system absorbs energy from an HTF and stores it. Another one is the discharge process, whereby the solar field is by-passed, and the TES system is allowed to discharge energy into the Rankine Cycle, thereby producing energy at night or in cloudy days (Qiu *et al*., 2019).

Another challenge as mentioned earlier, is enhancing heat transfer of TES materials. One of the ways of enhancing the heat transfer properties of TES materials is adding nanoparticles or nanofluids to molten salts. Nanofluids are applied by dispersing nanoparticles of smaller than 100 nm to HTFs. The primary objective of nanoparticles is to enhance both the thermal conductivity and specific heat capacity while minimizing the viscosity of the HTF fluids.

Molten salts show positive response to the addition of nanoparticles, they are appropriate materials for this enhancement method. Theoretically, conventional CSP can attain about 10% more in efficiency when solar concentration ratio is in the range of 10-1000 (Nagarajan *et al*., 2014). While there is a positivity in using nanoparticles, there are also challenges faced with application of nanoparticles. That includes corrosion, erosion, etc. (Fernandez *et al*., 2019), however, research and development is in progress so that nanoparticles can be applied in CSP technology.

2.12.4 Chemical storage

Another option under consideration is the energy storage via chemical storage, which uses a reversible chemical reaction to store and release energy. The enthalpy change during a reversible chemical reaction is used in this process. While a chemical reaction is endothermic, energy is retained, and when it is exothermic, energy is released. Reactants are stored separately during energy storage, but reactants are recombined during energy release. Ammonia-based chemical storage was investigated by the Solar Thermal Group in Australia, where a receiver generated 15 kW with the use of a PDC sytem. For improving the ammonia-based chemical reaction, pressures of up to 30 MPa have been suggested. At 10 MPa, a storage capacity of 40 MWth/m^3 is reached. Chemical storage is still in its early stages of production, so there are no any pilot demonstrations yet. However, there are currently research groups working on a chemical storage system (Steinmann, 2012).

2.13 Heat Transfer Fluids

Thermal oils, particularly synthetic oils and molten salt are commonly used as HTFs in PTC systems (Mohammadi *et al*., 2019). Thermal oils are a mixture of diphenyl and diphenyl oxide. They are organic fluids which possesses good heat transfer properties. Examples of thermal oils are Therminol VP-1, Dowtherm, and so on. Thermal oils are currently expensive, and high care is needed when handling them. Leaks of thermal oil will degrade the environment, moreover they cause a fire hazard when the oil is vaporized and contacted with air (Alva *et al*., 2018). The fire hazard for thermal oils is below the CSP system operational temperatures (Batuecas *et al*., 2017). When thermal oils are at temperature above the operating range, the degradation process of oils start, thus causing acids which may initiate corrosion which will eventually damage pipes and tanks. The advantage of thermal oils over molten salts is that their melting points is very low (less than 12°C), which implies that, they will not freeze, hence there is no

need for any antifreeze mechanism. Their maximum operating temperature is 400℃ and they are mostly used in PTCs (Alva *et al*., 2018).

For application in systems, which require more than 400℃, Molten salts are required. Molten salts are characterized by high boiling point, high volumetric heat capacity and high thermal stability. The maximum operating temperature limit for molten salts is about 565℃. As compared to thermal oils, molten salts are cheap, non-toxic, non-flammable and can easily be accessed. Due to their high melting point of more than 200℃, freezing takes place when there is no solar energy at night. Desirable conditions are that the melting point must be close to the ambient temperature and the boiling point must be high to promote a high operating range. The advantage of molten salts is that they can be used as both an HTF and energy storage (Alva *et al*., 2018).

2.14 Solar Tracking

To maximise energy yield and efficiency, concentrating solar collectors are installed with tracking devices to follow the sun. There are two methods of tracking, namely: one axis tracking and double axis tracking. Trackers can either be mechanical or electric-electronic devices. Electrical-electronic devices are more accurate (Baronea *et al*., 2019). In single axis tracking, concentrating solar collectors are either aligned to a North-South direction and the sun is tracked from east to west or aligned to East-West direction and the sun is tracked from North to South. The North-South orientation has a best collector optical efficiency, thereby resulting in a more energy produced in a year (Baronea *et al*., 2019). For North-South orientation, the PTCs experience the highest incidence angle (cosine losses) at noon and the lowest in the mornings and evenings. The North-South orientation has a higher energy production in summer and less energy in winter (Kalogirou, 2014). The East-West orientation experiences high cosine losses in the mornings and because of that, the collector performance becomes reduced. The advantage of using the East-West Orientation is that during the day, little collector adjustment is required and the collector's full aperture area faces the sun at noon. During winter, more energy is produced by the East-West Orientation. The selection of the orientation of the solar collector depends on the application of the solar system. The specific time (summer or winter) when the most energy is needed for a particular application is important in selecting an orientation (Baronea *et al*., 2019). Double axis tracking systems track the sun in both axis, and thus more efficient but that comes with a high cost (Baronea *et al*., 2019). This tracking system is commonly used in PDC and HFC.

2.15 Solar Thermal Steam Generating Systems

Three concepts of solar steam generation for IPH exists, namely: steam flash concept, direct steam generation and unfired boiler concept. All of them are associated with advantages and disadvantages.

2.15.1 Steam flash concept

This method is an indirect process where water from the flash vessel is pressurized and circulated through the solar collector (see Figure 2.5). The heated water can reach temperatures between 180 and 200℃. The circulating pump is used to pressurize the system and maintains the required pressure in order to prevent boiling of water in the collectors and pipe network of the solar system (Fernandez-Garcıa *et al*., 2010). Some of the pressure supplied by the circulating pump is lost on the flash valve (Kalogirou, 2004). The circulating pump is also used to recirculate the sub-cooled water. Part of the heated water turns into steam when it enters the flash vessel, this happens because of the change in pressure inside the flash vessel. Flashing is in the range of 4 to 6%. The steam exits through the steam mains and is directed to industrial process. The remaining water is circulated through the solar collector. Storage water tank feeds the solar steam generating system with make-up water (Fernandez-Garcıa *et al*., 2010).

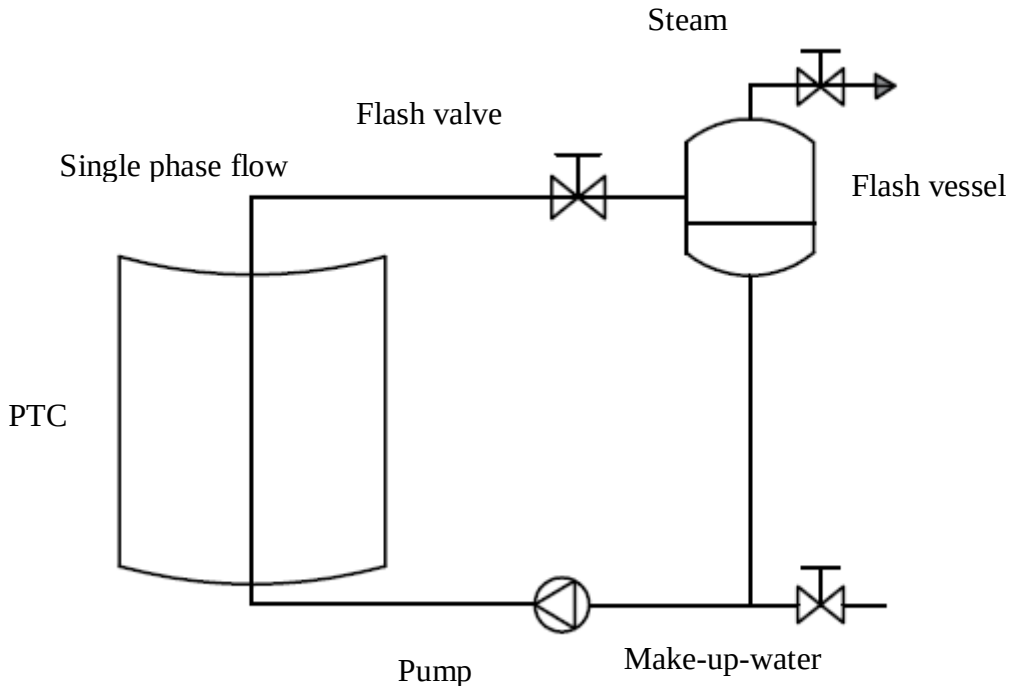


Figure 2.5 Schematic diagram of a flash boiler steam generation concept (Modified from Kalogirou, 2004)

2.15.2 Direct steam generation (DSG)

This method is a direct process, where water is partially or completely boiled in the solar collector (See Figure 2.6). There are two types of direct steam generation systems. The first type is designed in such a way that feed water is added to the steam drum or mixed with the recirculated water at a rate that is controlled by a level controller in the drum. Water is passed through a steam drum where the separation between steam and water takes place. In the second type, feed water is added directly to the solar collector inlet (Fernandez-Garcıa *et al.*, 2010). The disadvantage of using DSG is that even with good, treated feed water, scaling on the receiver tube is inevitable. Capital costs for both DSG and steam flash steam generating systems are approximately the same (Kalogirou, 2004).

.

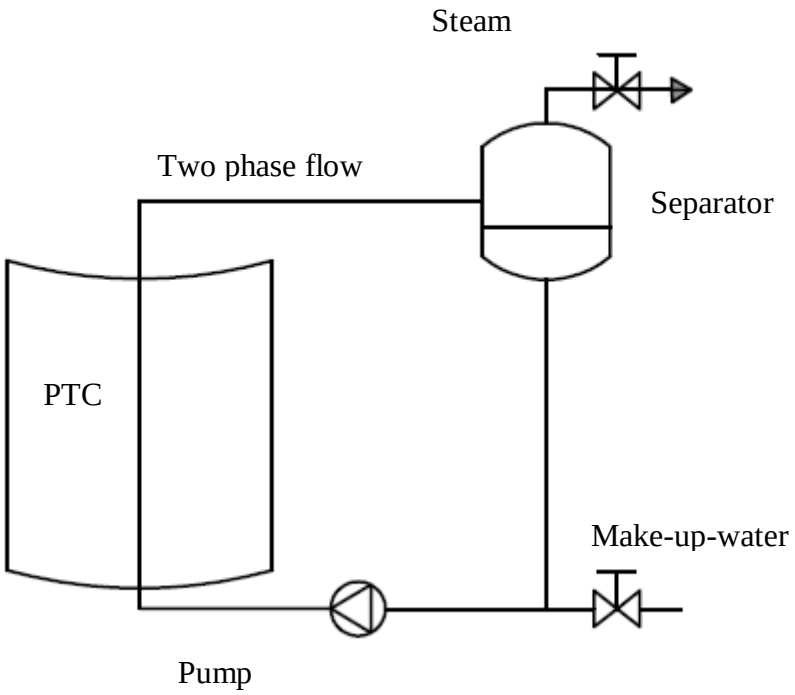


Figure 2.6. Schematic diagram of a direct steam generation concept (Modified from Kalogirou, 2004)

2.15.3 Unfired boiler concept

In this method, there is a heat transport loop, which transport the heated HTF from the collector to an unfired boiler or heat exchanger (Refer to Figure 2.7). An HTF is recirculated to the collectors by a circulating pump. In this boiler or heat exchanger, an HTF transfers heat required to feed water, which in turn, converts into saturated or superheated steam at the required pressure and temperature. An HTF that is often used is thermal oil (Fernandez-Garcıa *et al*., 2010).

Unfired steam generating systems operate at low pressure and the system is simple to operate. HTFs should be non-freezing and non-corrosive. These characteristics of an HTF have made the system to gain more popularity over the DSG systems, and they are the main reasons for the common use of heat transfer oil systems in current industrial steam-generating solar systems. The major disadvantage of using heat transfer oil systems lie in the characteristics of an HTF. The fluids are difficult to handle, and most of them are flammable. HTFs are decomposed when they are exposed to air, and due to that, ignition-point temperatures can be lower, and leakages can cause fire in other types of insulation even at temperatures that are

largely lower than the measured auto-ignition temperatures of the thermal oil. HTFs are relatively costly and have a potential to pollute the environment and this renders them inappropriate for the food industry (Kalogirou, 2004).

When compared to water, HTFs have low heat transfer characteristics. They are characterized by more viscosity at ambient temperatures, lower density, lower specific heat capacities and lower thermal conductivities as compared to water. This implies that to obtain the same quantity of energy transferred by solar steam generating systems using water, the higher flow rates, higher collector differential temperatures, and higher pumping power are required. Moreover, heat transfer coefficients are lower, thus causing a larger temperature differential between the receiver tube and an HTF. Higher temperatures are a necessity to attain cost effective heat exchange process and this results in reduced collector efficiency (Kalogirou, 2004).

.

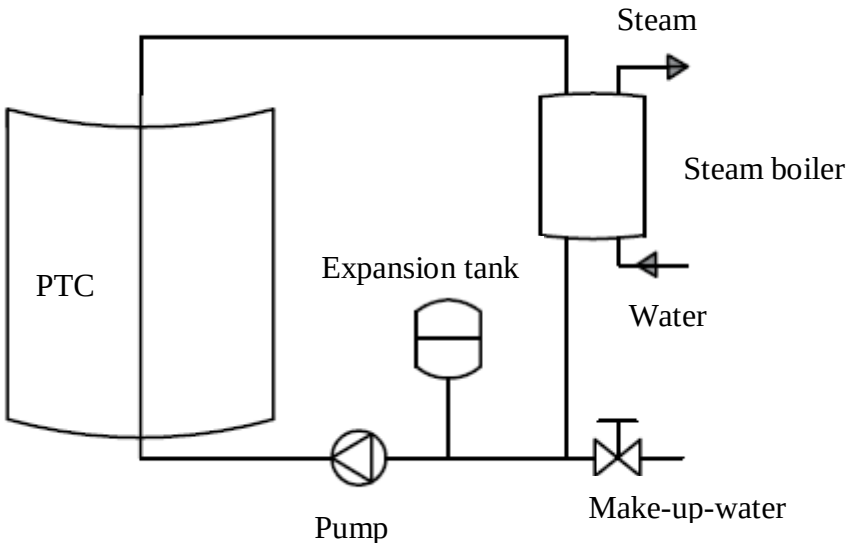


Figure 2.7. Schematic Diagram of an Unfired Boiler Concept (Modified from Kalogirou, 2004)

2.16 South African Solar Resource

All CST technologies concentrate sunlight. The DNI component is relevant as optical concentration cannot be achieved based on diffuse light coming from various directions. Diffuse light or global horizontal insolation (GHI) operates differently; it includes both the direct insolation and the diffuse insolation. GHI is appropriate for the assessment of energy

yields for non-concentrating technologies. For example, GHI can be used for the estimation of energy yield for PV systems, while DNI is applied for estimation of energy yields for CST technologies (Meyer *et al*., 2012). This section will be focused on DNI in Africa, and particularly in South Africa.

Africa is one of the continents that have countries with the highest solar potential (Refer to Figure 2.8). Total theoretical potentials in the whole of Africa are estimated at around 470 Petawatt hours (PWh) for CST Technology (Hermann *et al*., 2014). DNI is usually the highest in the countries which lie in the regions between 40 degrees north and south of the equator. These bands on both sides of the equator are also called the 'sunbelts'. This region includes the Middle East, North Africa, South Africa, India, the Southwest of the United States, Mexico, Peru, Chile, Western China, Australia, southern Europe and Turkey, but not limited to these countries (International Renewable Energy Agency and The Energy Technology Systems Analysis Programme, 2013). The global distribution of GHI (Top) and DNI (Bottom) are shown on Figure 2.8. Countries which have the highest CST potential in Africa are Algeria, Egypt, Namibia, South Africa, Sudan and Tanzania (Hermann *et al*., 2014).

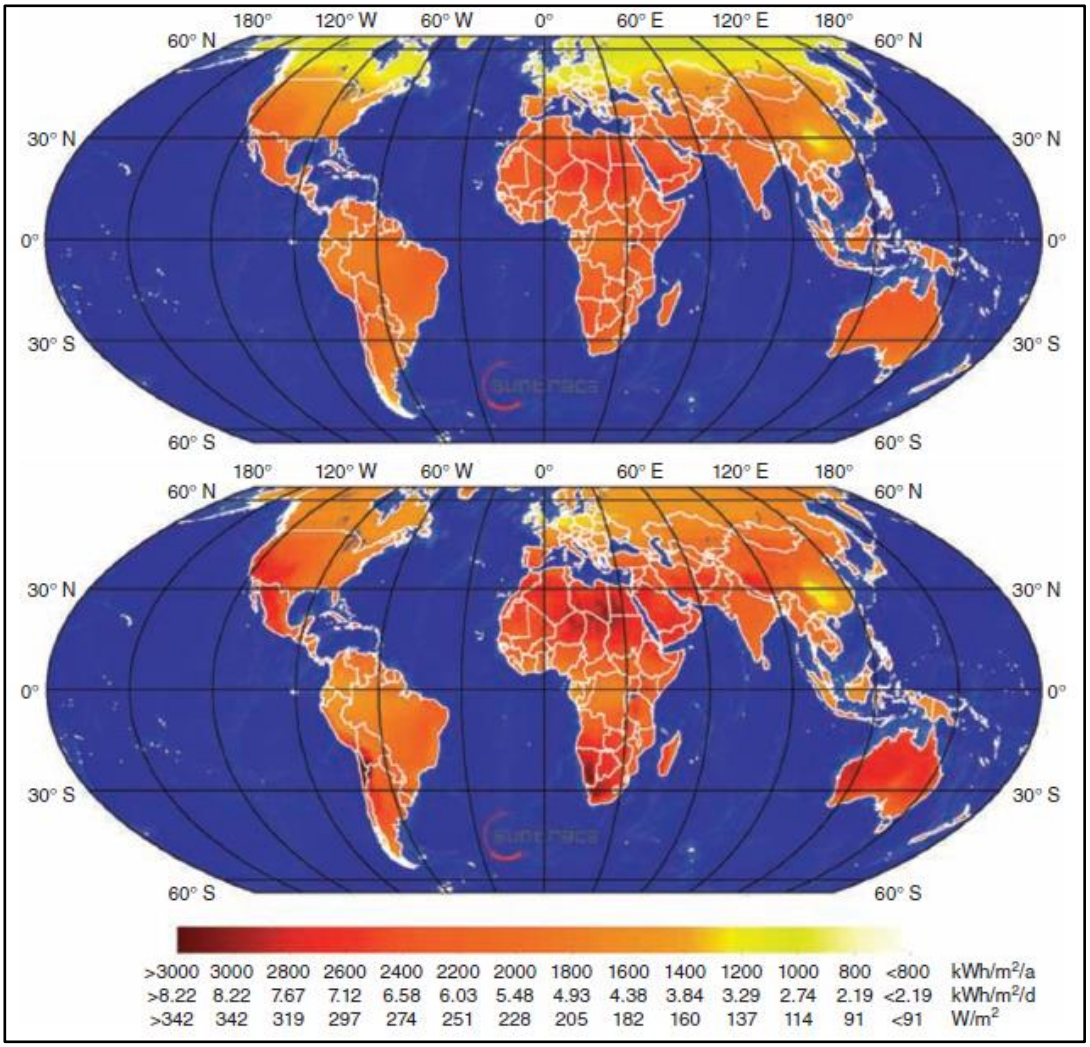


Figure 2.8 Global distribution of GHI(Top) and DNI(Bottom)(Meyer *et al*., 2012

South Africa is privileged to be one of the 5 countries in the whole continent of Africa to have the highest annual sunshine hours and has an average of more than 2,500 hours of sunshine a year, making it more suitable for harnessing solar energy for different applications. Solar-radiation levels range between 4.5 and 6.5kWh/m^2 in one day (South Africa. Department of Energy, 2009). Figure 2.9 shows a solar resource map for South Africa. South Africa is located between latitude 22 to 35 S, and longitude 17 to 33 E. It can clearly be seen on the map that most areas receive a high DNI, thus creating an enabling environment for decentralized renewable energy systems.

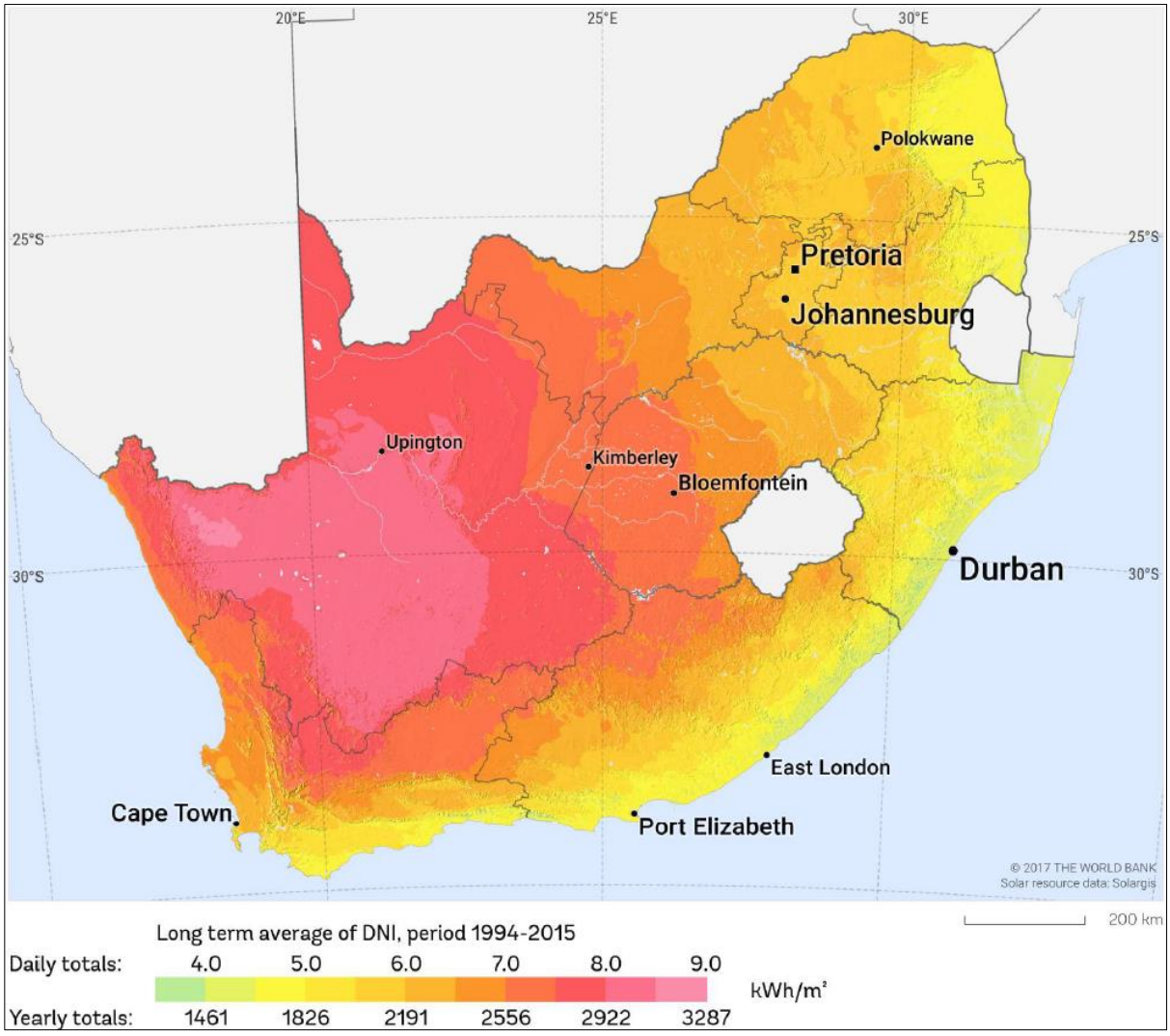


Figure 2.9. Long term average DNI for South Africa (Solargis, 2017)

The following information on table 2.3 shows the amount of area across different suitability classes, whereas Table 2.4 shows suitability classes for categorizing areas with CST and CSP potential.

Table 2.3. Sizes of areas with CSP potential in South Africa (Modified from Hermann *et al*., 2014)

Country	**Total area**	**Exclusion area**	**CSP (Potential categories)-Associated areas Direct Normal Insolation (kWh/m^2/year)**			
			1800	1800-2000	2000-2500	2500-3000
	[km^2]	[km^2]	[km^2]	[km^2]	[km^2]	[km^2]
South Africa	1220394	202816	13530	171651	517904	314494

Table 2.4. Suitability classes (Modified from Hermann *et al*., 2014)

	Limited Suitability	**Suitable**	**Highly Suitable**	**Excellent**
Concentrating Solar Power	below 1800 kWh/ m^2 /year (DNI)	1800 – 2000 kWh/ m^2 /year(DNI)	2000 – 2500 kWh/ m^2 /year(DNI)	2500 – 3000 kWh/m^2 /year (DNI)

According to Table 2.1, the following applies: (1) An area of 13530 Km^2 in South Africa receives 1800 kWh/ m^2, this places this area under limited suitability; (2) An area of 171651 Km^2 receives a DNI from 1800-2000 kWh/ m^2 /year, implying that the area is suitable for CSP/CST; (3)An area of 517904 Km^2 receives a DNI of 2000-2500 kWh/ m^2, which implies the area is highly suitable for CSP/CST, (4) An area of 314494 Km^2 is the biggest of all 4 areas, and it also receives the highest DNI, it is classified as an area with excellent capabilities for CSP/CST. From the map it is shown that most areas are covered by DNI ranging from 1800 to 3287 kWh/ m^2 /year, making South Africa generally suitable for CSP or solar thermal technologies. It is important to mention that although 1800 kWh/ m^2 is categorized as limited suitability, it still has a potential for CST technologies.

2.17 Conclusions

In the literature review, the project topic has been considered both in a broader context and in a specific context. This literature survey has showed that the world is shifting toward renewable energy in order to minimize carbon dioxide emissions and provide clean energy to an increasing population. In addition to this global effort to shift to renewable energy, there are researchers working on designing energy efficient technologies that are aimed at decreasing the contribution of industry to non-sustainable development. However, some of these technologies are still at laboratory scale or developmental stage, while others have found it difficult to transition to industrial scale and even if they do, they become expensive. On the other hand, continued use of conventional energy sources have not shown to be sustainable because of their high cost and environmental impact.

Solar energy is an alternative promising renewable energy source that helps to reduce carbon emissions while also providing energy in a sustainable manner. There are numerous solar technologies available, some of which are not yet mature, while others are. Despite the fact that South Africa has adequate solar radiation, South Africa has fewer projects on CST and those that are existent are mostly for large-scale power production. PTC is a mature solar thermal technology that is not widely used in small-scale applications, although it has a great potential in meeting the energy requirements for industrial processes requiring medium temperatures. Small-scale solar energy applications are critical, particularly for agro-based processes that require thermal energy in medium temperature range.

Steam distillation of essential oils is one of the agro-based processes, however, only a few studies using CPC and PDC for essential oil steam distillation, have been conducted. It is important to remember that these two CST technologies are not yet established technologies, making them difficult to suggest to a customer who is simply interested in seeing the technology in action and making profit. PTCs, unlike CPC and PDC, have a long history of successful operation and are considered the safest technology. While several small PTCs have been produced, they are rarely used in essential oil steam distillation processes. Although the use of large commercial PTCs has a lot of technological credibility, combining a small PTC with the essential oil steam distillation method requires a lot of caution, hence a need to focus research on CST technologies and industrial operations.

The use of PTC in combination with the most popular and favoured method of essential oil extraction, steam distillation, poses challenging questions that can only be addressed through research. Such concerns include whether PTCs can be combined with the essential oil steam distillation process, and if so, whether the energy gains and losses are sufficient to justify recommending the system to potential stakeholders, and whether the system is competitive when compared to traditional energy generation methods. The overall efficiency of the PTC system is crucial in proving the utility of solar energy in critical oil steam distillation or other agro-based processes. As a result, this project will examine the overall output as well as the factors/parameters that have direct influence on the performance of the system.

CHAPTER 3: MATERIALS AND METHODS

The experiments were divided into two parts; the first part consisted of laboratory experiments using a steam distillation glassware, while the second part consisted of field experiments. The first part was a steam distillation of orange, lemon and mandarin peels. The second part was also a steam distillation of orange, lemon and mandarin peels, but the apparatus used was a gas-powered steam distillation and a PTC-powered steam distillation unit. Both field steam distillation experiments used the same distillation tank and condenser, with the source of power being the only main difference. This chapter presents an experimental procedure for all the experiments and the description of apparatus used.

3.1 Laboratory Steam Distillation of essential oils

3.1.1 Description of steam distillation laboratory apparatus

Figure 3.1 shows a schematic diagram of essential oil steam distillation. In steam distillation, water is heated to a boiling point by a heating a mantle, releasing steam in the flask, as shown in the diagram. The steam that is produced rises in a column that contains the more or less finely ground plant. The steam leaves the extraction vessel and moves to the spiral condenser, where it is cooled to room temperature. The cooled liquid, which includes both oil and hydrosol, is guided to a separation funnel. The essential oil and hydrosol are divided in layers within the separation funnel, with the essential oil on top and the hydrosol on the bottom. The immiscibility of oil and water at room temperature is used to distinguish the two liquids. The essential oil is left behind after the hydrosol layer is drained from the bottom of the separation funnel by opening the valve.

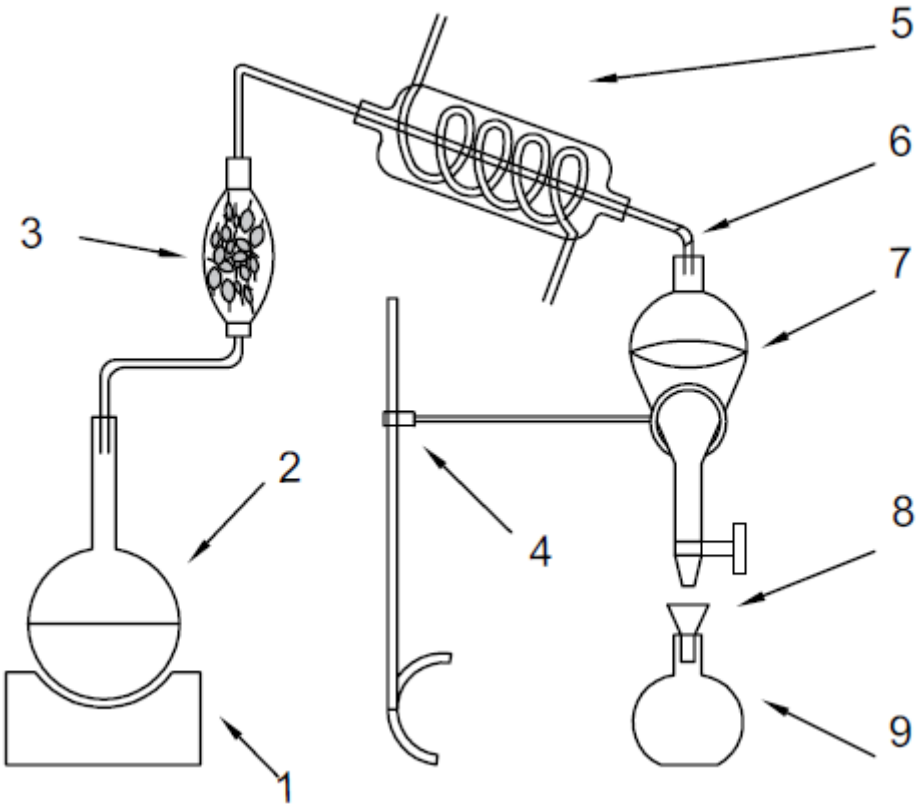


Figure 3.1. Glassware Apparatus: (1) heating mantle, (2) flask, (3) extraction vessel, (4) stand and clamp, (5) spiral condenser, (6) adaptor, (7) separation funnel (8) funnel, (9) florentine (Modified from Shakir and Salih, 2015)

As explained earlier in previous sections of chapter 2, various forms of energy can be supplied to generate steam. In laboratory experiments, instead of using a heating mantle powered by electricity, a 2.75 kW portable gas stove was used to provide heat to a one-litre flask carrying water meant for steam generation. Figure 3.2, 3.3, and 3.4 shows an actual laboratory steam distillation set-up, essential oil harvested in a separation funnel and bottled essential oils in amber vials.

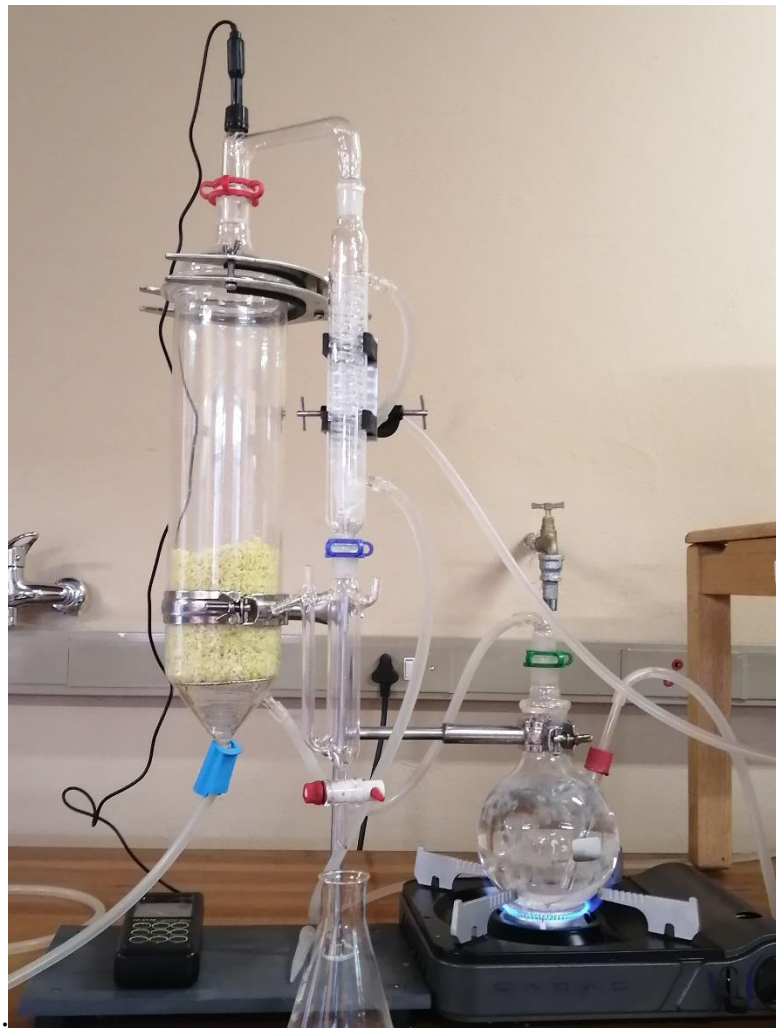


Figure 3.2. Laboratory steam distillation system glassware



Figure 3.3. Essential oil separation



Figure 3.4. Collected essential oil

3.1.2 Laboratory methodological approach used for steam distillation

The steam distillation glassware was assembled and made ready for steam distillation of citrus fruit peels. The distillation process was powered from a portable gas burner stove with a nominal heat input of 2.75 kW and a nominal butane gas consumption of 200 g/h. For the purpose of measuring the amount of heat used for every experiment, the weight of gas cartridge before and after an experiment was measured. Citrus fruits, namely orange, lemon and mandarin were sourced from the local market (Tshwane Fresh Produce Market). The peels of these fruits were then peeled from the fruits and a blender was used to cut them into pieces of 2 to 5 mm. The total mass of the peels was measured before and after distillation. The samples of prepared citrus peels were dried in the oven for 24 hours at 105℃, after which, the moisture content in percentage wet basis (%wb) was determined. In order to start an experiment, the distillation still or extraction vessel was charged with a known mass of ground citrus peels. The heat from the stove was introduced by turning on the ignition control knob. A total of 27 experiments were conducted, with each citrus peels experiment repeated 3 times at 250, 300 and 350 g. The heating time was measured from the time the distillation started to the time when the experiment is stopped, the distillation temperature was also recorded. After time of extraction, depending on how much time each experiment takes to extract, the quantity of hydrosol, reflux and the water remaining in the boiling flask were measured. The quantity of essential oil was measured, and the essential oil's yield calculated as the ratio of the quantity of oil measured to a quantity of peels (plant material) extracted. The oil was stored in an amber essential oils vial at 4 ℃. The Gas Chromatography was used to analyse the oil.

3.2 Gas-powered Essential Oil Steam Distillation

3.2.1 Description of gas-powered essential oil steam distillation

Figure 3.5 shows a schematic diagram of a gas-powered essential oil steam distillation.

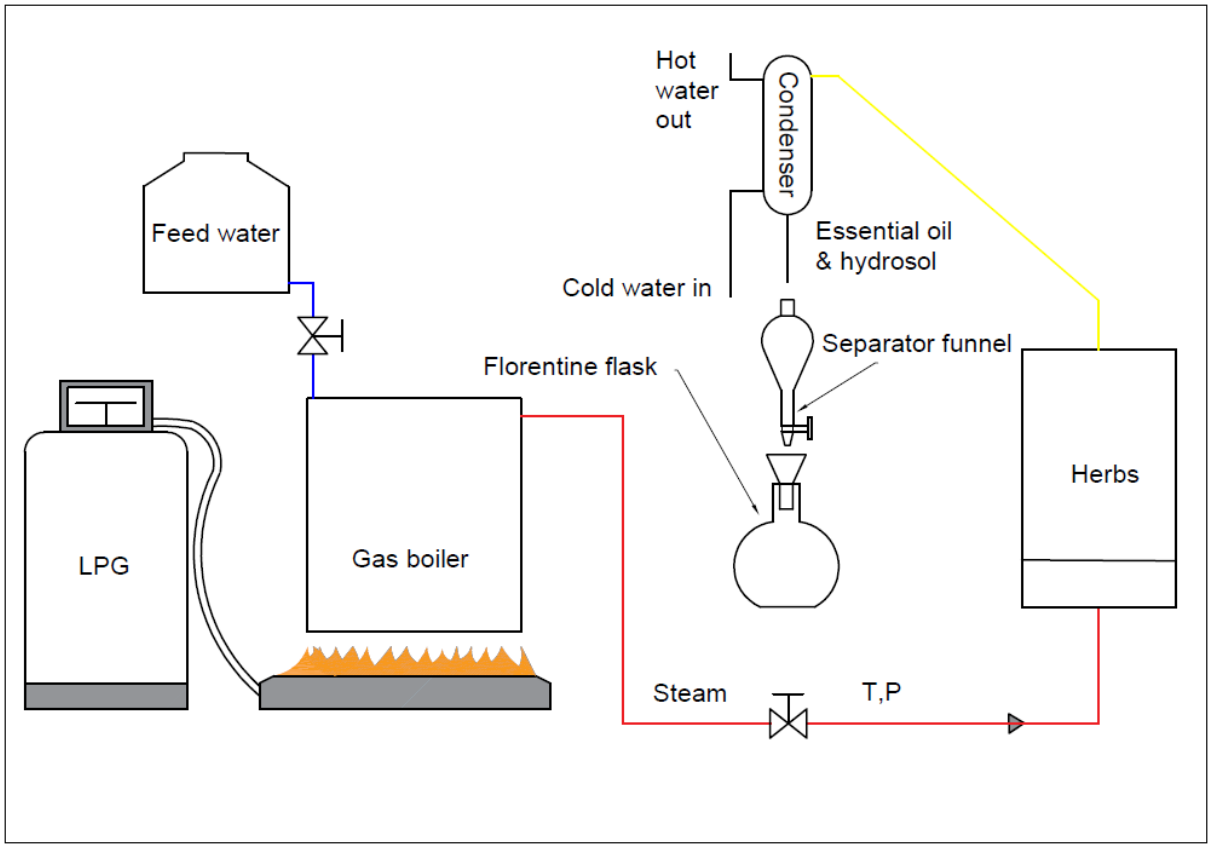


Figure 3.5. LPG-powered essential oil steam distillation unit

Figure 3.6 shows the actual picture of a set-up for steam distillation.



Figure 3.6. Gas-powered essential oil steam distillation unit in operation

3.2.2 Methodological approach used for gas-powered essential oil steam distillation unit

A gas-powered boiler was used as a source of steam for a distillation process. The feed water valve was opened and the boiler was filled to the recommended volume of water before the valve was closed. The gas boiler's burner was connected to a 19 kg LPG cylinder with a gas mixture of propane and butane on a mix ratio of 60:40. The distillation tank's steam inlet pipe from the steam distillation unit was connected to a steam supply pipe from the gas-powered boiler. The condenser, was connected to a water source at ambient temperature for cooling the

vapour. Citrus fruits, namely orange, lemon and mandarin were sourced from the local market (Tshwane Fresh Produce Market). The peels of these fruits were then peeled from the fruits and a blender was used to cut them into pieces of 2 to 5 mm. The total mass of the peels was measured before and after distillation. The samples of prepared citrus peels were dried in the oven for 24 hours at 105℃, after which, the moisture content in wet basis was determined. In order to start an experiment, the distillation tank was charged with 1.3 kg of citrus peels and each citrus peels experiment was repeated at least 3 times to determine mean values. The gas-powered boiler was turned on, by igniting the burner. The heating time was measured from the time the distillation started to the time when the experiment is stopped, both the inlet and outlet distillation temperatures on the distillation tank were recorded. After time of extraction, the quantity of hydrosol and essential oil were measured, and the essential oil's yield calculated as the ratio of the quantity of oil measured to a quantity of peels (plant material) distilled. The oil was also stored in an amber essential oils vial at 4 ℃. The Gas Chromatography was used to analyse the oil.

3.3 Selection of the Concentrating Solar Thermal Technology for Steam Distillation of Essential Oils

The central focus of this research is to have an effective decentralized solar power supply for essential oil distillation processes. FPC and ETC systems with maximum temperatures of below 100^{o}C are predominantly used for heating water, buildings and swimming pools. There are technological advancements developed to increase the temperature of FPC and ETC. They include (1) multiple glazing for FPC (up to 110℃), (2) transparent insulation material, and the use of inert gas or an ultra-high vacuum for FPC (up to 150℃), and (3) the use of solar tracking of FPC and ETC (International Renewable Energy Agency and The Energy Technology Systems Analysis Programme, 2015). New developments of selective coatings have enabled FPCs to reach stagnation temperatures of 200℃, but even with these high temperatures reached, better efficiencies can only be achieved at temperatures below 100℃ (Kalogirou, 2003). The challenges faced with these systems is their inability to operate at high temperature as their efficiency becomes compromised, moreover the space requirement also becomes a problem. Different CST technologies are available and that can operate efficiently at higher temperature. Such examples of CST technologies are HFC and PDC, LFC, and PTC. However, not all these CST technologies can be used for industrial process heat (Kalogirou, 2003). For example, HFC and PDC reach high temperatures that are undesirable for IPH. Moreover, the use of such high

temperature systems will not justify the high capital costs associated with this high temperature CST technology. However, many efforts have been made by researchers to modify Parabolic dish collector to suit for the needs of IPH but such a system may not be suitable for either distillation or cooking as it requires a frequent change of focus position (Munir, 2010).

The problems presented earlier can easily be solved by using PTC. PTCs are predominantly employed for IPH where steam is required (Kalogirou, 2004). Small sized parabolic trough can be used to generate saturated steam at medium temperatures (Kalogirou, 2003 and Kalogirou, 2014). The advantages of PTCs over the traditional solar collectors used in domestic water heating and other water heating facilities are their ability to operate at (1) lower thermal losses, (2) higher efficiency while at higher working temperatures, (3) smaller collector surface, and no risk of dangerous stagnation temperatures, because the solar collector can be defocused (Fernandez-Garcia *et al*., 2010). Moreover, PTCs are the most mature technology as over the years, more technical credibility has been gained. Components of the PTC system are also available in the market and the structural part of the PTC can easily be built on site or in the local workshops. For this project and after considerations of various options for IPH, PTC was selected (Refer to APPENDIX B.1 and C.1 for preliminary calculations and solar resource assessment used for selecting a right size of PTC). The selection of a CST system was also based on the fact that; the place where the system was constructed, receives a sufficient long term average DNI of 2138 kWh/m^2. According to suitability classes used by Hermann *et al*. (2014), to determine if an area or region is suitable for CST technology or not, the selected area (of geographical coordinates: -25.729533°, 28.276100° (-25°43'46", 28°16'34") for installation of PTC, falls under 'highly suitable' category (see Table 2.4 of Chapter 2) , implying that the deployment of a CST project in the area will be successful in terms of thermal energy output. For ease of use, particularly for a farmer who may not have an in-depth knowledge of steam production, an unfired steam solar steam generating concept was selected.

3.4 PTC-Powered Essential Oil Steam Distillation

3.4.1 Description of PTC-powered essential oil steam distillation

Figure 3.7 below is a schematic diagram of the PTC-powered essential oil steam distillation.

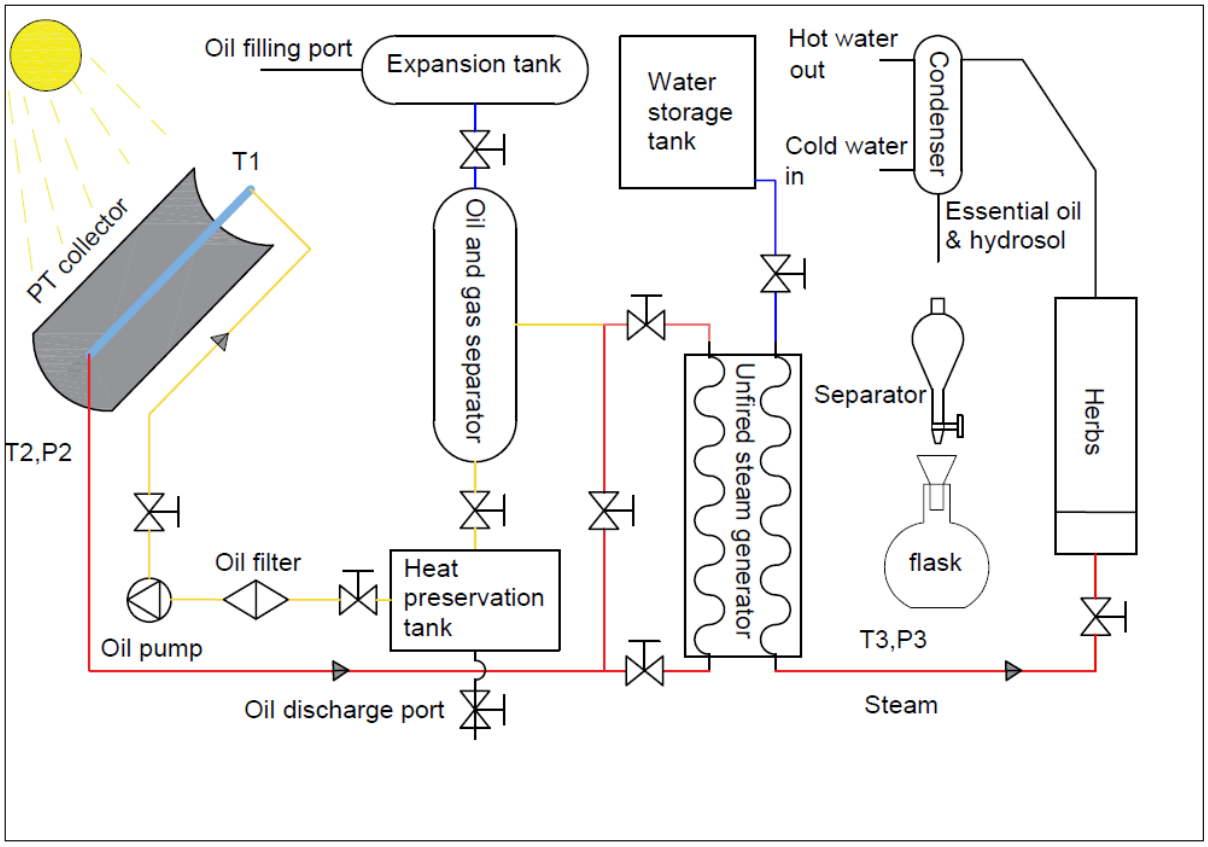


Figure 3.7. Schematic diagram of the PTC-powered essential oil steam distillation

Various functions of the system components are summarized below:

1. 15.3 m^2 parabolic trough collector: transforms solar energy to thermal energy.
2. Receiver tube: absorbs solar energy reflected from the PTC.
3. Tracking and drive device: continually tracks and positions the PTC to the Sun's direct position.
4. Steam generator: used to generates steam and feed to the distillation tank.
5. Distillation tank: essential oil plant material is charged into the tank for steam distillation.
6. Condenser: condenses the vapour mixture of oil and water into a separation funnel.
7. Separation funnel: used to separate essential oils and hydrosol.
8. Florentine flask: collects hydrosol.

9. Expansion tank: A tank through which an HTF can expand into at operating conditions, it prevents HTF from damaging pumps, and seals.
10. Heat Preservation tank: stores thermal energy.
11. Water storage tank: stores cold purified or softened water to be delivered to the steam generator.

The following sections further expands in details on the selected system components.

3.4.2 Parabolic trough collector

PTC consists of plastic sprayed galvanized steel frame, which supports the mirrors in a parabola shape as shown in Figure 3.8. Square shape torque tube of 6 m has attachments which are used to mount the mirrors on a parabolic shape. The torque tube derives its motion directly from a slew drive, which is connected directly to a planetary reducer motor. Mirrors are made of a 1 mm silver tempered glass covering a layer of high reflective silver coating. The silver coating is protected by copper and two or three protective paints underneath. The mirrors have a solar weighted specular reflectance of more than 92% and an aperture width of 2.55 m. These mirrors fall within the category of silvered thin-glass mirrors discussed in section 2.12.



Figure 3.8. Parabolic trough (PT20) installed at ARC-AE premises

Table 3.1 shows some of the important parameters of the PTC.

Table 3.1. Parameters of the selected parabolic trough Collector (PT-20)

Parameters of the PT-20 collector	
Parameter	Value/type
Collector rim angle	67,6℃
Reflective surface	4 mm Silvered tempered glass
Receiver material	Stainless Steel 304
Collector aperture area	15,3 m^2
Receiver surface treatment	-
Glass envelope diameter	90 mm
Glass envelope transmittance	≥ 0,93
Absorber outside diameter	40 mm
Absorbance	0,95
Absorber Emittance	≤ 10%
Tracking mechanism accuracy	≤ 0,2^o
Collection orientation	Axis in N-S direction
Mode of tracking	E-W horizontal

3.4.3 Heat collecting element (Receiver tube)

The receiver consists of an inner metal tube (absorber) which is made of a Stainless Steel 304, and an outer glass tube, which is made of borosilicate glass. The absorber is coated with selective coating. The receiver is evacuated tube type with a vacuum degree of 3.0 x 10^{-4} Pa (at 200℃).

3.4.4 Single axis tracking system

PTC consists of a single axis tracking system, which consists of a 30 W, 24 V direct current (DC) motor that transmits torque to a torque tube, which in turn allows the tracking motion of the solar collector. The motor is a planetary reducer motor of gear ratio 782.4:1, it delivers a current of less than 1.25 Ampere(A) at a rated output speed and torque of 1.2 RPM (revolution

per minute) and 45 N.m(Newton meter), respectively. In order to reduce the speed of the planetary reducer motor, the DC motor speed is reduced through a slew drive at a worm gear ratio of 73:1. The slew drive has rated output speed and torque of 0.016 rpm and 985.5 N.m, respectively and can support maximum radial and axial loads of 53 and 133 KN, respectively. The slew drive facilitates tracking at a precision of 0.2 º. Mirrors are placed on a North-South orientation. The North-South orientation was selected based on its best collector optical efficiency, thus resulting in a more energy production annually. In addition, the North-South orientation has a higher energy production in summer and as a result, it is more suitable for many essential oils that grow and mature in summer. Figure 3.9 shows a fully constructed PTC aligning with True North-South line for a maximum capture of sunshine.

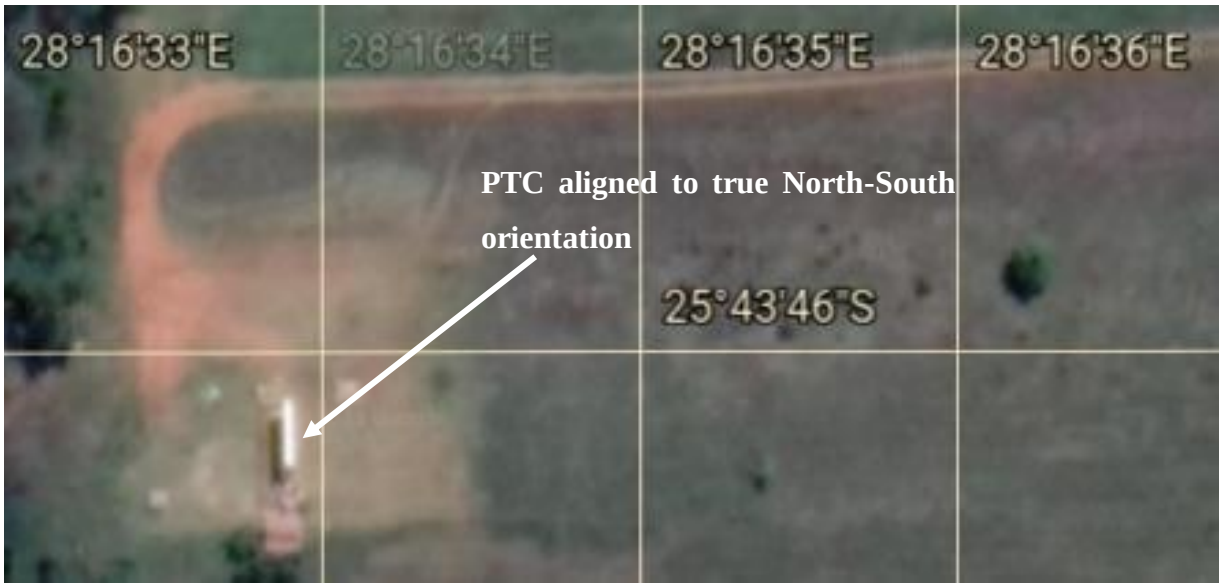


Figure 3.9 Image of True North-South aligned PTC as captured from the Satellite at Agricultural Research Council (-25°43'46", 28°16'34")

3.4.5 Water, steam and synthetic oil pipe network

Two operating fluids exist in the system, namely Therminol 66 and water. Therminol 66 is the thermal oil, pumped from the heat preservation tank to the collector, refer to Table 3.2 for selected physiochemical properties of Therminol 66 (See APPENDIX D.1 for complete data sheet). It enters the collector through the inlet of the receiver and exits the collector through the exit of the receiver tube and flows down to the PHE and back to the heat preservation tank, the cycle repeats itself since it is a closed system. A three phase, 3.7 A, 1.5 kW motor with a speed

of 1415 rev/min, power factor of 0.79 and efficiency of 79%, is used to drive a high temperature thermal oil pump that circulates therminol 66.

Because of the liquid expansion of therminol 66 at high temperature as the oil becomes less dense, an expansion tank of 48 litres has been integrated into the system to contain the fluid expansion. The expansion tank is located at the highest point in the PTC-powered essential oil steam distillation unit with a single drop leg piping arrangement as shown in schematic diagram of the PTC (Figure 3.10). The single drop leg piping was used since the only function of the expansion tank was to facilitate fluid expansion. The expansion tank also plays a critical role in system venting. It vents moisture and low-boiling degradation products from the system. Due to the elevated position (2.6 m) of the expansion tank, a positive head pressure is developed in the inlet of the pump, causing a flooded pump suction. This supplies an uninterrupted flow of oil from the pump. An SC250H flow meter, which provides reading on volumetric flow rates, is fitted on the collector inlet line. With temperature data recorded on the collector inlet and outlet, this volumetric flow rate is later used for calculations of the density of the therminol 66 oil. The calculated density is in turn used for calculating the mass flow rate in kg/s. Temperature gauges are fitted on the collector inlet and outlet. A pressure gauge is also inserted on the outlet of the collector for pressure reading of the exiting thermal oil from the receiver tube.

Table 3.2. Thermo-physical properties of therminol 66

Property	**Value**
Composition	Modified terphenyl
Max. bulk temperature	345℃
Kinematic viscosity at 40℃	29,6 cSt (mm^2/s)
Density at 25 ℃	1005 kg/m^3
Thermal conductivity at 27℃	0,11732 W/(m.k)
Flash point COC(ASTM D-92)/ (ASTM D-93)	184/170℃
Auto ignition temperature ASTM E-659/DNI 51794	374/399℃
Normal boiling point	359℃
Coefficient of thermal expansion at 200℃	0,000819/℃

The heated oil is directed to a heat exchanger and transfers heat to the water, which transforms to saturated steam. The flow of water to the heat exchanger is by gravity from the water tank to the PHE. The generated steam is directed to a distillation tank, which contain plant material (see Figure 3.11 showing steam output from the heat exchanger). Along the steam generation pipe, temperature gauge, pressure gauge and a flow meter for steam flow rate were fitted.

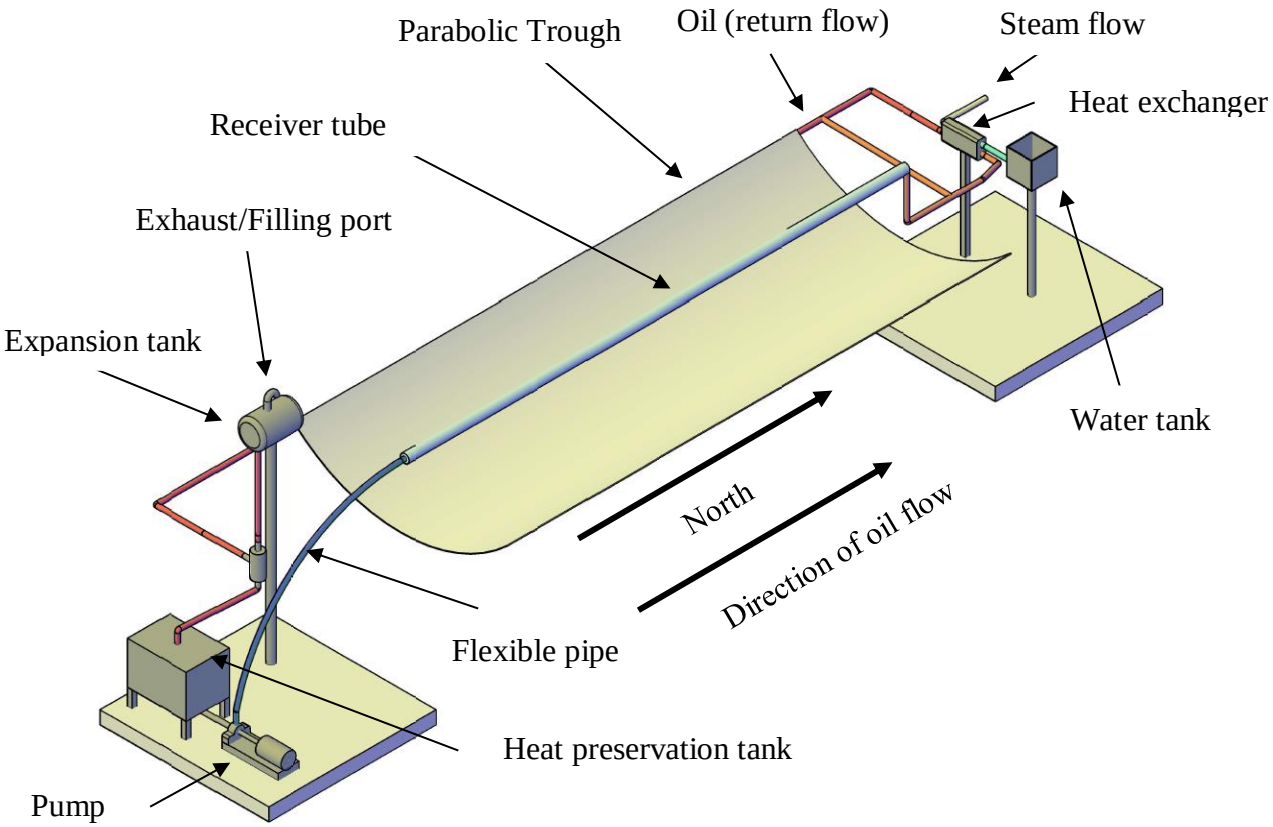


Figure 3.10. Schematic diagram of fluid flow of the PTC-powered essential oil steam distillation unit apparatus (South East Isometric View)



Figure 3.11 Steam production during system test

3.4.6 Distillation tank

A distillation tank is cylindrical in shape, with a diameter of 207 mm, a height of 502 mm, and a thickness of 2 mm, and is used to apply steam to the plant material as well as extract essential oils. The distillation tank receives the saturated steam produced by the PTC System. A perforated grill is built into the distillation tank to provide a bed for plant material. At the bottom of the distillation tank, one pressure gauge and one temperature gauge were installed, while one temperature gauge was installed near the top. The sealable lid is 6 mm thick and has a seal. A condenser is a device that is directly connected to the distillation tank and is used to condense the vapours.

3.4.7 Methodological approach used for PTC-powered essential oil steam distillation unit.

In the study, experiments were conducted using the steam distillation method (see Figure 3.12 for a complete set-up of the steam distillation unit). Experiments were conducted with a known mass of a plant material and for each quantity of plant material selected, experiments were repeated at least three times in order to determine mean values of yields and operational parameters. Oranges, lemon and Mandarin peels were obtained fresh from the local market. Small samples of the citrus peels were used for proximate analysis, and the rest of the plant material was prepared as a feedstock to the distillation tank. Sample of the known mass of each fruit peel (1.3 kg) was uniformly packed inside the distillation tank. The PTC was adjusted to supply a required pressure, temperature, and flow rate. Immediately, after the top stainless steel cap/lid was fastened after charging the vessel with plant material, the steam was directed to the

distillation tank. The steam volatized the oils in the plant material. The steam and volatile components of the plant material were directed to the condenser and separation funnel, where the essential oils were separated from the hydrosol (see Figure 3.13 for essential oil and hydrosol condensed into separation funnel). Essential oil and water condensate have different densities and form an immiscible two-liquid mixture at low temperature. The separation of oil extracts and hydrosol condensate utilized these differing properties to separate essential oil from hydrosol condensate. The essential oil collected were stored and analyzed using a Gas Chromatography (GC) to determine the fatty acid profile and other components.



Figure 3.12 Steam distillation unit set-up



Figure 3.13 Essential oil and hydrosol separation

CHAPTER 4: RESULTS AND DISCUSSIONS

This chapter contains the summary and discussions of results. Firstly, the proximate analyses are presented, followed by results and discussions of all experiments conducted.

4.1 Characterization: Proximate Analysis

Table 4.1, 4.2 ,4.3 and 4.4 show results of proximate analysis. The calculated values such as carbohydrates, hemicellulose, and cellulose are also listed. For each proximate item analysed, an appropriate method was used as briefly discussed below.

4.1.1 Dry matter, ash, total solids, moisture contents of fresh citrus peels

AOAC Official Methods 930.15 is the oven-drying methods for dry matter and moisture content determination, the feed sample is dried at 135°C for 2 h. It is one of the commonly used method for feed moisture analysis due to its ease of use (Ahn *et al*., 2014). For ash content, the feedstock material was tested based on the prescribed conditions of AOAC Official Methods 942.05, the test ran for 2 hours at a temperature of 600°C, and other similar rigorous conditions were adhered to (Thiex and Novotny, 2019).

Table 4.1. Dry matter, ash, total solids, moisture contents of fresh citrus peels

Analysis	Method number	Unit	Fresh citrus peels before distillation		
			Orange Peels	Lemon Peels	Mandarin Peels
Dry matter	ASM013	%	86,83	86,92	83,41
Ash	ASM 048	%	3,41	3,69	2,43
Total Solids	Calculated		83,42	83,23	80,98
Moisture	ASM 013	%	13,17	13,08	16,59

Table 4.2. Dry matter, ash, total solids, moisture contents of fresh citrus peels after distillation

Analysis	Method number	Unit	Distilled samples		
			Orange Peels	Lemon Peels	Mandarin Peels
Dry matter	ASM013	%	86,77	88,12	84,86
Ash	ASM 048	%	3,48	3,58	2,42
Total Solids	Calculated	%	83,29	84,54	82,44
Moisture	ASM 013	%	13,23	11,88	15,14

4.1.2 Protein, fat and carbohydrates

The protein content was determined by using AOAC Official Method 954.01, whereby the feedstock samples are digested with sulphuric acid to convert amino groups of protein to ammonia which distilled into a boric acid receiver and measured by titration with sulphuric acid solution. The nitrogen content was multiplied by a universal factor of 6.25 to obtain the protein content (Petterson *et al.*,1999). For fat content analysis, a traditional organic solvent method, called soxtec system was used. During the extraction process, fat is dissolved in the solvent inside the extraction unit, after which, the solvent is vaporized from the extraction cup and passes through condenser leaving the fat behind. Diethyl was used in the process. AOAC Official Methods 978.10, which uses a fritted glass crucible, was used for crude fibre. The method was conducted by extracting the feed material with acid and alkali (Petterson *et al.*,1999). Carbohydrates were calculated from the known dry matter, protein, fat and ash content (Greenfield and Southgate, 2003).

Neutral detergent fibre (NDF) was determined by using an NDF method, which was based on the extraction of feed with a hot neutral solution of sodium lauryl sulphate (Van Soest and Wine,1967). Acid detergent fibre (ADF) was determined by using ADF method, the method used heat treatment of the sample with sulphuric acid containing cetyltrimethyl ammonium bromide (Goering and Van Soest, 1970). Acid detergent lignin (ADL) is determined by treating the ADL residue with 72% sulphuric acid (Goering and Van Soest, 1970). The difference between NDF and ADF value gives an estimate of the content of non-cellulosic polysaccharides. The ADF residue contains mainly cellulose and lignin. The lignin content was determined and the resulting residue give the cellulose content. NDF = lignin + cellulose + hemicellulose, ADF = lignin + cellulose, ADL = acid detergent lignin, NDF – ADF = hemicellulose and ADF – ADL = cellulose.

Table 4.3.Composition before distillation

Analysis	Method number	Unit	Fresh citrus peels before distillation		
			Orange Peels	Lemon Peels	Mandarin Peels
Protein (N x 6,25)	ASM 078	%	10,49	4,88	5,9
Fat (ether extraction)	ASM 044	%	1,42	1,17	1,4
Carbohydrates (calculated)	ASM 075	%	71,51	77,18	73,68
Total non-structural carbohydrates	ASM 073	%	41,35	33,05	45,07
Fibre (crude)	ASM 059	%	11,57	12,27	8,1
Neutral detergent fibre	ASM 060	%	15,2	18,28	10,37
ADF		%	16,12	14,94	10,16
ADL		%	0,71	1,09	0,48
Cellulose	Calculated	%	15,41	13,85	9,68
Hemicellulose	Calculated	%	-0,92	3,34	0,21

Table 4.4. Composition after distillation

Analysis	Method number	Unit	Distilled samples		
			Orange Peels	Lemon Peels	Mandarin Peels
Protein (N x 6,25)	ASM 078	%	5,17	5,64	5,88
Fat (ether extraction)	ASM 044	%	1,39	1,14	1,43
Carbohydrates (calculated)	ASM 075	%	76,73	77,76	75,13
Total non-structural carbohydrates	ASM 073	%	42,4	30,63	46,93
Fibre (crude)	ASM 059	%	10,62	14,04	8,73
Neutral detergent fibre	ASM 060	%	14,88	18,67	11,92
ADF		%	15,31	17,93	11,99
ADL		%	1,54	2,16	2,43
Cellulose	Calculated	%	13,77	15,77	9,56
Hemicellulose	Calculated	%	-0,43	0,74	-0,07

Complete experimental data for the above analysis is provided in APPENDIX F.1

4.2 Laboratory Experiments

4.2.1 Yields of orange, lemon and mandarin peels

Citrus peels have been the subject of several laboratory studies. Many factors that can affect the efficiency of the distillation process; temperatures, essential oil quality, and yield were observed during the experiments. For all of the experiments, parameters such as butane gas

consumption, citrus peels weight before and after distillation, heating time, extraction vessel temperature (°C), quantity of hydrosol, essential oil, and water in the flask before and after steam generation were registered (See APPENDIX G.1 to G.3 for all the data collected). In addition, percentage of the moisture content before each citrus peel extraction was determined (See APPENDIX H.1 to H.2 for raw data). The calculated data yielded a variety of useful details. For each experiment, a stop watch was started and stopped when the oil column in the separator funnel was almost constant, but an average distillation time was determined for each citrus peels. Orange peels took an average of 18 minutes for steam distillation, while lemon and mandarin took an average of 22 minutes. For orange and mandarin, the distillation temperatures were found to be constant at 93 °C. Both of the lemon tests on 250 and 300 g ran at an average temperature of 95°C, but at a plant material loading of 300 g, the temperatures fell dramatically (see Figure 4.1). Despite the fact that the boiling points of some chemical compounds in essential oils are higher than 100 °C, all of the essential oils were separated from the source plant at a temperature just below 100 °C. The compounds of lemon peels and their respective boiling temperatures are γ-terpinene 183°C, β-pinene 166°C, Myrcene 166 °C, β-Bisabolene, Neryl acetate 240°C, Sabinene 163°C, a-Pinene 156°C, Geranial 299°C, and p-Cimene 177°C (Nooh, 2019). However, because of the partial pressure phenomena, these chemical compounds were able to be separated at temperatures below 100°C. Any essential oil with a high boiling point can be evaporated with steam in a ratio such that their combined vapour pressures are equal to the atmospheric pressure (Tandon, 2008).

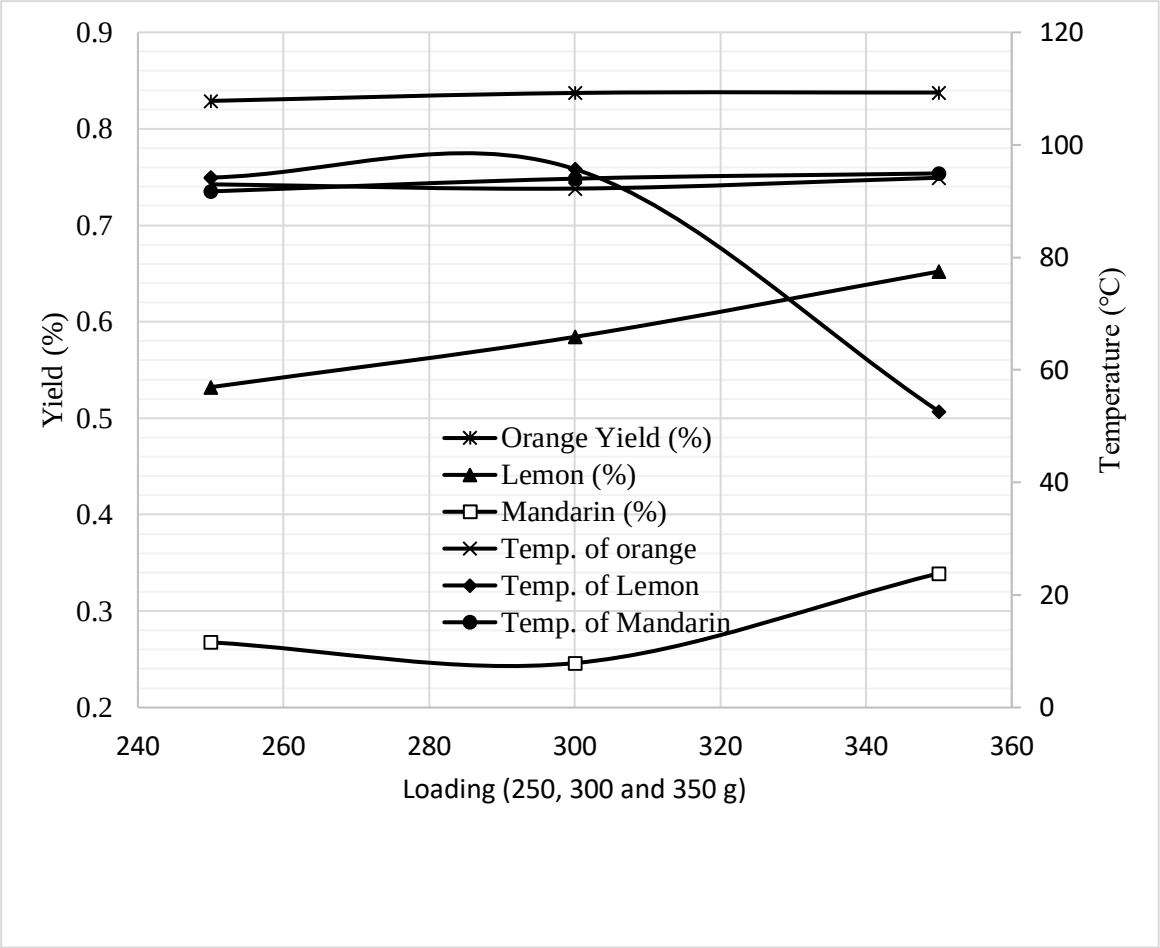


Figure 4.1: Yield and temperature

The yields as seen in Table 4.5 were calculated on a mass to mass basis (gram of oil per gram of plant material). The extraction yield for orange peels were found to be 0.83 %, followed by lemon peels (0.59 %) and mandarin peels (0.28 %). The percent yield of orange, lemon and mandarin peels were found to be 58.77, 50.39 and 20.3 %, respectively.

Table 4.5. Yields of orange, lemon and mandarin peels

Essential oil Sample	**Actual extraction yield (%)**	**Theoretical yield (%)**	**Percent yield (%)**
Orange peels	0,83	1,42	58,77
Lemon peels	0,59	1,17	50,39
Mandarin peels	0,28	1,4	20,3

According to M'hiri *et al*. (2017), essential oils for citrus oils range from 0.6 to 1%, however, literature on the individual source plants show that great amounts of essential oil can be achieved. For example, citrus reticulate peels yielded a low amount of 0.22 % when harvested at stage one (green colour and immature) but increased to amounts of 2.7 % for stage 2 (yellow colour and semi-immature) and 1.3 % for stage 3 (orange color and mature) (Franco-Vega1, 2016). Gök *et al.* (2015), with the use of a standard clevenger-type apparatus obtained a yield of 4.34% from fresh peel with yield experiments repeated at least three times. It can be concluded that for all laboratory citrus peels experiment, all the yields were at least within the expected range of 0.6 – 1%.

4.2.2 Energy consumption analysis in a laboratory scale

Energy consumption plays a very important role in the economics of the steam distillation process. As previously mentioned, essential oils steam distillation processes consume great quantities of energy, it is thus vital to factor energy consumption for each experiment. The quantity of energy was measured by first taking note of the measurements of the butane gas consumed before and after the experiment and the difference was converted to kWh of usage per experiment. Figure 4.2 shows the amount of power consumed per 100 g of plant material. Orange peels showed to be consuming less energy per 100 g, 0.21 kWh, followed by lemon energy consumption of 0.237 kWh, and mandarin consumption of 0.254 kWh.

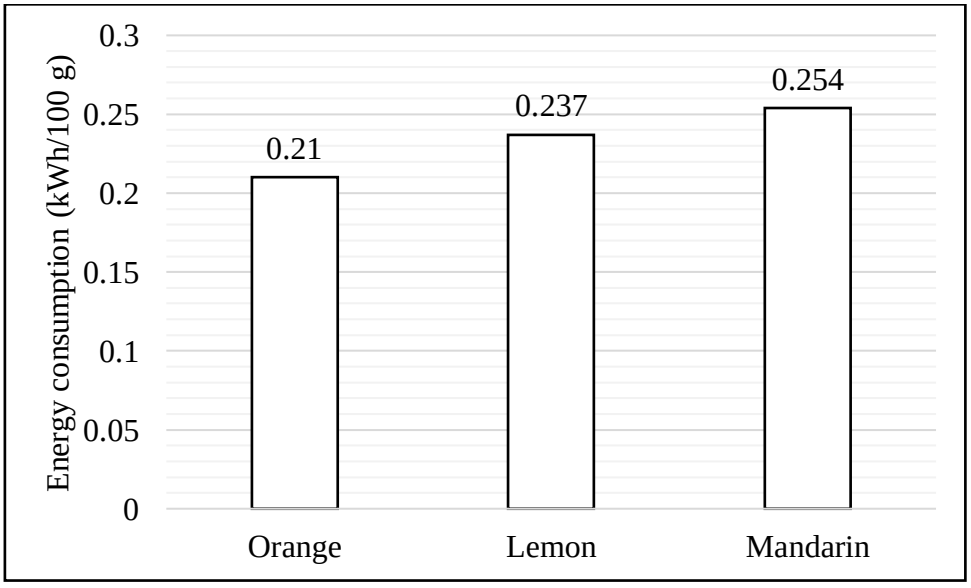


Figure 4.2 : Energy consumption per 100 gram of plant material

In terms of the energy consumption per one gram of oil produced, orange peels consumed 0.26 kWh, whereas lemon and mandarin peels consumed 0.42 and 0.975kWh, respectively (See Figure 4.3).

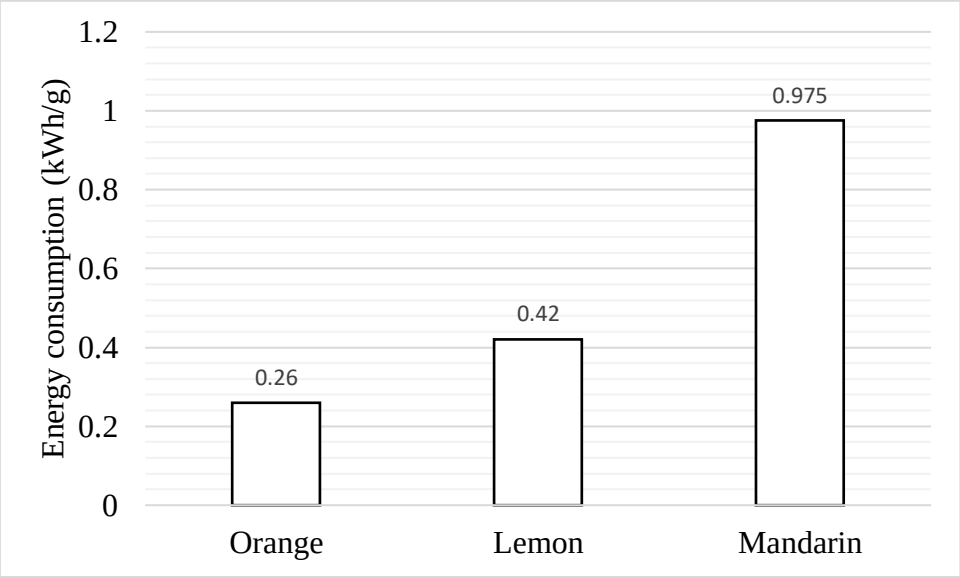


Figure 4.3 Energy consumption per one gram of oil produced

Table 4.6 shows total energy consumption, essential oil yield and the quantity of essential oil extracted per unit plant dry matter.

Table 4.6. Yields and energy consumed

Citrus peels	Weight (kg)	Moisture content (wb)(%)	Energy consumed(kWh)	Essential oil extracted (g)	Essential oil extracted/unit plant dry matter (g/kg)
Orange	0,25	72,51	0,51	1,8861	27,44
Lemon	0,25	83,19	0,64	1,3318	31,68
Mandarin	0,25	78,67	0,77	0,6114	11,47
Orange	0,3	72,51	0,56	2,532	30,70
Lemon	0,3	83,19	0,76	1,4531	28,81
Mandarin	0,3	78,67	0,75	0,7568	11,83
Orange	0,35	72,51	0,65	2,5578	26,58
Lemon	0,35	83,19	0,70	2,2744	38,65
Mandarin	0,35	78,67	0,82	1,1272	15,10

4.2.3 Average instantaneous power supply into the system

Steam distillation requires uninterrupted reliable power supply so that volatile chemicals can be released at constant temperature, thereby maintaining high yields and the constant standards of the quality of the essential oil. All the laboratory experiments were powered by a portable gas stove with a maximum potential of 2.75 kW. To make full use of this power, precautions were taken in order to avoid either applying more energy or applying less energy. The power knob switch was used to adjust this power input according to steam requirements. Observations of possibility of the condensation in the distillation vessel were made, and thereafter power input was adjusted accordingly. The power input is the rate at which energy is supplied to the system, it is the average instantaneous power given in kW. It was calculated by dividing the average power consumption by the distillation time.

The average instantaneous power available for orange, lemon, and mandarin were 2.15 kW, 1.94 and 2.08 kW, respectively. The incremental changes of the feedstock mass for distillation did not show significant changes in input energy required. For example, in the case of mandarin peels, 250 and 350 g samples both required 2.02 kW, whereas 300 g samples required 2.19 kW, which is only 8.4 percentage change from 250 g sample to 300 g sample of mandarin. For orange peels, 250 g samples consumed heat energy at an average rate of 2.33 kW whereas for 300 and 350 g samples the heat transfer rates were 2.04 and 2.08 kW, respectively. However, for large amounts of plant material, high amounts of input energy will be required, this is because larger amounts of sensible energy and latent heat of vaporization will be required as the mass of moisture in the plant material and essential oil increase.

4.3 Field Experiments

4.3.1 Gas-powered field experiment

During the gas-powered field experiment, average operating temperature for orange, lemon and mandarin were found to be 95.8, 96 and 95.8 °C, respectively, as seen in Table 4.7 (See APPENDIX I.1 for experimental data). In terms of the operational steam flow rates, on average the steam flow rate was 4.2 kg/h. The percent yields were 45.67, 37.19 and 83.22 % (see Table 4.8). Mandarin experienced a higher extraction and percent yield.

Table 4.7. Distillation temperature

Experiment	Orange	Lemon	Mandarin
1	96	96	96
2	96	96	95,8
3	95,5	96	95,6
Average	95,8	96,0	95,8

Table 4.8. Yields of orange, lemon and mandarin peels

Essential Oil Sample	Extraction yield (%)	Theoretical yield (%)	%Yield
Orange peels	0,65	1,42	45,67
Lemon peels	0,44	1,17	37,19
Mandarin peels	1,17	1,4	83,22

With regards to energy consumption per 100 gram of plant material, orange, lemon and mandarin peels had energy consumption of 0.339, 0.254 and 0.323 kWh, respectively. The comparison of the 3 citrus peels is shown on Figure 4.4.

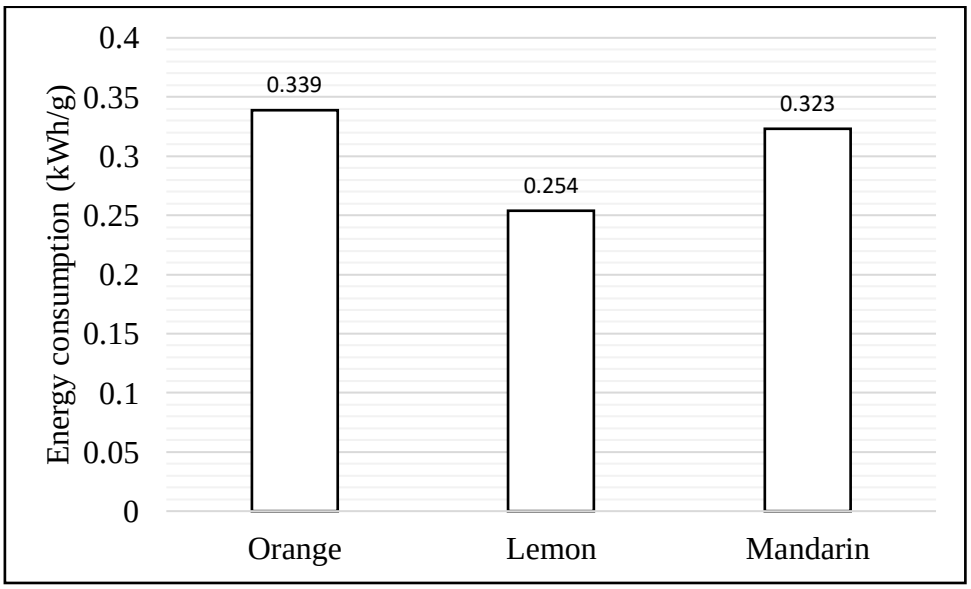


Figure 4.4 Energy consumption per 100 g of plant material

On a kWh per gram of oil basis, the energy consumed for orange, lemon, and mandarin peels were 0.534, 0.605, and 0.277 kWh, respectively as on Figure 4.5.

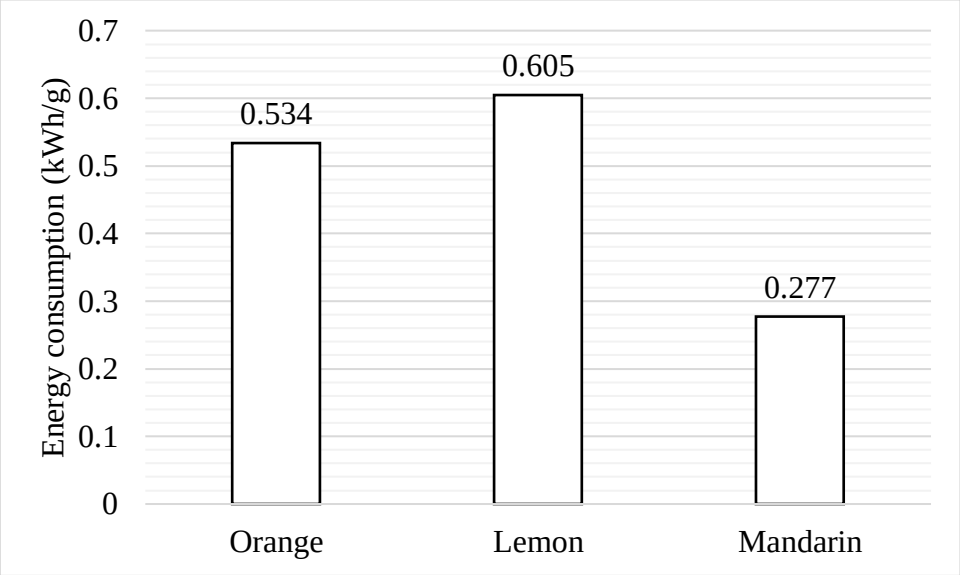


Figure 4.5 Energy consumption per gram of essential oil

The total amount of energy consumed on a 1.3 kg samples of orange, lemon and mandarin peels is shown on table 4.9. The amount of essential oil extracted per unit plant dry matter was also calculated.

Table 4.9 Essential oil extracted per unit plant dry matter

Citrus peels	Weight (kg)	Moisture content (wb)(%)	Energy consumed(kWh)	Essential oil extracted (g)	Essential oil extracted/Unit plant dry matter (g/kg)
Orange	1,3	80,29	3,562	8,0675	31,49
Lemon	1,3	81,13	2,544	5,6998	23,24
Mandarin	1,3	70,72	3,181	15,0972	39,66

With regards to the average instantaneous power required, orange experiments with 1.3 kg samples required 7.2 kW. Lemon and mandarin required 8 and 7.9 kW, respectively. Overall, the amount of average instantaneous power is 6.8 kW, regardless of which citrus peel is used.

4.3.2 Comparative analysis of results (Laboratory and gas-powered field experiment)

Table 4.10 shows the comparison data of laboratory and field gas-powered experiments, showing the amounts of moisture content of citrus samples before steam distillation and the amount of oil produced per citrus peel dry matter (d.m).

Table 4.10. Laboratory and field experiments

	Orange peels		Lemon peels		Mandarin peels	
	Lab	**Field (LPG powered)**	**Lab**	**Field (LPG powered)**	**Lab**	**Field (LPG powered)**
Weight (kg)	0,35	1,3	0,35	1,3	0,35	1,3
Moisture Content (%Wb)	72,5	80,29	83,2	81,13	78,67	70,72
Oil quantity (g)	2,5578	8,0675	2,2744	5,6998	1,1272	15,0972
Oil/d.m of plant material (g/kg)	26,57	31,49	38,68	23,24	15,10	39,66

With regards to yields for laboratory and field experiments, there were significant trends of changes. In the case of orange, the yield was 0.83 %, for laboratory and 0.65% for field experiment, with 21.69% decrease in yield from laboratory to field experiment, for lemon peels, the yield was 0.59 % for laboratory and 0.44 % for field experiment, with 25.42% decrease in yield from laboratory to field experiment, for mandarin peels, the yield was 0.28 % for laboratory and 1.17 for field experiment, with 317.86 % increase in yield from laboratory to field experiment.

In terms of energy consumption per 100 gram basis, the energy consumption for orange peels for laboratory experiment was 0.21kWh and 0.44kWh for field experiment, with 109.52 % increase in energy consumption from laboratory to field experiment. The energy consumption for lemon peels for laboratory experiment was 0.237 and 0.254kWh for field experiment, with 7.17 % increase in energy consumption from laboratory to field experiment. The energy consumption for mandarin peels for laboratory experiment was 0.254, and 0.323kWh for field experiment, with 27.17 % increase in energy consumption from laboratory to field experiment.

In terms of energy consumption per one gram of oil produced, the energy consumption for orange peels for laboratory experiment was 0.26 and 0.534kWh for field experiment, with 105.38 % increase in energy consumption from laboratory to field experiment. The energy consumption for lemon peels for laboratory experiment was 0.42 and 0.605kWh for field

experiment, with 44.05 % increase in energy consumption from laboratory to field experiment. The energy consumption for mandarin peels for laboratory experiment was 0.975 and 0.277 kWh for field experiment, with 71.59 % decrease in energy consumption from laboratory to field experiment.

Overall it can be concluded that more energy was used in the field or pilot experiment when extracting the essential oil, whereas in the laboratory experiments less energy was used. This was demonstrated in the amount of energy consumption per 100 gram of plant material. With regards to energy consumption per one gram of oil produced, the same trend continued (i.e. more energy was consumed per one gram of oil) except with mandarin experiment. The amount of energy consumed per one gram of oil in laboratory experiment was found to be very high (0.975kWh) as compared to field experiments of orange and lemon peels.

With regards to essential oil's yields, for both orange and lemon peels, generally yields decreased significantly from laboratory experiments to field experiments, whereas with mandarin, there was a significant increase in the yields. This observation may probably be attributed to the fact that, before distillation, the blended plant material of mandarin was not uniformly ground or blended, thus making it difficult for steam to penetrate the plant material, hence the inefficiency in the use of energy. The high moisture content of mandarin as compared to samples used in the laboratory experiment can be a source of difficulties in blending the plant material.

4.3.3 PTC-powered field experiment

The yields of orange, lemon and mandarin are as presented in Table 4.11. They also fall within expected ranges, with one exception where lemon showed lower amounts than the expected ranges.

Table 4.11 Yields of orange, lemon and mandarin peels

Essential oil sample	Extraction yield (%)	Theoretical yield (%)	%Yield
Orange peels	0,668618	1,42	47,08577
Lemon peels	0,527097	1,17	45,05106
Mandarin peels	1,09029	1,4	77,87784

With regards to energy consumption, orange, lemon and mandarin peels had energy consumption per gram of essential oil of 0.184, 0.186 and 0.193 kWh, respectively. The comparison of the three citrus peels is shown on Figure 4.6 below.

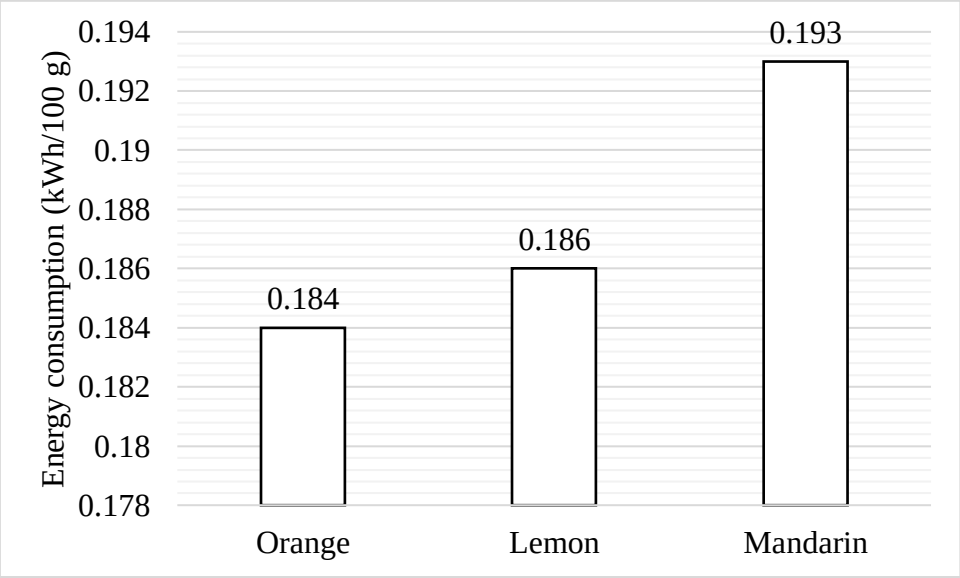


Figure 4.6 Energy consumption per 100 g of plant material

On a kWh per gram of oil basis, the energy consumed for orange, lemon, and mandarin peels were 0.277, 0.353, and 0.177 kWh, respectively as shown in Figure 4.7.

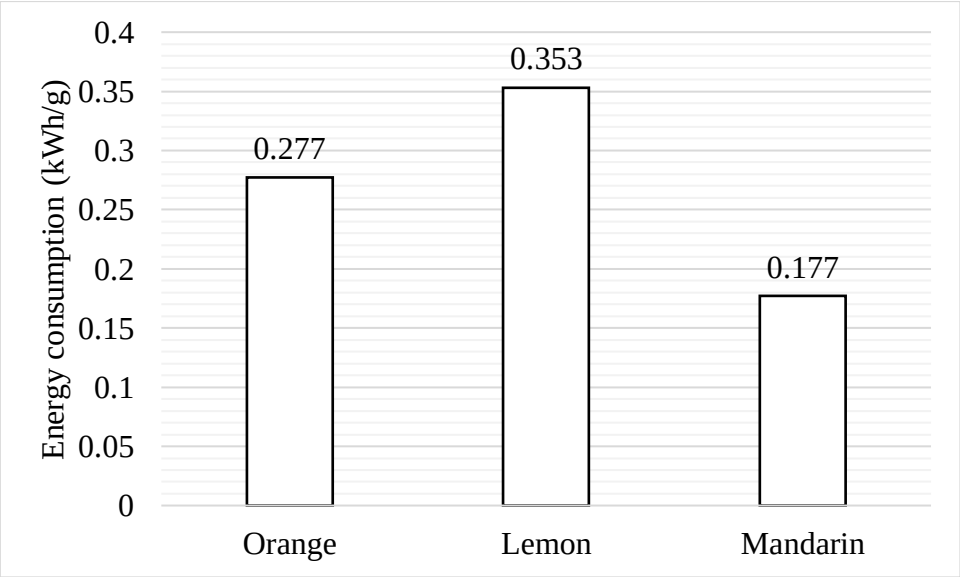


Figure 4.7 Energy consumption per gram of essential oil

The total amount of energy consumed on a 1.3 kg samples of orange, lemon and mandarin peels is shown in Table 4.12. The amount of essential oil extracted per unit plant dry matter was also calculated.

Table 4.12 Essential oil extracted per unit plant dry matter

Citrus peels	Weight (kg)	Moisture content (wb)(%)	Energy consumed(kWh)	Essential oil extracted (g)	Essential oil extracted/Unit plant dry matter (g/kg)
Orange	1,3	77,61	2,460	8,3251	28,602
Lemon	1,3	83,89	2,497	7,005	33,448
Mandarin	1,3	76,12	2,554	13,9555	44,954

4.3.4 Comparative analysis of gas-powered laboratory and field experiments

Yields of Essential Oils

Figure 4.8 shows a variation of essential oil yields of orange, lemon and mandarin peels. It can be concluded that the essential oils yield from the laboratory experiments were found to be higher than that of field experiments, with one exception on both mandarin field experiments where it was found that both field experiments yielded more essential oil than the laboratory experiment. This can be attributed to the fact that during the laboratory experiment of mandarin peels, the mandarin peels could not be well ground by the blender to produce finely ground, even particle size distribution, thus making it difficult for steam to penetrate the mandarin peels. An indication of relatively higher yields for laboratory experiments is a sign that essential oil yields from both field experiments can still be improved further.

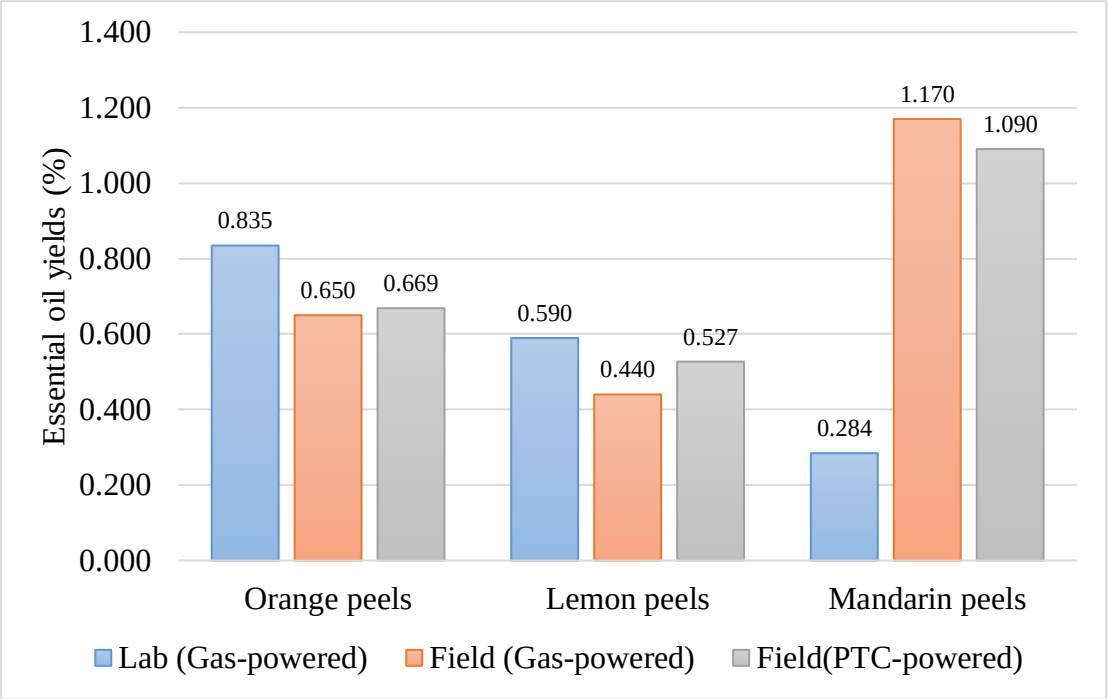


Figure 4.8 Comparison of essential oil yields (%)

The yields of orange, lemon and mandarin essential oils were found to be 0.67, 0.53 and 1.09 %, respectively, for PTC, whereas for gas-powered steam distillation, the yields were 0.65, 0.44 and 1.17% for orange, lemon and mandarin peels, respectively. The results of orange and lemon indicated a 3%, and 20% decrease, respectively, in oil yield when moving from gas-powered experiments to PTC-powered experiments, whereas in the case of mandarin, the change from gas to PTC-powered experiments produced a slightly opposite results, which is an 8% drop in oil yield when changing from gas to PTC-powered experiment. The yields for orange and mandarin peels for the PTC-powered experiments are within the ranges found in literature. However, with lemon, the yield was a little lower than the expected range (0.6-0.1 %), and the same trend continued with gas-powered experiment. Comparison of the laboratory results and PTC-powered steam distillation showed relatively higher yields for laboratory experiments, thus showing a need for improvement of the field experiments.

Consumption of energy per 100 g of plant material

Figure 4.9 shows energy consumption per 100 gram of plant material. A consumption of energy per 100 g of the plant material is also an important basis for comparisons. When comparing all the experiments, PTC-powered shows relatively low consumption of power per 100 gram of plant material. The fact that the walls of the distillation tank had already gained heat because

of the sun's radiation before the experiment start, can possibly reduce the sensible heat required to raise the contents of the distillation tank to saturated conditions, thus reducing the energy and time taken for steam distillation. In all laboratory experiments, energy consumptions were found to be lower than those of gas-powered field experiments.

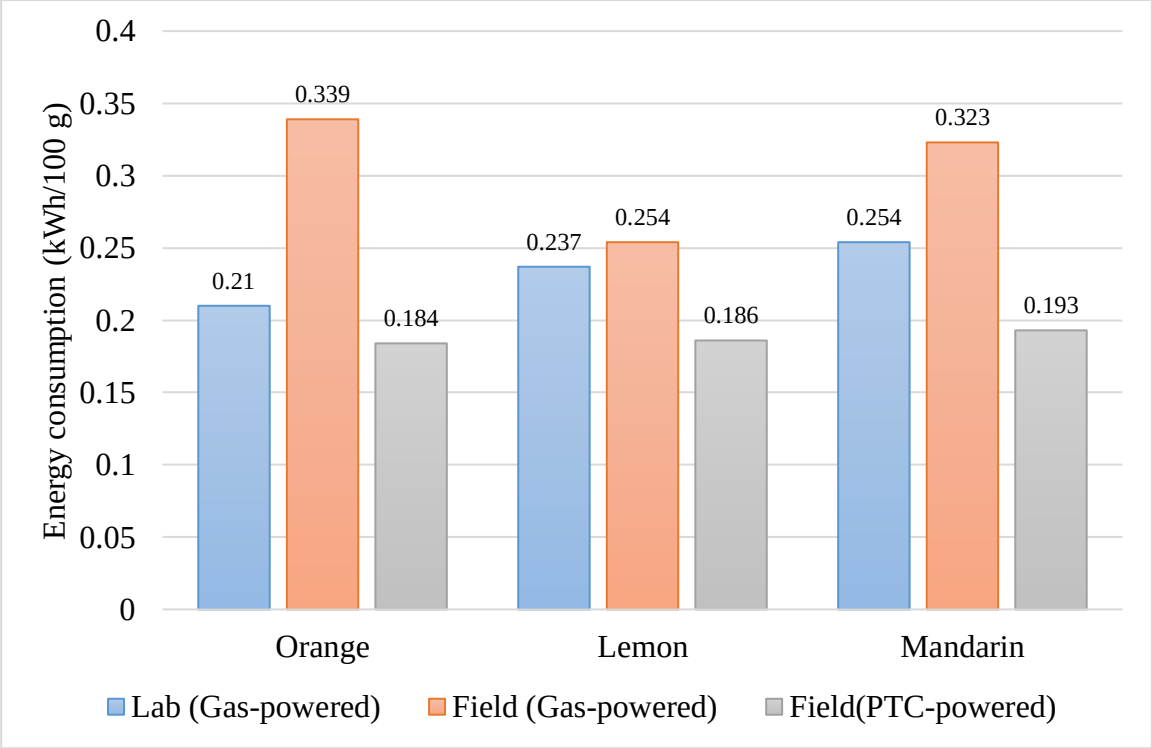


Figure 4.9 Energy consumed per 100 gram of essential oil produced in laboratory and field experiments

Energy Consumption of Essential Oil Manufacturing Process

Because of the energy intensive nature of the steam distillation operation of the essential oil extraction, it is vital to take into consideration how much energy is needed to produce one gram of oil because inefficiencies in distillation consequently translate into huge energy losses. The parameter (kWh/gram of oil produced) measures the efficiency of steam distillation and is used in Figure 4.10 to compare different experiments.

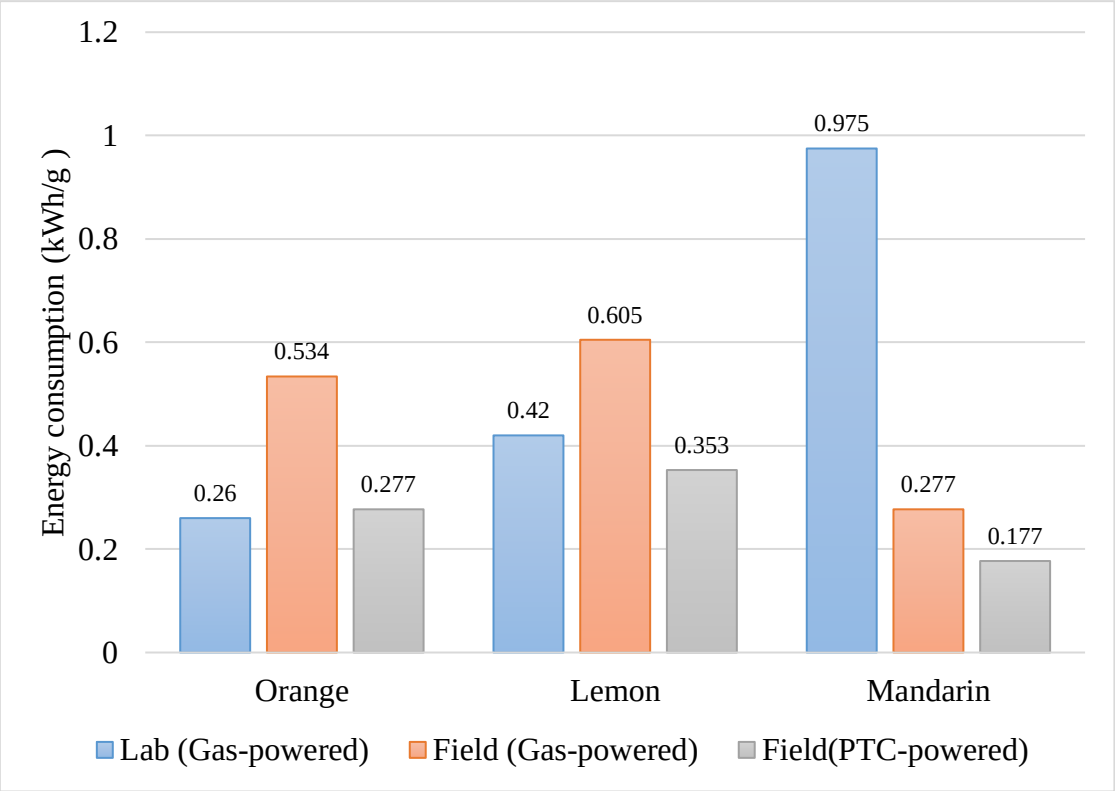


Figure 4.10 Comparison of energy consumed per one gram of essential oil produced in laboratory and field experiments

The energy consumed in the laboratory steam distillation during orange experiments is 0.26 kWh and lower than the two field experiments. However, it is opposite with lemon, where the PTC consumed low amount of kWh to produce one gram of essential oil as compared to the 0.42 kWh consumed in the laboratory experiment. Lemon and orange in gas-powered field experiments performed poorly, with one gram of oil produced at 0.534 and 0.605 kWh for orange and lemon, respectively. On the other hand, an almost one kWh (0.975 kWh) was consumed by the laboratory steam distillation of mandarin peels. It is more energy consumed, as compared to other experiments. This observation reiterates further about the importance of particle size of plant material before steam distillation. When comparing field (gas-powered experiment) and field (PTC-powered experiment), it can clearly be seen that the distillation tank used less power when powered by a PTC (see Table 4.13 for a percentage decrease of energy consumption from gas to PTC). However, it will be prematurely to assume that the CST system (PTC) was more efficient than the distillation tank powered by the gas. Reason being that, during the calculations of the heat energy used by gas-powered experiment, a total amount of gas used was accounted for, whereas in the case of PTC, the heat energy was simply an addition of a sensible heat required to reach saturated conditions plus the total latent heat of

vaporization until the experiment is completed. This approach obviously overlooks the fact that not all the gas is efficiently burned for useful power, which consequently generate saturated steam. For example, according to the Energy Technology Systems Analysis Programme (2010), boilers operate at an efficiency of 75%. This reality may explain why all gas-powered experiments reflected a high consumption of heat or thermal energy per one gram of oil produced. Applying a 75% efficiency will make the results of the two experiments even more comparable.

Table 4.13 Percentage decrease of energy consumption

Citrus peel	Lab (Gas-powered)	Field (Gas-powered)	Field(PTC-powered)	Percent change (%)
Orange	0,26	0,534	0,277	-0,48
Lemon	0,42	0,605	0,353	-0,42
Mandarin	0,975	0,277	0,177	-0,36

Carbon footprint (CO_2 Emissions)

An 800 gram of CO_2 is released when burning fossil fuels generating heat energy of one kWh (Kusuma *et al*., 2017). The amount of CO_2 emisions can be expressed as:

$$E_{CO_2} = \frac{800E_c}{1000} \qquad 4.1$$

E_{CO_2} is CO_2 emissions (kg), and E_c is energy consumption (kWh). In order to investigate the impact of CO_2 emissions, the CO_2 emissions for gas-powered experiments were calculated as seen on Table 4.14.

Table 4.14 Comparison of CO_2 emissions

Citrus peel	Laboratory (Gas-powered)/Total kWh	Total CO_2 emissions (g)
Orange	0,534	427,2
Lemon	0,605	484
Mandarin	0,277	221,6

The CO_2 emissions were found to be 472.2, 484 and 221.6 grams, respectively. These values may not appear significant if considered from a perspective of per gram basis of essential oil produced. It should be taken into consideration that, although CO_2 emissions are in the range

of grams, it takes more energy and more plant material to produce one gram of oil, thus producing more CO_2 emissions. In order to further show the extent of CO_2 emissions and negative impact to the environment, few gas (LPG)-powered field experiments as seen in Figure 4.15 were randomly selected from the recorded experimental data of total kWh consumed during the steam distillation (See APPENDIX I.2 for energy consumption data). The CO_2 emissions were found to be 3.9 2.2 and 2.5 kg for orange, lemon and mandarin, respectively. The experiments were run between 30 and 40 minutes but each produced CO_2 emissions in the range of kgs. This shows how conventional extraction methods can affect the environment.

The amount of total energy and CO_2 emissions can appreciably be higher than what it appears to be on Table 4.15, depending on which plant material is extracted. Certain plants consume more energy on a per gram basis and as a result, more CO_2 is emitted into the atmosphere. For example, Kusuma *et al.* (2017) reported that conventional extraction methods like water distillation consumed more than 6.5 kWh total energy when extracting vetiver oil. Kusuma *et al.* (2017) also reported that the production of patchouli oil on a per gram of oil resulted in an energy consumption of 6.55 kWh when extracted with water distillation. That is an equivalent of 5.24 kg of CO_2 emissions for every gram of essential oil produced. These are substantial amounts of both energy and harmful CO_2 emissions, which can be mitigated by solar energy.

Table 4.15 Total CO_2 emissions emitted during steam distillation of orange, lemon and mandarin

	Field (Gas-powered)/Total kWh)	**Total CO_2 emissions (g)**
Orange	4,834	3867,56
Lemon	2,799	2239,11
Mandarin	3,181	2544,44

In terms of the solar energy, CO_2 emissions are expected to be zero, provided that ancillary components such as the fluid circulatory pump and PTC tracker are also powered by solar energy. In conventional solar thermal systems, pumps and tracker or any ancillary components depend on electricity from an external source. These components can significantly add on the CO_2 emissions if the source of the electricity is not from renewable energy sources. There are already novel hybrid photovoltaic (PV) / CST systems that generate electricity and process heat at the same time. PV system is used to offset the electrical energy cost while the CST system is used to generate thermal energy (Riggs *et al.*, 2019). According to Riggs *et al.* (2019), these

hybrid systems have a potential to improve energy or exergy efficiency of the CST systems. The advantage of PV / CST systems is that in terms of scalability, even small installation on a small-scale is practical, thus allowing even residential customers (Riggs *et al*., 2019).

Average Power Supply of Field Gas And PTC-Powered Systems

The energy consumption for individual field experiments for gas-powered system ranged from:

- 3.562 to 4.834 kWh for orange, with an average of 4.41 kWh.
- 2.544 to 4.58 kWh for lemon, with an average of 3.307 kWh.
- 3.181 to 4.834 kWh for Mandarin, with an average of 4.198 kWh.

In order to fulfil these power requirements, an average power supply (rate of heat transfer in kW) was maintained, which is equal to the amount of total kWh consumed per steam distillation experiment divided by the time it took to complete the distillation. For orange peels, the rate of heat transfer was ranging from 6.107 to 8.057 kW, with an average of 7.201 kW. For lemon peels, the rate of heat transfer was 3.915 to 7.427 kW, with an average of 5.335 kW, whereas for mandarin, the heat transfer rate was found to be 6.361 to 9.357, with an average of 7.857 kW.

On the other hand, the energy consumption for individual field experiments for PTC-powered systems are as follows:

- 2.348 to 2.46 kWh for orange, with an average of 2.387 kWh.
- 2.376 to 2.497 kWh for lemon, with an average of 2.417 kWh.
- 2.424 to 2.554 kWh for mandarin, with an average of 2.506 kWh.

With regards to the rate of heat transfer, the net thermal output power delivered by the PTC is considered. The solar energy flux incident on the collector aperture plane, which is the product of the aperture area of the PTC, DNI (measured through a pyrheliometer device), and some efficiency factor, is an important parameter, particularly for PTC efficiency calculations. However, because of the non-availability of the pyrheliometer mounted on the site, there were no real time, site specific ground measurements recorded on the day of experiments. This is however, not critical since the most important parameter, namely: (1) temperature of an HTF

at the PTC inlet, (2) temperature of an HTF at the PTC outlet and lastly (3) the volumetric flow rate (measured by an SC250H variable area flowmeter) were recorded.

During the experiments, the average net thermal output was calculated to be 12.509 kW for orange, 12.943 kW for lemon and 12.704 kW for mandarin (See APPENDIX A.1 for thermal analysis and APPENDIX J.1 for data collected on PTC). These net thermal outputs are obviously large amounts of energy from the collector as compared to the 9.1 kW rated output thermal energy that was specified by the mirror and receiver tube collector manufacturer. Several possibilities may have applied which accounted to this amount. For example, the mirror and receiver tube collector manufacturer may have tested the system at a time when the DNI is less than what the solar site received on the days of experiments. The PHE which is a plate heat exchanger may have been the wrong size (smaller) or inefficient in transferring or dissipating heat to the water, thus causing elevated temperatures in the solar collector. In relation to the heat transfer rate delivered by the field gas-powered experiments (7.201, 5.335, and 7.857 KW), 12.704 kW delivered by the PTC is still high, but it should be noted that the original PTC thermal capacity designed or sized for a distillation tank was 7.5 kW rated energy of the PTC, however, the manufacture supplied the nearest standard PTC collectors sizes, of which 9.1 kW was the nearest suitable collector on the shelf.

Heat Losses

Because heat losses form part of inefficiencies in the system, an effort was made to quantify them, for estimating the final useful power. The theory of thermal network resistance, together with theory on convective heat losses were used in the designing of an excel thermal model (See APPENDIX A.2 and A.3 for detailed calculation procedure followed). Firstly, certain assumptions about the surface temperatures of the cylinder walls had to be made, to allow the iterative calculations so that the calculated surface temperatures on the walls of the distillation tank can be used to calculate the heat transfer losses on the top, bottom and vertical walls of the tank. The input to the thermal model include the assumed outside surface temperatures of the distillation tank, and the measured inside temperature of the distillation tank, which is the average of the temperatures at the steam inlet and the temperatures at the steam outlet. The output parameters of the model include the convective heat transfer coefficients for all the three walls, the calculated temperatures after several iterations, as well as the heat transfer losses, which is one of the important parameters that the model aimed to quantify.

For orange, lemon, and mandarin, the heat losses in the gas-powered field experiment were found to be 124, 6.5 and 13 W, for cylindrical, top, and bottom walls, respectively, which is about 144 W in total. On the other hand, the heat losses for orange, lemon, and mandarin in the PTC-powered experiment were found to be 125, 6.5 and 13 W, for cylindrical, top, and bottom walls, respectively, which is about 145 W in total. The difference between the heat losses were not found to be very significant. This is due to the fact that there were only minimal distillation temperature differences between the gas and PTC-powered experiments. The efficiency of the distillation tank is the difference between the heat input and the heat losses divided by the heat input into the distillation tank. That is about 6 % for both gas and PTC-powered experiments. This value may look unrealistic if considered in isolation of the boiler efficiency, which is about 75 %. If the boiler efficiency is considered, overall efficiency becomes the product of the thermal efficiency of the distillation tank and gas boiler efficiency, which is calculated to be 70.5 %. If the boiler efficiency of 75% (as found from the literature) is for boilers which are thermally insulated, then probably the efficiency of the gas-powered field experiments will drop even further below 70.5 % because the boiler was not insulated when experiments were conducted. Given the above explanation about lack of thermal insulations from the boiler, significant energy losses are still expected.

In terms of the PTC experiments, it is not simple to calculate the overall thermal efficiency without knowing the DNI data during hours of experiments. However, in the absence of data for DNI, receiver tube and reflective mirror manufacturer catalogue data can be trusted. Moreover, the information on the efficiency of PHE is also critical in the determination of the overall efficiency. After considering the thermal efficiency of 65% (from the manufacturer's catalogue/data sheet), 94% distillation tank efficiency (as calculated) and 90 % efficiency of plate heat exchanger, the overall efficiency of the system was found to be 54.99 %. Swiss Rotors (2020) reported a maximum efficiency of 90% for PHE, while Reay *et al.* (2013) reported a maximum efficiency 95% for PHE. However, to avoid overestimating the overall efficiency of the PTC-powered steam distillation, a maximum of 90% was used in the calculations. It should also be noted that the 90 and 95% are upper values in the efficiency ranges of PHEs, thus implying that the calculated overall system efficiency can still be a little lower. In a similar study conducted by Kültürel and Tarhan (2016) with CPCs, where perpermint was extracted through steam distillation, overall efficiencies ranging from 27.9% to 34.3% were found. This significant improvement from PTC over the CPC may be attributed to the fact that CPC are stationary, non-tracking solar collectors, thus compromising the overall efficiency of the

system. In addition, the PTC which was used for the experiment used evacuated tube collectors which improved the efficiency of the system.

4.4 Gas Chromatography Results

Table 4.16, 4.17 and 4.18 show the chemical compositions appearing in three citrus fruits peels. In most of the cases, main chemical components of orange, lemon and mandarin peels were shown in significant amounts, showing that even solar system can operate well in the extraction of essential oils. For example, steam distillation of mandarin peels is one such case where PTC-powered system had a significantly higher concentrations of limonene compound than all other experiments. Limonene is predominant in orange, lemon and mandarin, and therefore traces of high concentration of limonene are vital in steam distillation. There are however, other major compounds of citrus peels, which were also successfully extracted. They include linalool, geranyl acetate, sabinene, β-sinensal, decanal (cas), γ-terpinene, β-myrcene, d-carvone, neryl acetate, and citronella. Most of these chemical compounds were shown to be in great amounts, which is what is required to keep the defining and important characteristics of these essential oil.

Orange

Table 4.16 Orange peels chemical compositions

Chemical Compound	Orange Experiments		
	Lab (Gas-powered)	Field (Gas-powered)	PTC - powered
Linalyl propionate	1,21	-	-
dl-Limonene	75,3	1,79	-
Linalool	1,79	2,67	-
p-mentha-E-2,8(9)-dien-1-ol	1,09	-	
1-Nonanol (CAS)	1,21	-	1,42
Nerol (CAS)	4,14	-	-
1-Decanol (CAS)	3,28	-	-
Geranyl acetate	1,01	-	-
Dodecanal (CAS)	1,22	-	-
Naphthalene, 1,2,3,5,6,7,8,8a-octahydro-1,8a-dimethyl-7-(1-methylethenyl)-, [1R-(1.alpha.,7.β.,8a.alpha.)]-	1,78	-	-
D-Limonene	-	1,57	-
Cycloheptene, 5-ethylidene-1-methyl- (CAS)	-	1,44	-
Cyclobutane, 1,2-bis(1-methylethenyl)-, trans- (CAS)	-	1,68	-
cis-2-(2-Pentenyl)furan	-	2,44	-

1,5-Cyclooctadiene, 1,5-dimethyl-	-	1,7	-
D-Limonene	-	1,16	-
β-Terpinyl acetate	-	1,24	-
Cyclobutane, 1,2-diethenyl-3-methyl- (CAS)	-	1,95	-
Bicyclo[2.2.1]heptane, 2-(1-methylethenyl)-	-	1,14	-
Cyclohexene, 1-methyl-5-(1-methylethenyl)-	-	0,98	-
Sabinene	0,03		
Limonene oxide	-	1,46	2,08
β-Sinensal	0,44		0,19
Citronella	-	0,99	2,35
3-Cyclohexen-1-ol, 4-methyl-1-(1-methylethyl)- (CAS)	-	1,3	-
Decanal (CAS)	-	3,25	12
Nerol (CAS)	-	2,4	-
6-Octen-1-ol, 3,7-dimethyl-, (R)-	-	1,86	-
Z-Citral	-	2,83	3,91
2-Cyclohexen-1-one, 2-methyl-5-(1-methylethenyl)-, (S)- (CAS)	-	1,08	1,49
Geraniol	-	3,27	-
2-Propenoic acid, 2-methyl-, decyl ester (CAS)	-	4,61	-
Undecanal (CAS)	-	0,96	-
Geranyl acetate	-	1,36	-
L-linalool	-	-	3,44
3-Cyclohexen-1-ol, 4-methyl-1-(1-methylethyl)- (CAS)	-	-	1,88
3-Cyclohexene-1-methanol, .alpha.,.alpha.,4-trimethyl-, (S)- (CAS)	-	-	1,09
α -Pinene	0,11		
carveol 1	-	-	1,49
2,6-Octadien-1-ol, 3,7-dimethyl- (CAS)	-	-	5,83
Trans-Geraniol	-	-	4,5
1-Decanol (CAS)	-	-	6,56
1-Cyclohexene-1-carboxaldehyde, 4-(1-methylethenyl)-, (S)-	-	-	1,4
Undecanal (CAS)	-	-	1,3
NERYL ACETATE	-	-	1,77
2,6-Octadien-1-ol, 3,7-dimethyl-, acetate, (Z)-	-	-	2,24
β-ELEMENE	-	-	2,16
Dodecanal (CAS)	-	-	1,38
Trans-Caryophyllene	-	-	2,95
Trans-Caryophyllene	-	-	2,73
Naphthalene, 1,2,3,5,6,7,8,8a-octahydro-1,8a-dimethyl-7-(1-methylethenyl)-, [1R-(1.alpha.,7.β.,8a.alpha.)]-	-	-	2,7
Naphthalene, 1,2,3,5,6,7,8,8a-octahydro-1,8a-dimethyl-7-(1-methylethenyl)-, [1R-(1.alpha.,7.β.,8a.alpha.)]-	-	-	5,64
Valencene (CAS)	-	-	
(-)-Caryophyllene oxide	-	-	1,85
Dodecanal (CAS)	-	-	2,13
Bicyclo[5.2.0]nonane, 2-methylene-4,8,8-trimethyl-4-vinyl-	-	-	1,46
Trans-Caryophyllene	-	-	2,01

Valencene (CAS)	-	-	1,16
Valencene (CAS)	-	-	4,96
Valencene (CAS)	-	-	4,18
(-)-Caryophyllene oxide	-	-	1,49
(1S,4aS,7R,8aS)-1,4a-Dimethyl-7-(prop-1-en-2-yl)decahydronaphthalen-1-ol	-	-	0,59

Lemon

Table 4.17 Lemon peels chemical compositions

Chemical Compound	Lemon experiments		
	Lab (Gas-powered)	Field (Gas-powered)	PTC-powered
(-)-β-Pinene	2,39	2,54	2,45
β-Myrcene	1,63	-	-
2- β -PINENE	0,91	-	-
2- β -PINENE	0,93	-	-
1,5-CYCLOOCTADIENE, 1,6-DIMETHYL-	54,97	55,34	56,46
1,5-Cyclooctadiene, 1,6-dimethyl-	6,15	-	-
γ-Terpinene	2,17	2,23	2,15
1,6-OCTADIEN-3-OL, 3,7-DIMETHYL-	1,07	-	-
Limonene oxide	1,39	-	-
3-CYCLOHEXEN-1-OL, 4-METHYL-1-(1-METHYLETHYL)-	1,24	-	1,33
3-Cyclohexene-1-methanol, .alpha.,.alpha.,4-trimethyl-, (S)-(CAS)	1,59	1,63	1,82
Nerol (CAS)	3,06	-	3,61
Sabinene	0,66	0,93	
Trans-Geraniol	3,2	-	3,68
Undecanal (CAS)	0,9	-	0,95
NERYL ACETATE	2,26	-	-
Geranyl acetate	1,18	5	5,55
2- β -PINENE	0,91		
Caryophyllene	1,59	-	-
Valencene (CAS)	1,25	-	2,18
β-Bisabolene (CAS)	1,63	1,79	1,95
Isomyrcenyl acetate	-	1,14	-
α -TERPINOLENE	-	1,11	1,12
CITRONELLA	-	1,19	-
Isogeranial	-	1,03	-
Z-Citral	-	3,35	-
3,7-DIMETHYL-2,6-OCTADIENAL	-	3,32	-
Trans-Caryophyllene	-	2,1	-

Naphthalene, 1,2,3,5,6,7,8,8a-octahydro-1,8a-dimethyl-7-(1-methylethenyl)-, [1R-(1.alpha.,7.beta.,8a.alpha.)]-	-	1,94	-
cis-(-)-1,2-Epoxy-p-menth-8-ene	-	-	1,11
CIS-CARYOPHYLLENE	-	-	1,99
cis-alpha-Bergamotene	-	-	1,07
BICYCLO[3.1.1]HEPTANE, 6,6-DIMETHYL-2-METHYLENE-, (1S)-	-	-	0,9

Mandarin

Table 4.18 Mandarin peels chemical compositions

Chemical Compound	Mandarin experiments		
	Lab (Gas-powered)	Field (Gas-powered)	PTC-powered
β-Myrcene	0,93	-	1,34
dl-Limonene	60,06	0,68	90,24
7-Oxabicyclo[4.1.0]heptane, 1-methyl-4-(1-methylethenyl)-	1,97	-	-
Decanal (CAS)	2,08	7,45	-
Spiro[4.5]dec-6-en-8-one, 1,7-dimethyl-4-(1-methylethyl)-	1,23	-	-
D-Carvone	1,67	-	-
1-Decanol	1,2	-	-
1,4-CYCLOHEXADIENE, 1-METHYL-4-(1-METHYLETHYL)-	-	5,17	-
3,4-Dimethylbenzyl alcohol	-	1,57	-
Linalool	-	5,31	1,18
Limonene oxide	-	1,08	-
1-Nonanol (CAS)	-	1,15	-
3-Cyclohexen-1-ol, 4-methyl-1-(1-methylethyl)-, (R)-	-	1,53	-
6-Octen-1-ol, 3,7-dimethyl-, (R)-	-	2,79	-
Z-Citral	-	1,2	-
2-Cyclohexen-1-one, 2-methyl-5-(1-methylethenyl)-, (S)- (CAS)	-	1,15	-
2-Decenal, (E)- (CAS)	-	1,81	-
1-Decanol (CAS)	-	3,57	-
1-Cyclohexene-1-carboxaldehyde, 4-(1-methylethenyl)-, (S)-	-	2,42	-
p-Mentha-1(7),8(10)-dien-9-ol	-	2,73	-
Undecanal (CAS)	-	2,21	-
2,4-Decadienal, (E,E)- (CAS)	-	0,92	-
(-)-cis-Isopiperitenol acetate	-	1,06	-
Trifluoroacetyl-lavandulol	-	1,58	-
NERYL ACETATE	-	3,61	-
α -Cubebene	-	2,72	-
Geranyl acetate	-	2,91	-
β-ELEMENE	-	3,51	-

α -PINENE, (-)-		0,1	
Dodecanal (CAS)	-	3,55	-
Limonen-10-yl acetate	-	2,22	-
Trans-Caryophyllene	-	2,18	-
p-Mentha-1,8-dien-7-yl acetate	-	1,37	-
(1S,5S,6R)-6-Methyl-2-methylene-6-(4-methylpent-3-en-1-yl)bicyclo[3.1.1]heptane	-	3,82	-
(1S,5S,6R)-6-Methyl-2-methylene-6-(4-methylpent-3-en-1-yl)bicyclo[3.1.1]heptane	-	1,3	-
GERMACRENE-D	-	1,2	-
Valencene (CAS)	-	1,26	-
NAPHTHALENE, 1,2,3,4,4A,5,6,8A-OCTAHYDRO-7-METHYL-4-METHYLENE-1-(1-METHYLETHYL)-, (1. α.,4A. α.,8A. α.)-	-	1,02	-
Farnesene (CAS)	-	5,59	-
Farnesene (CAS)	-	1,85	-
8-ISOPROPYL-1,3-DIMETHYLTRICYCLO[4.4.0.0~2,7~]DEC-3-ENE	-	3,21	-
Cadinene	-	0,96	-
γ-Terpinene	-	1,87	-

4.5 Techno-Economical Analysis

4.5.1 Techno-economic review

There is a common view that fossil energy technologies are cheaper as compared to renewable energy technologies. However, this view overlooks the operation and maintenance cost of the two technologies, the negative impacts, and other costs associated with nuclear and coal-fired power plants (Gets, 2013). For example, in the case of solar thermal energy systems, the initial capital investment is high, but the operation and maintenance cost which include electricity consumed by pumps are low, and solar energy is free (no fuel costs). On the other hand, fossil fuel-fired boilers have a smaller initial investment but maintenance and operational costs are high (Joubert *et al.*, 2016). For example, throughout the lifespan of fossil fuel-fired boilers, fuel contributes 96% of the total cost while capital, operation and maintenance costs contribute 4% (Energy Technology Systems Analysis Programme , 2010). According to Walwyn and Brent (2014), the cost of renewable energy has reduced significantly over the past decade when compared to the cost of energy from fossil fuels and this cost pattern is predicted to continue until 2030. The levilized cost of electricity (LCOE) from PV panels, wind generators, geothermal sources are close to and essentially equal to the cost of electricity from coal or nuclear sources (Walwyn and Brent, 2014).

In the study conducted by Walwyn and Brent (2014) of the costs of electricity from the renewable energy independent power producer procurement programme (REIPPP), it was found that the weighted average cost of electricity from the renewable energy technologies has reduced progressively since the beginning of the programme from 211 to 84 $/MWh. The three dominating solar energy technologies under REIPPP are wind, PV and CSP systems. Among these three, wind contributes a bigger share in the national grid, whereas CSP is behind. Over the years, wind energy has established itself, and this has significantly reduced the cost of wind energy. Its low cost has boosted its preference or dominance in the REIPPP over other renewable energy technologies (Graig *et al.*, 2017). According to Joubert *et al.* (2016), the costs of large-scale solar thermal plants in South Africa are still high when compared to system cost in other countries, the main barrier being the low cost of coal, but current systems are competing well with paraffin, diesel, petrol, and gas, and the projected savings are high.

To this far, the important aspects of the CST technologies discussed are more applicable to large-scale implementation of PTCs. However, to an extent, the techno-economic factors in the large-scale operation of the CST technologies for electricity production also apply to CST technologies for industrial process heat. For example, the initial capital investment of CST technologies for industrial process heat is also high. High upfront investment costs and low energy prices are typical barriers to the deployment of solar thermal installations in industrial and power production processes (International Renewable Energy Agency and The Energy Technology Systems Analysis Programme, 2015). Other factors, which stall the progress in deployment of industrial systems, include (1) The complexities associated with integrating CST technologies with old systems, (2) Subsidized Low fuel prices, and (3) Lack of technical capacity (professionals), financing and public awareness. As a result of these influencing factors, the economic potential for CST technologies is low. However, it is estimated that approximately 180 Gigawatt of thermal power can be implemented economically if CST technology costs continue to decrease (International Renewable Energy Agency and The Energy Technology Systems Analysis Programme, 2015).

One of the CST components that contributes a significant share in high capital investment is the need to store energy. Storage systems are costly but a simple method to reduce the overall cost of the CST technology is by excluding TES system. In such a case, the process heat is directed to an industrial process. When this type of system is adopted, the maximum energy input to the process must not be considerably larger as this will cause energy losses. However,

with the TES excluded, it implies that industry operations, which use the CST technology at night, early or late hours, will not be running cost effectively (Kalogirou, 2003). Further options exist for reducing the cost of a CST technology, for example, non-evacuated tube receivers are ideal for industrial process applications since they are low cost receivers as compared to evacuated tube receivers. Further cost savings are realized when proper operation and maintenance are conducted in order to ensure that the CST systems operate at optimal conditions throughout their lifespan (South African National Energy Development Institute, 2017), which is generally assumed to range from 20 to 30 years (Bologna *et al*., 2020).

In order for CST systems to compete well with natural gas, an important parameter namely; the levelized cost of heat (LCOH), which is a ratio of the life time cost of the system to life time production of energy, must be decreased in such a way that it is more economically feasible to use CST technology than to use natural gas. In order to reduce the LCOH, either the lifetime cost (numerator) must be decreased or the lifetime production (denominator) must be increased (see Eq. [4.2]). The cash flows (operation and maintenance) can be decreased by cost mitigations whereas, the lifetime production of energy can be increased by technical advancement aimed at improving performance of the system. In a techno-economic analysis conducted by Musi *et al*. (2017), it was predicted that the LCOE or LCOH is decreasing over time, and that given the favourable times and market conditions, the LCOE will drop to 6 ¢/kWh by 2020.

$$LCOH = \sum \frac{Cash\ Flow}{Thermal\ energy\ generated} \qquad 4.2$$

There are different ways of investigating the economic viability of a CST technology. Many commercial customers have an understanding of the LCOH as a measure of how much they pay for the process heat. There are however, many that are interested in the payback time. The payback time takes into account the initial capital investment and the cost difference between LCOH and the current fuel prices. The internal rate of return (IRR) and net present value (NPV) are also taken as indicators of financial performance during the financial analysis of CST systems (Mathur *et al*., 2013).

According to South African National Energy Development Institute (2017), solar thermal systems have shorter pay back periods when compared with other forms of renewable energy. When South African National Energy Development Institute (2017) performed techno-economic analysis of fossil fuel and renewable energy hybrid technologies for large-scale

commercial CST projects, it was proved that a simple payback period of 6.75 years can be achieved if the company was to sell carbon credits. However, this can be riskier for private developers. This situation may however, prove to be different in the case of small-scale industrial process heat applications. For example, when Afzal *et al*. (2017) performed cost analysis on a steam distillation of essential oil with scheffler concentrator, it was found that the payback time can be half a year. Generally, the customers or the process heat industries prefer a payback period of three to five years. The payback period varies with the cost of fuel, which is intended to be replaced by renewable energy. South African industries use LPG, electricity, diesel, coal paraffin and heavy fuel oil (HFO) for process heat. When a solar thermal process replaces an expensive fuel such as LPG, the economics can be improved, thus lowering the payback time. The advantage of using solar thermal technologies for industrial process heat is the fact that, over the years, the costs of the CST technologies have been declining with the size of the collector area, they have been between 400 and 800 € per m² (Solar Payback, 2019). In terms of costs per energy output, PTC costs ranged from 600 to 2 000 $/kW, whereas for PTCs intended for commercial, utility-scale production of electricity, the costs ranged from 6000-34000 $/kW. That indicates that the implementation of CST at a small-scale industrial level is becoming more and more economical (International Renewable Energy Agency and The Energy Technology Systems Analysis Programme, 2015).

CHAPTER 5: CONCLUSIONS AND RECOMMENDATIONS

5.1 CONCLUSIONS

The steam distillation unit, integrated with PTC was developed and tested experimentally, with the main aim to determine if this type of a CST system can be successfully used for steam distillation of essential oils in the agro-based industry that is already cost-burdened by conventional steam distillation essential oil extraction techniques. In order to accomplish the tests and subsequently the aim, three tests were conducted, namely: laboratory and two field tests comprising of the gas and PTC-powered steam distillation. Results were generated and which gave rise to conclusive arguments as detailed below:

a. Firstly, the operation of the low pressure (< 1bar), PTC-powered steam distillation was conducted successfully, reaching high temperatures of 295 ℃, with the maximum bulk temperature (345 ℃) of the therminol 66 being the only limiting factor to reaching even higher temperatures.
b. The system generated a net thermal output of 12 kW, with the collector inlet and outlet temperatures, as well as volumetric flow rate being about 50℃, 295℃ and 100 l/h, respectively.
c. During this successful operation, the operational steam distillation temperatures for orange, lemon and mandarin were about 96 ℃. These temperatures compare well with temperatures usually expected from a steam distillation operating under atmospheric conditions.
d. The above operating conditions created by the PTC-powered essential oil steam distillation created an enabling environment for essential oils to break free from essential oil plants and produce essential oil at quantity and quality marching that found in the literature.
e. The average yields of orange, lemon and mandarin essential oils were found to be 0.67, 0.53 and 1.09 % whereas for gas-powered steam distillation, the average yields were 0.65, 0.44 and 1.17 % for orange, lemon and mandarin peels, respectively. Concerning the gas- and PTC-powered experiments, the majority of essential oil yields from individual experiments fell within the expected ranges. Low amounts of lemon oil may be associated with the lemon peels and further research may identify the problem.

f. With regards to energy efficiency, the two field experiments were evaluated and results compared. The gas-powered steam distillation experiment showed that the overall efficiency of the system was 70.4 %, with high probability of even getting less, considering the fact that the boiler was not thermally insulated. On the other hand, the overall system efficiency of the PTC-powered steam distillation was found to be 54.99 %, which is 15.41 % less than that of the gas-powered steam distillation. Although the overall system efficiency is relatively small, it still compares very well with other similar research studies on CST technologies and in some cases a little bigger.

In light of the collected data and analysis of yield, essential oil quality, distillation efficiency and solar resource, it can be concluded that PTC can compete with fuel gas (LPG) and possibly other fuel sources, but it depends on the fluctuations of the fuel price. Each fuel selected has its own price and a different payback period associated with replacing that particular fuel. The higher the fuel price, the better the economics for CST projects. It is thus advisable that for each case of evaluating economic and financial viability of an industrial process heat CST project, prevailing factors must be analyzed as it is not the only fuel that affects the payback period; discount rates, current costs of CST technology components, DNI radiation all affect the payback time.

5.2 RECOMMENDATIONS

Proposed Changes on the Solar Collector Field And Steam Production Side

a) Replacement of PHE with solar steam generator (for example shell and tube type solar steam generator) as PHEs would normally be suitable for low temperature applications. PHE with design limitations of 148.89 to 232.22℃ and 10.34 to 20.68 bar, was subjected to heat transfer oil which could potentially reach 300 ℃. Potential problems can be expected, whether it is compromised efficiency of the system or technical problems.
b) A steam /water separator must be fitted to remove the condensate from the steam in order to allow dry steam into the distillation tank.
c) Changing the feed water supply from gravity fed to feed water supply using a feed pump to promote a more controllable flow of water into the condenser.
d) Supply of pre-heated feed water to the steam generator to avoid delays in steam generation.

e) Bypass the heat storage tank as it currently lowers the temperature of the return flow of the therminol 66 oil, thus dropping the temperature at the collector inlet. There has to be a valve to isolate the tank storage, so that it is only used for the purpose of storing the oil when the system is not in operation.
f) Installation of a throttle valve for a proper flow control of therminol 66 is required.
g) A thorough study on the exergy of the system. This will bring about a comprehension of all the heat losses incurred in the pipelines, receiver collector and heat exchanger. The results of the study will help the engineer to accurately march the thermal energy output of the PTC with the energy requirements of the distillation tank so that the thermal energy output is not appreciable larger than the chemical process or the distillation tank's heating requirements. This is very important, especially in a system where there is no thermal energy storage system where an excess heat can be stored.
h) The installed PTC is a low pressure system (less than a bar) and limited to certain operating temperature and pressure, and therefore an effective control system should be installed and set to control the temperature and pressure for optimal and safe operation.
i) The whole system of PTC-powered steam distillation unit was developed and constructed to discharge the steam at atmospheric pressure and temperature and therefore an option to modify the system to a modern pressurized system at elevated pressures of 1.38 to 3.4 bar and a temperature above 150 ℃ will be suitable for a system processing tons of plant material. This modification will also reduce the distillation times.
j) Powering a solar tracker and other ancillary components with PV system instead of using alternating current (AC) to DC rectifier (Power supply), which are currently adding to carbon footprint and AC to DC conversion losses.
k) Constant low flow rates of 100 l/h (0.02514 kg/s) of therminol 66 has been a technical problem that had developed a char in the receiver tube. This can potentially cause low heat transfer from the stainless steel pipe and selective coating to the therminol 66 oil, and blockages of the pipeline. Therefore, the pump must be sized to increase the flow rate, but also to increase the pressure slightly.
l) In an effort to reduce the cost the PTC system, future projects can focus on adopting to non-evacuated tube receivers instead of using costly evacuated tube receivers which are suitable for temperatures of more than 300℃.
m) Likewise, first surface mirrors like aluminium reflectors can also be used, as they are suitable for medium temperature applications.

Proposed Changes to the Chemical Process (Essential Oil Steam Distillation) Components Receiving the Process Heat or Steam.

a) Insulation of the distillation tank and other uncovered parts of the PTC to reduce the heat losses that are occurring. Thermal insulation keeps the heat transfer coefficient low, thus minimizing the heat losses.
b) Conversion of the system to hybrid system, for example, integrating a gas-powered boiler to feed steam into the distillation tank during early and late hours or at night. A system of isolation valves can be used to achieve that by using the current gas-powered steam distillation tank.
c) A changeover tank and a second distillation tank must be fitted to reduce the time taken between loading and off-loading of the plant material, thus increasing the overall efficiency of operations.
d) Permanent housing at a point where the hydrosol and essential are received so that the harvested oils are protected from the direct contact with sunlight before they are bottled and stored.
e) In the presence of more financial resources, a potential of PTC technology in steam distillation should also be tested with a variety of essential oil bearing plants to discover further on how the system performs.

CHAPTER 6: REFERENCES

Afzal, A., Munir, A., Ghafoor, A. and Alvarado, J.L. (2017) 'Development of hybrid solar distillation system for essential oil extraction', *Renewable Energy*, 113, pp. 22-29, *ScienceDirect* [Online]. Available at: https://www.sciencedirect.com/science/article/pii/S0960148117304123 (Accessed: 29 December 2017)

Ahmed, F.E., Hashaikeh, R. and Hilala, N. (2019) 'Solar powered desalination–Technology, energy and future outlook', *Desalination*, 453, pp. 54-76, *ScienceDirect* [Online]. Available at: https://www.sciencedirect.com/science/article/pii/S0011916418321258 (Accessed: 2 May 2020)

Ahn, J.Y., Kil, D.Y., Kong, C. and Kim, B.G. (2014) 'Comparison of oven-drying methods for determination of moisture content in feed ingredients', *Asian-Australasian Journal of Animal Sciences (AJAS)*, 27(11), pp. 1615-1622, *PubMed* [Online]. Available at: https://pubmed.ncbi.nlm.nih.gov/25358322/ (Accessed: 5 December 2017)

Ali, B., Al-Wabel, N.A., Shams, S., Ahamad, A., Khan, S.A. and Anwar, F. (2015) 'Essential oils used in aromatherapy: A systemic review', *Asian Pacific Journal of Tropical Biomedicine*, 5(8), pp. 601-611, *ScienceDirect* [Online]. Available at: https://www.sciencedirect.com/science/article/pii/S2221169115001033 (Accessed: 5 February 2017)

Alva, G., Lin, Y. and Fang, G. (2018) 'An overview of thermal energy storage systems', *Energy*, 144, pp. 341-378, *ScienceDirect* [Online]. Available at: https://www.sciencedirect.com/science/article/pii/S036054421732056X (Accessed: 2 November 2019)

Aramesh, M., Ghalebani, M., Kasaeian, A., Zamani, H., Lorenzini, G., Mahiane, O. and Wongwises, S. (2019) 'A review of recent advances in solar cooking technology', *Renewable Energy*, 140, pp. 419-435, *ScienceDirect* [Online]. Available at: https://www.sciencedirect.com/science/article/pii/S096014811930326X (Accessed: 12 February 2020)

Ayub, I., Munir, A., Amjad, W., Ghafoor, A. and Nasir, M.S. (2018) 'Energy- and exergy-based thermal analyses of a solar bakery unit', *Journal of Thermal Analysis and Calorimetry*, 133, pp. 1001-1013, *SpringerLink* [Online]. Available at:

https://link.springer.com/article/10.1007/s10973-018-7165-3 (Accessed: 13 November 2018)

Aziz, Z.A.A., Ahmad, A., Setapar, S.H.M., Karakucuk, A., Azim, M.M., Lokhat, D., Rafatullah, M., Ganash, M., Kamal, M.A. and Ashraf, G.M. (2018) 'Essential oils: extraction techniques, pharmaceutical and therapeutic potential - a review', *Current Drug Metabolism*, 19, *ResearchGate* [Online]. Available at: https://www.researchgate.net/publication/326598166 (Accessed: 7 April 2021)

Barba, F.J., Gavahian, M., Ismail, E., Zhu, Z., Chemat, F., Lorenzo, J.M. and Khaneghah, A.M. (2019) 'Solar radiation as a prospective energy source for green and economic processes in the food industry: From waste biomass valorization to dehydration, cooking, and baking', *Journal of Cleaner Production*, 220, pp. 1121-1130, *ScienceDirect* [Online]. Available at: https://www.sciencedirect.com/science/article/pii/S0959652619305748 (Accessed: 15 September 2019)

Baronea, G., Buonomanoa, A., Forzanoc, C. and Palomboa., A. (2019) 'Solar thermal collectors', in Calise, F., D'Accadia, M. D., Santarelli, M., Lanzini, A. and Ferrero, D. (eds.) *Solar hydrogen production: processes, systems and technologies.* UK: Academic Press, pp. 179-235.

Batuecas, E., Mayo, C., Díaz, R. and Pérez, F.J. (2017) 'Life cycle assessment of heat transfer fluids in parabolic trough concentrating solar power technology', *Solar Energy Materials and Solar Cells*, 171, pp .91-97, *ScienceDirect* [Online]. Available at: https://www.sciencedirect.com/science/article/pii/S0927024817303392 (Accessed: 17 March 2018)

Bologna, A., Fasano, M., Bergamasco, L., Morciano, M., Bersani, F., Asinar, P., Meucci, L. and Chiavazzo, E. (2020) 'Techno-Economic analysis of a solar thermal plant for large-scale water pasteurization', *Applied Sciences*, 10, pp. 4771. DOI: 10.3390/app10144771 (Accessed: 14 December 2020)

Bundschuh, J., Chen, G., Tomaszewska, B., Ghaffour, N., Mushtaq, S., Hamawand, I., Reardon-Smith, K., Maraseni, T., Banhazi, T., Mahmoudi, H., Goosen, M. and Antille, D.L. (2017) 'Solar, wind and geothermal energy applications in agriculture: back to the future?', in Bundschuh, J. (ed.) *Geothermal,wind and solar energy*

applications in agriculture and aquaculture. Netherlands: CRC Press Taylor & Francis Group, pp. 1-32.

Cengel, A.Y. (2006). *Heat and mass transfer: A practical approach*, 3rd edn. New York: McGraw-Hill Companies.

Chemat, F. and Boutekedjiret, C. (2015). 'Extraction // Steam Distillation' in Ramos, L. (ed.) Encyclopedia of Separation Science, pp. 1434-1441, *ScienceDirect* [Online] Available at: https://www.researchgate.net/publication/285643201_Extraction_Steam_Distillation (Accessed: 1 November 2017)

Chemat, F., Vian, M.A. and Cravotto, G. (2012) 'Green extraction of natural products: concept and principles', *International Journal of Molecular Sciences,* 13 (7), pp. 8615 -8627, *ResearchGate* [Online]. Available at: https://www.researchgate.net/publication/230784575_Green_Extraction_of_Natural_Products_Concept_and_Principles (Accessed: 7 November 2017)

Energy Technology Systems Analysis Programme (2010) *Industrial Combustion Boilers.* [Online]. Available at: https://iea-etsap.org/E-TechDS/HIGHLIGHTS%20PDF/I01-ind_boilers-GS-AD-gct%201.pdf (Accessed: 6 April 2021)

Essential Distillation Equipment South Africa (2017) *The distillation process. Available at:* https://www.edesa.co.za/essential-oil-distillation-process/ (Assessed: 19 December 2017)

Farjana, S.H., Huda, N., Mahmud, M.P. and Saidur, R. (2018) 'Solar process heat in industrial systems – A global review', *Renewable and Sustainable Energy Reviews*, 82(3), pp. 2270-2286, *ScienceDirect* [Online]. Available at: https://www.sciencedirect.com/science/article/pii/S1364032117312108 (Accessed: 15 February 2017

Favre-Marinet, M. and Tardu, T. (2009) *Convective heat transfer*. Great Britain: ISTE Ltd and John Wiley & Sons, Inc.

Fernandez-Garcıa, A, Gomez-Vidal, J., Oro, E., Kruizenga, A., Sole, A. and Cabeza, L.F. (2019) 'Mainstreaming commercial CSP systems: A technology review', *Renewable Energy*, 140, pp.152-176, *ScienceDirect* [Online]. Available at:

https://www.sciencedirect.com/science/article/pii/S0960148119303544 (Accessed: 15 October 2019)

Fernandez-Garcıa, A., Sutter, F., Fernandez-Reche, J, E. and lupfert, E. (2017). 'Mirrors', in Heller, P. (ed.) *The performance of concentrated solar power (CSP) systems*. UK:Woodhead Publishing, pp. 76-107.

Fernandez-Garcıa, A.F., Zarza, E., Valenzuela, E. and Perez, M. (2010) 'Parabolic-trough solar collectors and their applications', *Renewable and Sustainable Energy Reviews,* 14(7), pp. 1695-1721, *ScienceDirect* [Online]. Available at: https://www.sciencedirect.com/science/article/pii/S1364032110000675 (Accessed: 15 February 2017)

Franco-Vega1, A., Reyes-Jurado1, F.,Cardoso-Ugarte1, G.A., Sosa-Morales, M.E., Palou1, E. and López-Malo1, A**.** (2016) 'Sweet Orange (*Citrus sinensis*) Oils', in Preedy, V.R. (ed) *Essential oils in food preservation, flavor and Safety*. USA: Nikki Levy, pp. 783-9.

Gets, A. (2013). *Powering the Future: Renewable Energy Roll-out in South Africa*. Johannesburg: Greenpeace Africa by AGAMA Energy (Pty) Ltd Cape Town, South Africa

Giacometti, J., Kovačević, D.B., Putnik, P., Gabrić, D., Bilušić, T., Krešić, G., Stulić, V., Barba, F.J., Chemat, F., Barbosa-Cánovas, G. and Jambrak, A.R. (2018) 'Extraction of bioactive compounds and essential oils from Mediterranean herbs by conventional and green innovative techniques: A review', *Food Research International*, 113, pp. 245-262, *ScienceDirect* [Online]. Available at https://www.sciencedirect.com/science/article/pii/S0963996918304824 (Accessed: 7 March 2019)

Goering, H.K. and Van Soest, P.J. (1970). *Forage Fibre Analyses. Agricultural Handbook No 379*. A.R.S., U.S. Department of Agriculture

Gök, A., Kirbaşlar, Ş.İ. and Kirbaşlar, F.G. (2015) 'Comparison of lemon oil composition after using different extraction methods', *Journal of Essential Oil Research,* 27(1), pp.17-22, *Research Gate* [Online]. Available at: https://www.researchgate.net/publication/273404571 (Accessed: 2 October 2017)

Graig, O.O., Brent, A.C. and Dinter, F. (2017) 'Concentrated solar power (csp) innovation analysis in South Africa', *South African Journal of Industrial Engineerng*, 28 (2), pp. 14-27, *ResearchGate*[Online]. Available at: https://www.researchgate.net/publication/319875894_Concentrated_solar_power_CSP_innovation_analysis_in_South_Africa (Accessed: 21 December 2017)

Greenfield, H. and Southgate, D.A.T. (2003) *Food composition data -Production, Management and Use*. 2nd edn. Rome: FAO Publishing Management Service

GreenTrust (2017) *Industrial scale solar heat in South Africa. Opportunities in agri-processing and textiles.* [Online]. Available at: https://www.greencape.co.za/assets/Uploads/Industrial-Scale-Solar-Heat-in-South-Africa-opportunities-in-agri-processing-and-textiles.pdf (Accessed: 18 January 2019)

Häberle, A. (2012) 'Concentrating solar technologies for industrial process heat and cooling', in Lovegrove, K. and Stein, W. (eds.) *Concentrating solar power technology*.UK: Woodhead Publishing Limited, pp. 602-619.

Hamid, A.A., Aiyelaagbe, O.O. and Usman, L.A. (2011) 'Essential oils: its medicinal and pharmacological uses', *International Journal of Current Research*, 3(2), pp. 086-098, *ResearchGate* [Online]. Available at: https://www.researchgate.net/publication/229041773_Essential_oils_Its_medicinal_and_pharmacological_uses (Accessed: 5 January 2021)

Handa, S.S A. (2008) 'An Overview of Extraction Techniques or Medicinal and Aromatic Plants', in Handa, S.S., Khanuja, S.P.S., Longo, G. and Rakesh, D.D. (eds.) *Extraction technologies for medicinal and aromatic plants*. trieste: United Nations Industrial Development Organization and the International Centre for Science and High Technology, pp. 9-54.

Herman, R.A., Ayepa, E., Shittu, S., Fometu, S.S. and Jun Wang, J. (2019) 'Essential oils and their applications -a mini review', *Advances in Nutrition and Food Science*, 4(4), pp. 1-13, *ResearchGate* [Online]. Available at: https://www.researchgate.net/publication/336305801 (Accessed: 14 August 2020)

Hermann, S., Miketa, A. and Fichaux, N. (2014) *Estimating the renewable energy potential in Africa*. [Online]. Available at:

https://www.irena.org/publications/2014/Aug/Estimating-the-Renewable-Energy-Potential-in-Africa-A-GIS-based-approach (Accessed: 28 October 2017)

Hesham, H.A.R., Abdurahman, H.N. and Rosli, M.Y. (2016) 'Techniques for extraction of essential oils from plants: a review', *Australian Journal of Basic and Applied Sciences*, 10(16), pp. 117-127, *ResearchGate* [Online]. Available at: https://www.researchgate.net/publication/326598166_Essential_Oils_Extraction_Techniques_Pharmaceutical_And_Therapeutic_Potential_-_A_Review (Accessed: 21 October 2017)

Indora, S. and Kandpal, T.C. (2019) 'Institutional cooking with solar energy', *Renewable and Sustainable Energy Reviews*, 84, pp. 131-154, *ScienceDirect* [Online]. Available at: https://www.sciencedirect.com/science/article/pii/S1364032117315320 (Accessed: 18 November 2020

International Renewable Energy Agency and The Energy Technology Systems Analysis Programme (2015) *Solar heat for industrial processes*. [Online]. Available at: iea-etsap.org/web/Supply.asp & www.irena.org/Publications, (Accessed: 20 August 2017).

International Renewable Energy Agency and the Energy Technology Systems Analysis Programme (2013) *Concentrating solar power*. [Online]. Available at: iea-etsap.org/web/Supply.asp and www.irena.org/Publications (Accessed: 05 July 2017).

Jain, S.H. and Ravikumar, G. (2010) 'A brief review on essential oil extraction and equipment', *Chemical Technology an Indian Journal CTAIJ*, 5(1), 19-24, *ResearchGate* [Online]. Available at: https://www.tsijournals.com/articles/a-brief-review-on-essential-oil-extraction-and-equipment.pdf (Accessed: 3 September 2017)

Joubert, E.C., Hess, S. and Van Niekerk, J.L. (2016) 'Large-scale solar water heating in South Africa: status, barriers and recommendations', *Renewable Energy*, 97, pp. 809-822, *ScienceDirect* [Online]. Available at: https://www.sciencedirect.com/science/article/pii/S096014811630550X (Accessed: 5 May 2017)

Kalogirou, S.A. (2003) 'The potential of solar industrial process heat applications', *Applied Energy*, 76(4), pp. 337-361, *ScienceDirect* [Online]. Available at:

https://www.sciencedirect.com/science/article/pii/S0306261902001769 (Accessed: 4 April 2019).

Kalogirou, S.A. (2004) 'Solar Thermal Collectors and Applications', *Progress in Energy and Combustion Science,* 30(3), pp. 231-295, *ScienceDirect* [Online]. Available at: https://www.sciencedirect.com/science/article/pii/S0360128504000103(Accessed: 9 September 2019)

Kalogirou, S.A. (2014) *Solar energy engineering, processes and systems.* Available at: https://www.sciencedirect.com/book/9780123972705/solar-energy-engineering (Accessed: 12 April 2017)

Kannan, N. and Vakeesan, D. (2016) 'Solar energy for future world: A review', *Renewable and Sustainable Energy Reviews*, 62, pp. 1092-1105, *ScienceDirect* [Online]. Available at: https://www.sciencedirect.com/science/article/pii/S1364032116301320 (Accessed: 5 December 2017)

Kedare, S.B., Paranjape, A.D. and Porwal, R. (2006) 'ARUN solar concentrator for industrial process heat applications', *Digicollection,* April [Online]. Available at: http://digicollection.org/eebea/documents/s20347en/s20347en.pdf (Accessed: 1 October 2017)

Khaled, S., Abdel-Azim, N.S., Saleh, I.A., Hegazy, M.F., El-Missiry, M.M. and Hammouda, F.M. (2015) 'Green technology: Economically and environmentally innovative methods for extraction of medicinal & aromatic plants (MAP) in Egypt', *Journal of Chemical and Pharmaceutical Research,* 7(5), pp. 1050-1074, *ResearchGate* [Online]. Available at: https://www.researchgate.net/publication/277569641_Green_technology_Economically_and_environmentally_innovative_methods_for_extraction_of_medicinal_aromatic_plants_MAP_in_Egypt (Accessed 18 April 2017)

Kröger, D.G. (2004) '*Air-cooled heat exchangers and cooling towers, thermal-flow performance evaluation and design.* University of Stellenbosch, Department of Mechanical Engineering

Kubeczka, K.H. (2010) ' History and sources of essential oil research', in Baser, K.H.C., and Buchbauer. (eds.). *Handbook of essential oils: science, technology, and applications*. USA: CRC Press Taylor & Francis Group, pp. 3-38.

Kültürela, N. and Tarhan,S. (2016) ‘ A solar distillery of essential oils with compound parabolic collectors (CPCs)’, *Anadolu Journal of Agricultural Sciences,* 31, pp. 72-83, *ResearchGate* [Online]. Available at: https://www.researchgate.net/publication/301561326_A_solar_distillery_of_essential_oils_with_compound_parabolic_collectors_CPCs (Accessed: 19 June 2017)

Kumaresana, G., Vigneswarana, V.S., Esakkimuthub, S. and Velraja, R. (2016) ‘Performance assessment of a solar domestic cooking unit integrated with thermal energy storage system’, *Journal of Energy Storage,* 6, pp.70-79, *ScienceDirect* [Online]. Available at: https://www.sciencedirect.com/science/article/pii/S2352152X16300445 (Accessed: 13 June 2018)

Kusuma, H.S., Altway, A. and Mahfud, M. (2017) ‘Alternative to conventional extraction of vetiver oil: Microwave hydrodistillation of essential oil from vetiver roots (Vetiveria zizanioides)’, *Earth Environmental Science,* 201, *IOP Science* [Online]. Available at https://iopscience.iop.org/article/10.1088/1755-1315/101/1/012015 (Accessed: 7 April 2021)

M’hiri, N., Ioannou, I., Ghoul, M. and Mihoubi Boudhrioua, N. (2017) ‘Phytochemical characteristics of citrus peel and effect of conventional and nonconventional processing on phenolic compounds’, *Food Reviews International,* 33(6), pp. 587-619, *Taylor and Francis Online* [Online]. Available at: https://www.tandfonline.com/doi/full/10.1080/87559129.2016.1196489 (Accessed: 5 January 2021)

Macaskill, C. (2017) 'Essential oils', in *Agrihandbook* [Online]. Available at https://agribook.co.za/adding-value/essential-oils/ (Accessed: 13 November 2017)

Masango, P. (2001) *Towards understanding steam distillation of essential oils by differential quantification of principal components using capillary gas chromatography*. PhD thesis. University of Surrey [Online]. Available at: https://core.ac.uk/download/pdf/322491823.pdf (Accessed: 14 June 2017)

Masango, P. (2005). ‘Cleaner production of essential oils by steam distillation’, *Journal of Cleaner Production,*13(8), pp. 833-839, *ScienceDirect*[Online]. Available at: https://www.sciencedirect.com/science/article/pii/S0959652604000654 (Accessed: 3 September 2017)

Mathur, A., Agrawal, G.D. and Chandel, M. (2013) 'Techno-economic analysis of solar parabolic trough type energy system for garment zone of Jaipur city', *Renewable and Sustainable Energy Reviews,* 17, pp. 104-109, *ScienceDirect* [Online]. Available at: https://www.sciencedirect.com/science/article/pii/S1364032112005163 (Accessed: 12 August 2017)

Meyer, R., Schlecht, M. and Chhatbar, K. (2012) 'Solar resources for concentrating solar power (CSP) systems', in Lovegrove, K. and Stein, W. (eds.) *Concentrating solar power technology*.UK: Woodhead Publishing Limited, pp. 68-90.

Milad T.J.A., Seyfollah, S. and Mohammad, A. (2017) 'Experimental investigation on a solar parabolic trough collector for absorber tube filled with porous media', *Renewable Energy,* 107, pp. 156-163, *ScienceDirect* [Online]. Available at: https://www.sciencedirect.com/science/article/pii/S0960148117300812 (Accessed: 15 Nov 2019]

Mills, D.R. (2012) 'Linear Fresnel reflector (LFR) technology', in Lovegrove, K. and Stein, W. (eds.) *Concentrating solar power technology*.UK: Woodhead Publishing Limited, pp. 153-196.

Mishra, A., Powar, S. and Dhar, A. (2019). 'Solar thermal powered bakery oven advances in solar research', in Agarwal, A.K. and Pandey, A. (eds.) *Advances in solar energy research.* Singapore: Springer Nature pp. 577-592.

Mohammad, K., Saghafifarb, M., Ellingwooda, K. and Powella, K. (2019) 'Hybrid concentrated solar power (csp) desalination systems', *Desalination,* 468, *ScienceDirect* [Online]. Available at: https://www.sciencedirect.com/science/article/pii/S001191641930894X (Accessed: 5 December 2020)

Munir, A. (2010) *Design, development and modeling of a solar distillation system for the processing of medicinal and aromatic plants*. Masters dissertation. University of Kassel, Witzenhausen [Online]. Available at https://kobra.uni-kassel.de/themes/Mirage2/scripts/mozilla-pdf.js/web/viewer.html?file=/bitstream/handle/123456789/2010081033973/DissertationMunir.pdf?sequence=3&isAllowed=y#pagemode=thumbs (Accessed: 12 May 2018).

Munir, A. and Hensel, O. (2010) ‘On-farm processing of medicinal and aromatic plants by solar’, *Biosystems Engineering*, 106(3), pp. 268-277, *ScienceDirect* [Online]. Available at: https://www.sciencedirect.com/science/article/pii/S1537511010000681 (Accessed: 13 May 2018)

Musi, R., Grange, B., Sgouridis, S., Guedez, R., Armstrong, P., Slocum, A. and Calvet, N. (2017) ‘Techno-economic analysis of concentrated solar power plants in terms of levelized cost of electricity’, *AIP Conference Proceedings*, 1850, pp. 160018. DOI: 10.1063/1.4984552 (Accessed: 04 April 2018)

Naeem, A., Abbas, T., Ali, T.M. and Hasnain, A. (2018) ‘Essential oils: brief background and uses, *Annals Short Reports*, 1(1), *Remedypublications* [Online]. Availale at: http://www.remedypublications.com/open-access/essential-oils-brief-background-and-uses-516.pdf (Accessed: 1 April 2021)

Nagarajan, P.K., J.Subramani, J., Suyambazhahan, S. and Ravishankar Sathyamurthy, R. (2014) ‘Nanofluids for solar collector applications: A Review’, *Energy Procedia*, 61, pp. 2416-2434, *Scienceirect* [Online]. Avilable at: https://www.sciencedirect.com/science/article/pii/S187661021403046X (Accessed: 15 November 2017)

Neumann, O., Neumann, A.D., Tian, S., Thibodeaux, C., Shubhankar, S., Müller, J., Silva, E., Alabastri, A., Bishnoi, S.W., Nordlander, P. and Halas N.J. (2010) ‘Combining solar steam processing and solar distillation for fully off-grid production of cellulosic bioethanol’, *ACS Energy letters*, pp. 8-13, *ResearchGate*[Online]. Available at: https://www.researchgate.net/publication/310665526_Combining_Solar_Steam_Processing_and_Solar_Distillation_for_Fully_Off-Grid_Production_of_Cellulosic_Bioethanol (Accessed: 17 February2017)

Nooh (2019) *How to make lemon essential oil*. Available at: https://www.youtube.com/watch?v=NlgZACkf3Q4 (Accessed: 23 May 2020)

Pangarkar, V.G. (2008) ' Microdistillation, thermomicrodistillation and molecular distillation techniques', in Handa, S.S., Khanuja, S.P.S., Longo, G. and Rakesh, D.D. (ed.) *Extraction technologies for medicinal and aromatic plants*. Trieste: United Nations Industrial Development Organization and the International Centre for Science and High Technology, pp. 129-143.

Panwar, N.L., Kaushik, S.C. and Kothari, S. (2012) 'State of the Art of Solar Cooking', *Renewable and Sustainable Energy Reviews*, 16(6), pp. 3776-3785, *ScienceDirect* [Online]. Available at: https://www.sciencedirect.com/science/article/pii/S1364032112002092 (Accessed: 27 August 2017)

Pernpeintner, J. (2017) 'Introduction to receiver types and design, performance parameters, impact on overall system', in Heller, P. (ed.). *The performance of concentrated solar power(CSP) systems*. UK: Woodhead Publishing

Petterson, D.S, Harris, D. J., Rayner, C. J., Blakeney, A. B. and Choct, M. (1999) 'Methods for the analysis of premium livestock grains', *Australian Journal of Agricultural Research*, 50, 775-787, *ResearchGate* [Online]. Available at: https://www.researchgate.net/publication/263004115_Methods_for_analysis_of_premium_livestock_grains (Accessed: 12 July 2018)

Platzer, W. and Hildebrandt, C. (2012). 'Absorber materials for solar thermal receivers in concentrating solar power (CSP) systems', in Lovegrove, K. and Stein, W. (eds.) *Concentrating solar power technology*.UK: Woodhead Publishing Limited, pp. 469-494.

Pouyfaucona, A.B., García-Rodríguez, L. (2018) 'Solar thermal-powered desalination: A viable solution for a potential market', *Desalination*, 435, pp. 60-69, *ScienceDirect* [Online]. Available at: https://www.sciencedirect.com/science/article/pii/S0011916417318374 (Accessed: 05 February 2019)

Pranesh, V., Velraj, R., Christopher, S. and Kumaresan, V. (2019) 'A 50 Year Review of Basic and Applied Research in Compound Parabolic Concentrating Solar Thermal Collector for Domestic and Industrial Applications', *Solar Energy*, 187, pp. 293–340, *ScienceDirect* [Online]. Available at: https://www.sciencedirect.com/science/article/pii/S0038092X19303974 (Accessed: 29 October 2020)

Qiu, L., Ouyang, Y., Feng, Y. and Zhang, X. (2019) 'Review on micro/nano phase change materials for solar thermal applications', *Renewable Energy*, 140, pp. 513-538, *ScienceDirec*t [Online]. Available at:

https://www.sciencedirect.com/science/article/pii/S0960148119303933 (Accessed: 08 September 2019)

Ranjitha, J. and Vijiyalakshmi, S. (2014) 'Facile methods for the extraction of essential oil from the plant species - a review'**,** *International Journal of Pharmaceutical Sciences and Research*, 5(4), pp. 1107-1115, *IJPSR* [Online]. Available at: https://ijpsr.com/bft-article/facile-methods-for-the-extraction-of-essential-oil-from-the-plant-species-a-review/?view=fulltext#:~:text=Essential%20oils%20are%20produced%20using,2%20supercritical%20fluid%20extraction%2C%20etc (Accessed: 19 December 2017)

Reay, D.A., Ramshaw, C. and Harvey, A.P. (2013) *Process intensification, engineering for efficiency, sustainability and flexibility isotopes in organic chemistry.* Available at: https://www.sciencedirect.com/science/article/pii/B9780080983042000146 (Accessed: 12 April 2021)

Riggs, B.C., Biedenharn, R., Dougher, C., Ji, Y.V., Xu, Q., Romanin,V., Codde, D.S., Zahler, J.M. and Escarra, M.D. (2017) 'Techno-economic Analysis of hybrid PV/T Systems for process heat using electricity to subsidize the cost of heat', *Applied Energy,* 208, pp. 1370-1378, *ScienceDirect* [Online]. Available at: https://www.sciencedirect.com/science/article/pii/S0306261917313041 (Accessed: 19

Rios, J.L. (2016) 'Essential oils: what they are and how the terms are used and defined', in Preedy, V.R. (ed.) *Essential oils in food preservation, flavor and Safety*. USA: Nikki Levy, pp. 3-9.

Saidur, R., Abdelaziz, E.A., Demirbas, A., Hossain, M.S. and Mekhilef, S. (2011) A review on biomass as a fuel for boilers. *Renewable and Sustainable Energy Reviews* 15, (5), pp. 2262-2289, ScienceDirect [Online]. Available at: https://www.sciencedirect.com/science/article/pii/S1364032111000578 (Accessed: November 2017)

Sansaniwal, S.K., Sharma, V. and Mathur, J. (2018) 'Energy and exergy analyses of various typical solar energy applications: a comprehensive review', *Renewable and Sustainable Energy Reviews,* 82 (1), pp. 1576-1601, *ScienceDirect* [Online]. Available at: https://www.sciencedirect.com/science/article/pii/S1364032117310638 (Accessed: 16 March 2020)

Sardeshpande, V. and Pillai, I.R. (2012) ‘Effect of micro-level and macro level factors on adoption potential of solar concentrators for medium temperature thermal applications’, *Energy for Sustainable Development*, 16(2), pp. 216-223, *ScienceDirect* [Online]. Available at: https://www.sciencedirect.com/science/article/pii/S0973082612000038 (Accessed: 1 January 2017)

Schmidt, E. (2010) ' Production of essential oils', in Baser, K.H.C. and Buchbauer. (eds.) *Handbook of essential oils: science, technology, and applications*. USA: CRC Press Taylor & Francis Group, pp. 83-790.

Shahsavari, A. and Akbari, M. (2018) ‘Potential of solar energy in developing countries for reducing energy-related emissions’, *Renewable and Sustainable Energy Reviews* 90, pp.275-291, *ScienceDirect* [Online]. Available at: https://www.sciencedirect.com/science/article/pii/S1364032118301527 (Accessed: 18 August 2019)

Shakir, I.B. and Salih, S.J. (2015) ‘Extraction of essential oils from citrus by-products using microwave steam distillation’, *Iraqi Journal of Chemical and Petroleum Engineering*, 16(3), pp. 11- 22, *ResearchGate* [Online]. Available at: https://www.researchgate.net/publication/328316284_Extraction_of_Essential_Oils_from_Citrus_By-Products_Using_Microwave_Steam_Distillation (Accessed: 05 July 2017)

Singh, A.K. (2008) ' Hydrolytic maceration, expression and cold fat extraction', in Handa, S.S., Khanuja, S.P.S., Longo, G. and Rakesh, D.D. (eds.) *Extraction technologies for medicinal and aromatic plants*. United Nations Industrial Development Organization and the International Centre for Science and High Technology, pp. 83-92

Solar Payback (2019) *Solar heat for industry*, Germany: German Solar Association

SolarGIS. (2017) *Solar Resource Maps of South Africa.* Available at: https://solargis.com/maps-and-gis-data/download/south-africa (Accessed: 05 November 2017).

South Africa. Department of Agriculture, Forestry and Fisheries (2012) *A guide to essential oil crops*. Pretoria: Directorate Communication Services

South Africa. Department of Energy (2009) *Renewable energy: solar power* [Online] Available at: http://www.energy.gov.za/files/renewables_frame.html (Accessed: 06 September 2017)

Srivastva, U. Malhotra, R. K. and Kaushik, S. C. (2017) 'Review of Heat Transport Properties of Solar Heat Transfer Fluids', *Journal of Thermal Analysis and Calorimeter*, 130, pp. 605-621, *SpringerLink* [Online]. Available at: https://link.springer.com/article/10.1007/s10973-017-6441-y (Accessed: 18 February 2018)

Steinmann, W.D. (2012) 'Thermal energy storage systems for concentrating solar power (CSP) plants', in Lovegrove, K. and Stein, W. (eds.) *Concentrating solar power technology*. UK: Woodhead Publishing Limited, pp. 362-394.

Stratakos, A.C. and Koidis, A. (2016) 'Methods for Extracting Essential Oils', In Preedy, V.R. (ed.) *Essential oils in food preservation, flavor and Safety*. USA: Nikki Levy, pp. 31-38

Swiss Rotors (2020) *How do you calculate the efficiency of a plate heat exchanger.* Available at: https://swissrotors.com/blog/how-do-you-calculate-the-efficiency-of-a-plate-heat-exchanger/#:~:text=With%20those%20factors%20embedded%20into,efficiency%20rates%20of%20approximately%2090%25 (Accessed: 5 April 2021)

Tandon, S.S. (2008) ' Distillation technology for essential oils', in Handa, S.S., Khanuja, S.P.S., Longo, G. and Rakesh, D.D. (eds.) *Extraction technologies for medicinal and aromatic plants*. Trieste: United Nations Industrial Development Organization and the International Centre for Science and High Technology, pp. 115-127.

Tandon, S.S., and Rane, S. (2008) 'Decoction and hot continuous extraction techniques', in Handa, S.S., Khanuja, S.P.S., Longo, G. and Rakesh, D.D. (eds.) *Extraction technologies for medicinal and aromatic plants*. Trieste: United Nations Industrial Development Organization and the International Centre for Science and High Technology, pp. 93-106.

Thiex, N. and Novotny, L. (2019) 'Determination of Ash in Animal Feed', *Journal of AOA C International*, 95 (5), pp. 1392-1397, *Oxford Academic* [Online]. Available at: https://academic.oup.com/jaoac/article/95/5/1392/5655282 (Accessed: 10 July 2020)

Tiwari, G.N. and Sahota, L. (2017). *Advanced Solar-Distillation Systems, Basic Principles, Thermal Modeling, and Its Application.* Singapore: Springer Nature

Tongnuanchan, P. and Benjakul, S. (2014) 'Essential oils: extraction, bioactivities, and their uses for food preservation', *Journal of Food Science,* 79(7), pp. 1231-1249, *Willey Online Library* [Online]. Available at: https://onlinelibrary.wiley.com/doi/full/10.1111/1750-3841.12492 (Accessed: 2 March 2017)

United Nations Industrial Development Organization and Food and Agriculture Organization of The United Nation (2005) *Herbs, spices and essential oils post-harvest operations in developing countries.* [Online]. Available at: http://www.fao.org/3/ad420e/ad420e.pdf (Accessed: 27 November 2017)

Valderrama, F. and Ruiz, F. (2018) 'An Optimal Control Approach to Steam Distillation of Essential Oils From Aromatic Plants', *Computers and Chemical Engineering*, 117, pp. 25-31, ScienceDirect [Online]. Available at: https://www.sciencedirect.com/science/article/pii/S0098135418301352 (Accessed: 2 December 2018)

Van Soest, P.J. and Wine, R.H. (1967) 'Use of detergents in the analysis of fibrous feeds. IV. Determination of plant cell-wall constituents', *Journal of Association of Official Analytical Chemists,* 50,pp. 50-55, *Oxford Academic Journals* [Online]. Available at: https://catalogo.latu.org.uy/opac_css/doc_num.php?explnum_id=1418 (Accessed: 1 October 2017)

Walwyn, D.R. and Brent, A.C. (2014) 'Renewable energy gathers steam in South Africa', *Renewable and Sustainable Energy Reviews*, 41, pp. 390-401, *ScienceDirect* [Online]. Available at: https://www.sciencedirect.com/science/article/pii/S1364032114007254 (Accessed: 16 August 2017)

Xu, B., Li, P. and Chan, C. (2015) 'Application of phase change materials for thermal energy storage in concentrated solar thermal power plants: A review to recent developments', *Applied Energy*, 160, pp. 286-307, *ScienceDirect* [Online]. Availabe at: https://www.sciencedirect.com/science/article/pii/S0306261915010867 (Accessed: 10 January 2018)

Zarza-Moya, E. (2012) ‘Parabolic-trough concentrating solar power (CSP) systems’, in Lovegrove, K. and Stein, W. (eds.) *Concentrating solar power technology*.UK: Woodhead Publishing Limited, pp. 197-239.

APPENDIX A: Thermal Analysis

APPENDIX A.1: Thermal analysis of the PTC

Thermal Efficiency

Thermal efficiency of the collector can be expressed by the following equation (Zarza-Moya, 2012):

$$\eta_t = \frac{\dot{Q}_s}{\dot{Q}_c} \qquad \text{A. 1}$$

Whereby,

η_t = Thermal efficiency of the collector,

$\dot{Q}_s$ = Solar energy flux incident on the collector aperture plane,

$\dot{Q}_c$ = Net thermal output power delivered by the collector,

The solar energy flux incident on the collector aperture plane, and the Net thermal output power delivered by the collector are expressed by the following equations:

$$\dot{Q}_s = A_a\, G_B \cos\varphi \qquad \text{A. 2}$$

$$\dot{Q}_c = \dot{m} c_p (t_o - t_i) \qquad \text{A. 3}$$

A_a is the aperture area of the collector, G_B is the direct beam solar irradiance, φ is the incidence angle of the collector, $\dot{m}$ is the mass flow rate through the collector which is determined by multiplying the volumetric flow rate by the temperature dependent density, c_p is the specific heat capacity of the HTF which is also temperature dependent, t_o and t_i are the collector outlet and inlet temperatures, respectively. The net thermal output can also be expressed by Eq. [A.4] below (Kalogirou, 2014). This equation and many other that are used in this section are explained in detail in the ASHRAE 93-1986 (RA91), which is a standard that is used in determining the collector performance.

$$\dot{Q}_c = F_R[G_B \eta_o A_a - A_r U_L (t_i - t_a)] \qquad \text{A. 4}$$

F_R is the heat removal factor, η_o is the optical efficiency, A_r is the surface area of the receiver, U_L is the overall heat loss coefficient of the collector, and t_a is the ambient temperature. From Eq. [A.4], the product of the U_L and the difference between the t_i and t_a, represent the thermal

energy loss through the collector to the surroundings. This thermal energy is lost through conduction, convection, and infrared radiations (Kalogirou, 2014).

The thermal efficiency can be determined by dividing Equation [A.4] by $G_B A_a$

$$\eta_t = F_R\left[\eta_o - U_L\left(\frac{t_i - t_a}{G_B C}\right)\right] \quad \text{A.5}$$

C is the concentration ratio, expressed as $C = A_a/A_r$

When operating under steady state conditions, the parameters F_R, U_L and η_o are nearly constant, given the steady state conditions of the solar irradiation and mass flow rate of HTF. A plot of η_t against $(t_i - t_a)/G_B C$ is linear, with a y-intercept of $F_R\eta_o$ and a gradient of $F_R U_L$.The gradient is an indication of how much energy has been removed from the solar collector, whereas the y-intercept denotes the maximum collector efficiency at which, the inlet temperature t_i is equivalent to the ambient temperature (Milad *et al*., 2017).

The heat removal factor is obtained from the following equation:

$$F_R = \frac{\dot{m}c_p}{A_r U_L}\left[1 - exp\left(\frac{U_L F' A_r}{\dot{m}c_p}\right)\right] \quad \text{A.6}$$

$F'$is the collector efficiency factor, which is computed from the following equation:

$$F' = \frac{{}^{1}/_{U_L}}{\frac{1}{U_L} + \frac{D_o}{h_{fi} D_i} + \left(\frac{D_o}{2k}\ln\frac{D_o}{D_i}\right)} \quad \text{A.7}$$

D_o and D_i are receiver outside tube diameter and receiver inside tube diameter, respectively. h_{fi} is the convective heat transfer coefficient inside the receiver tube.

$$F' = \frac{{}^{1}/_{U_L}}{\frac{1}{U_L} + \frac{D_o}{h_{fi} D_i} + \left(\frac{D_o}{2k}\ln\frac{D_o}{D_i}\right)} \quad \text{A.8}$$

The efficiency was calculated by using Eq. [A.1], therefore:

$$\eta_t = \frac{\dot{m}c_p(t_o - t_i)}{A_a\, G_B \cos\varphi} \quad \text{A.9}$$

Measured Parameters for Thermal Modelling of a Parabolic Trough Collector

The calculation of the net thermal output or useful energy requires a measurement of the inlet temperature and outlet temperature, as well as the volumetric flow of the HTF, which is multiplied by the density to determine the mass flow rate. Measured temperatures are used to determine the temperature dependent thermal properties, which are in turn used to calculate the useful energy. The most important thermal properties of HTFs are (Srivastva *et al*., 2017):

- Viscosity, which determines the flow characteristics of the HTF in the system,
- Density, which governs the viscosity as well as pumping requirements of the fluid,
- Heat capacity, which impacts on the volume of HTF required to carry thermal energy for any given output, and
- Thermal conductivity, which is critical in choosing the chemical nature of the HTF, thereby affecting the overall engineering of the solar collector.

For CST applications, the eutectic mixture of synthetic compounds diphenyl-oxide/diphenyl (operating up to 400°C) are generally used. For these HTFs, thermal properties are tabulated and are based on empirically derived formulae such as these 2 formulae below (Milad *et al*., 2017).

$$k = -0.819477 \times 10^{-5}t - 1.92257 \times 10^{-7}t^2 + 2.5034 \times 10^{-11}t^3 - 7.2974 \times 10^{-15}t^4 + 0.137743 \quad \text{A.10}$$

$$c_p = 0.002414t + 5.9591 \times 10^{-6}t^2 - 2.9879 \times 10^{-8}t^3 + 4.4172 \times 10^{-11}t^4 + 1.498 \quad \text{A.11}$$

k is the thermal conductivity, t is the temperature, and c_p is the specific heat capacity.

These thermal properties are inter-dependent and the heat transfer capacity of any HTF for any heat exchanger's system configuration is given by the sum of these thermal properties (Srivastva *et al*., 2017). Thermal properties play an important role in heat transfer calculations. Suppliers of HTFs provide tabulated data of thermal properties (refer to APPENDIX D.1). In some cases, empirically derived prediction models or formulae are provided in the data sheets

as is the case with data sheet for therminol 66 (See APPENDIX D.1). The following prediction models applies for Therminol 66 and were used for the calculation of the useful energy:

$$\rho = -0.614254 \times T(℃) - 0.000321 \times T^2(℃) + 1020.62 \qquad A.12$$

$$c_p = 0.003313 \times T(℃) + 0.0000008970785 \times T^2(℃) + 1.496005 \qquad A.13$$

$$k = -0.000033 \times T(℃)0.00000015 \times T^2(℃) + 0.118294 \qquad A.14$$

$$v = e^{\left(\frac{586.375}{T(℃)+62.5} - 2.2809\right)} \qquad A.15$$

v is the kinematic viscosity. Of the above prediction models, values obtained from Eqs [A.12] and [A.13] were substituted in Eq [A.3] to calculate the useful energy.

APPENDIX A.2: Thermal analysis of a distillation tank

Heat Input into the System

The total rate of heat transfer into the distillation tank is given by the amount of energy required to reach saturated conditions plus the amount of energy required to vaporize oil and water. According to Munir and Hensel (2010), the energy consumed by the distillation tank in KJ is the sum of sensible heat energy and latent heat of vaporization, therefore Eq. [A.16] represent the rate of heat transfer, whereby the first term in the numerator is the sum of sensible heat energy and the second term is the latent heat of vaporization.

$$E_t = \frac{\left[\{M_p m_p c_w + m_d c_s + m_p(1 - M_p)c_f\}\Delta T + M_p m_p h_w\right]}{t} \qquad A.16$$

E_t is the total heat transfer rate into the distillation tank, M_p is the moisture content of the plant material (wet basis), m_p is the mass of the plant material, c_w is the specific heat capacity of water, m_d is the mass of distillation tank, c_s is the specific heat capacity of stainless steel, c_f is the pecific heat capacity of fibre,, ΔT is the change in temperature, h_w is the latent heat of vaporization of water at atmospheric pressure. t is the time time taken to reach saturated conditions. The specific heat of water can be calculated from the following equation (Kröger, 2004):

$$c_p = 8.15599 \times 10^3 - 2.80627 \times 10T + 5.11283 \times 10^{-2}T^2 - 2.17582 \times 10^{-13}T^6 \quad \text{A. 17}$$

Whereby, T is the average temperature of the fluid.

The overall energy balance of the solar powered essential oil steam distillation unit can be expressed as:

$$E_t = E_u + E_l \quad \text{A. 18}$$

E_t is the input energy into the distillation tank, E_u is the useful energy directed to the essential oil extraction process. E_l is the heat losses through the walls of the distillation tank. The efficiency of the distillation tank was calculated as:

$$\eta_{Still} = \frac{E_u}{E_t} \quad \text{A. 19}$$

The overall efficiency of the whole system is given as the product of the thermal efficiency of the distillation tank and the thermal efficiency of the collector, thus the following equation applies:

$$\eta_o = \eta_{\text{distillation } tank} \times \eta_{\text{Collector}} \quad \text{A. 20}$$

<u>Heat Losses on the walls of the Tank</u>

This section explains the thermal modelling of the distillation tank. The distillation tank consists of 3 segments, namely, (1) the cylindrical segment, (2) the top wall, which is also a lead and the bottom segment, located close to where the steam inlet is. Figure A1 shows a schematic diagram of the distillation tank.

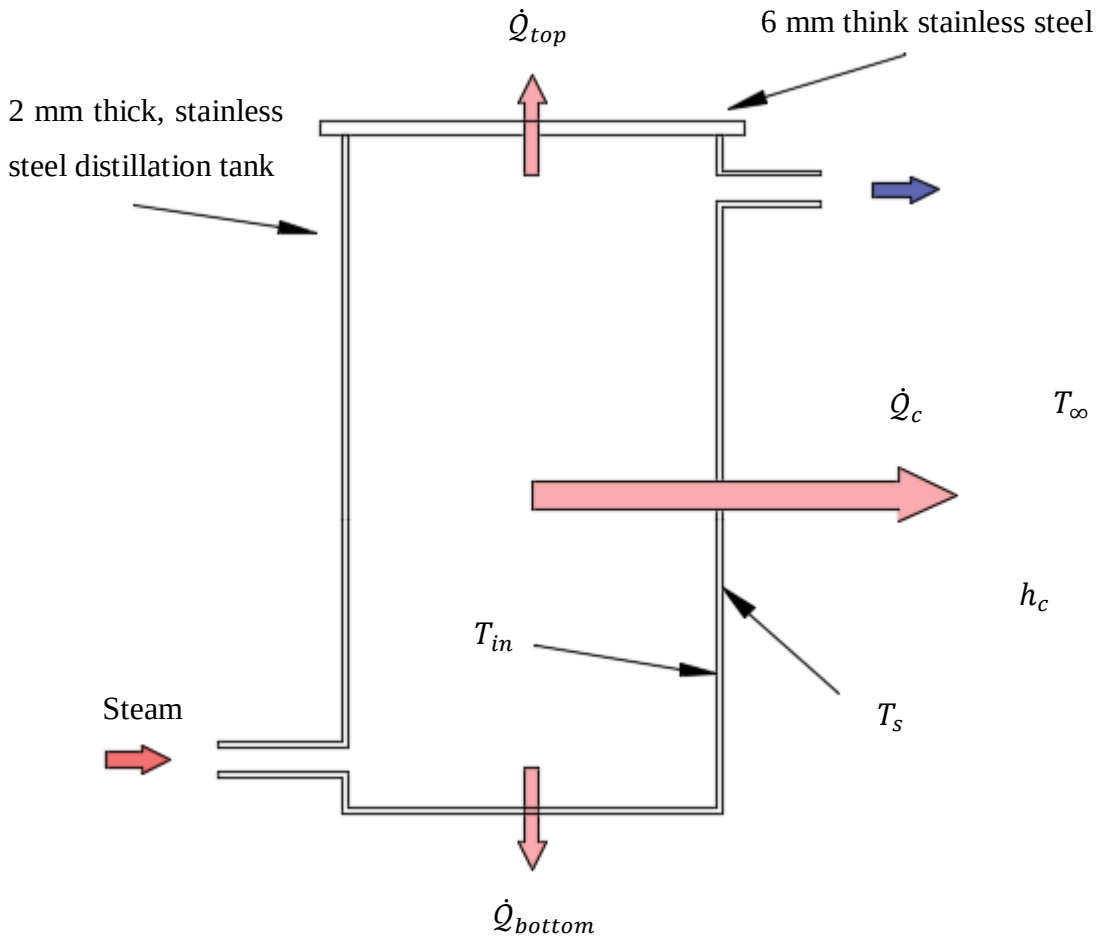


Figure A1. Schematic diagram of a distillation tank showing heat transfer

Cylindrical Losses

Heat losses from the cylindrical walls are expressed as follows:

$$Rate\ of\ heat\ conduction\ through\ the\ wall = Rate\ of convection\ from\ the\ wall$$

$$\dot{Q} = \frac{T_{in} - T_s}{L/KA} = \frac{T_s - T_\infty}{1/h_c} \qquad A.21$$

$$= \frac{T_{in} - T_s}{R_{cond}} = \frac{T_s - T_\infty}{R_{Conv}}$$

Adding numerator and denominator yields (Cengel, 2006):

$$\dot{Q} = \frac{T_s - T_\infty}{R_{Conv} + R_{Conv}} \qquad A.22$$

T_s is the temperature of the cylindrical surface, T_∞ is the temperature of the surroundings, R_{Cond} and R_{Conv} are the conductive and convective thermal resistances, respectively. Thermal resistances are calculated from the following formulae:

$$R_{Cond} = R_{cyl} = \frac{\ln(\frac{r_2}{r_1})}{2\pi kL} \quad \text{A. 23}$$

r_2 is the external radius of the cylinder, r_1 is the internal radius of the cylinder, k is the thermal conductivity of the cylinder material and L is the length of the cylinder. For the convective thermal resistance the following formula is used, whereby h and A are convective heat transfer coefficient and surface area of cylinder, respectively:

$$R_{Conv} = \frac{1}{hA} \quad \text{A. 24}$$

For the calculation of the convective heat transfer coefficient h, an initial estimate of h is necessary. Correlations for external natural convection are used for the estimation of h.

$$h = \frac{Nu\, k}{L} \quad \text{A. 25}$$

Nu is the nusselt number and k is the thermal conductivity of air. The Nu number is determined from the correlations for external natural convection. Eqs [A.26], [A.27] and [A.28] are correlations formulae for vertical walls and are also used for the estimation of Nu number of cylindrical walls when $D \geq 35L/GRa_L{}^{1/4}$, D is the diameter of the cylinder, G is the Grashof number, Ra_L is the Raleigh number(Cengel, 2006). In other texts, it is stated that when $D/L \geq Ra^{1/4}$, Eq.[A.28] can be applied for cylindrical walls (Favre-Marinet and Tardu, 2009). According to Cengel (2006), Eq.[A.26] and [A.27] are a simpler versions of the Nu number calculations and Eq.[A.29] is a more complex approach, yielding accurate results. For this study, in all cases, $D/L \geq Ra^{1/4}$, therefore, Eq.[A.28] was used to calculate Nu.

$$Nu = 0.59Ra_L{}^{1/4} \text{ (Range of } Ra_L\text{: } 10^4 - 10^9) \quad \text{A.26}$$

$$Nu = 0.1Ra_L{}^{1/3} \text{ (Range of } Ra_L\text{: } 10^9 - 10^{13}) \quad \text{A.27}$$

$$Nu = \left\{0.825 + \frac{0.387Ra_L{}^{1/6}}{[1 + (0.492/Pr)^{9/16}]^{8/27}}\right\}^2 \quad \text{A. 28}$$

The Ra_L is the product of the Grashof number and the Prandt number. Grashof number and the Prandt number are determined from the geometric properties of the fluid (see APPENDIX E.1 for geometric properties of air used in the calculations of Grashof number and the Prandt number). The raleigh number is expressed as follows:

$$Ra_L = GPr \qquad \text{A.29}$$

$$Ra_L = \frac{g\beta(T_s - T_\infty)L^3}{v^2} Pr \qquad \text{A.30}$$

g is the gravitational constant, β is the coefficient of volume expansion, given as $1/T$, T_s is the temperature of the surface and it is assumed in the beginning in order calculate h , T_∞ is the temperature of the fluid sufficiently far from the surface, L is the characteristic length of the geometry and v is the kinematic viscosity of the fluid. All fluid properties are evaluated at the film temperature of $T_f = T_s + T_\infty/2$ (Cengel, 2006).

When the average convection coefficient is known, the rate of heat transfer by natural convection from a cylinder at a uniform temperature T_s to the surrounding fluid can be expressed by Newton's law of cooling as (Cengel, 2006):

$$\dot{Q}_{conv} = hA(T_s - T_\infty) \qquad \text{A.31}$$

Newton's law of cooling can be rearranged as:

$$T_s = T_\infty + \frac{\dot{Q}_{conv}}{hA} \qquad \text{A.32}$$

$$T_s = T_\infty + R_{Conv}\dot{Q}_{conv} \qquad \text{A.32}$$

Because T_s is assumed in the beginning to determine the average h, Eq.[A.32] is used to calculate T_s and iterations are made until the assumed T_s and the calculated T_s are equal.

Top and Bottom Wall Losses

For top and bottom wall losses, calculation of heat losses are done in a similar way as the cylindrical wall losses, however, the estimation of th**e** average nusselt number and thus the average convection coefficient are based on different formulae for nusselt number, thus the following Nu number formulae were applied in the heat losses calculations (Cengel, 2006).

Top Wall:

For a horizontal plate heated side downward and Nu is expressed as:

$Nu = 0.27{Ra_L}^{1/4}$ (Range of Ra_L: $10^5 - 10^{10}$)

Bottom Wall:

For a horizontal plate hot side upward laminar regime, Nu is expressed as:

$Nu = 0.54{Ra_L}^{1/4}$ (Range of Ra_L: $10^4 - 10^7$)

For turbulent regime:

$Nu = 0.15{Ra_L}^{1/4}$ (Range of Ra_L: $10^7 - 10^9$)

When all the heat losses from the distillation tank have been calculated, the total heat losses are determined by adding all the heat losses. The efficiency of the distillation tank is calculating by dividing the useful energy by the energy input.

APPENDIX A.3: Thermal energy modelling

For ease of calculation of energy output and losses in the solar powered steam distillation, an excel model was developed to estimate the thermal output of the solar collector, input energy to the distillation tank, as well as the losses on the walls of the distillation tank. The following describes the model.

(a) Solar Output

Parameter	**Value**
T_{av}	=(ti+to)/2
p	=((-0,614254*Tav)-(0,000321*Tav^2)+1020,62)
m	=((V/1000)*p)/3600
C_p	=((0,003313*Tav)+(0,0000008970785*Tav^2)+1,496005)
Qu	=m*C_p*(to-ti)
Solar Input (Solar irradiation information)	
Q_s	=Gb*Aa/1000

(b) Energy input to the distillation tank

cw =((8,15599*10^3)-(2,80627*10*((Tf_outlet+Tf_inlet)/2+273))+(5,11283*10^(-2)*((Tf_outlet+Tf_inlet)/2+273)^2)-(2,17582*10^(-13)*((Tf_outlet+Tf_inlet)/2+273)^6))/1000

Et =((((M_p/100)*ms_p*c_w)+(m_d*c_s)+(ms_p*(1-(M_p/100)*c_f)))*((Tf_outlet+Tf_inlet)/2-(Ti_outlet+Ti_inlet)/2)+((M_p/100)*ms_p*h_w))/(t*60)

(c) Heat losses on the wall of a distillation tank

Cylinder Wall Heat Losses

T_f_1	=(Ts_assumed+T_surr_1)/2
Geometric properties of air (obtained through interpolation)	
ρ	=FORECAST(B5;OFFSET(Data!B5:B23;MATCH(B5;Data!A5:A23;1)-1;0;2); OFFSET(Data!A5:A23;MATCH(B5;Data!A5:A23;1)-1;0;2))
v	=FORECAST(B5;OFFSET(Data!E5:E23;MATCH(B5;Data!A5:A23;1)-1;0;2); OFFSET(Data!A5:A23;MATCH(B5;Data!A5:A23;1)-1;0;2))
k	=FORECAST(B5;OFFSET(Data!F5:F23;MATCH(B5;Data!A5:A23;1)-1;0;2); OFFSET(Data!A5:A23;MATCH(B5;Data!A5:A23;1)-1;0;2))
Pr	=FORECAST(B5;OFFSET(Data!H5:H23;MATCH(B5;Data!A5:A23;1)-1;0;2); OFFSET(Data!A5:A23;MATCH(B5;Data!A5:A23;1)-1;0;2))
Convective Heat Transfer Coefficient	
RaL_1	=(9,81*1/T_f_1*(Ts_assumed-T_surr_1)*(0,505)^3)*Pr_1/(v_1*10^-6)^2
Nu_1	=(0,825+((0,387*RaL_1^(1/6))/(1+(0,492/Pr_1)^(9/16))^(8/27)))^2
h	=(Nu_1*k_1)/0,505
Surface temperature of cylinder wall	
As	=PI()*0,205*0,505
Rcond_1	=1/(2*PI()*k_stainless_steel*L_1)*LN(0,1025/0,1005)
Rconv_1	=1/(h_1*As_1)
T_s(calc/°C)	=(T_surr_1-273)+((Tin_1-(T_surr_1-273))/(Rcond_1+Rconv_1))*Rconv_1
Ts_calc_K_1	= T_s(calc/°C) +273
Heat loss	
Q	=(Ts_calc_K_1-T_surr_1)/Rconv_1/1000

Top Wall Losses

T_f_2	=(Ts_assumed_2+T_surr_2)/2
Geometric properties of air(obtained through interpolation)	
ρ	=FORECAST(B32;OFFSET(Data!B5:B23;MATCH(B32;Data!A5:A23;1)-1;0;2); OFFSET(Data!A5:A23;MATCH(B32;Data!A5:A23;1)-1;0;2))
v	=FORECAST(B32;OFFSET(Data!E5:E23;MATCH(B32;Data!A5:A23;1)-1;0;2); OFFSET(Data!A5:A23;MATCH(B32;Data!A5:A23;1)-1;0;2))

k	=FORECAST(B32;OFFSET(Data!F5:F23;MATCH(B32;Data!A5:A23;1)-1;0;2); OFFSET(Data!A5:A23;MATCH(B32;Data!A5:A23;1)-1;0;2))
Pr	=FORECAST(B32;OFFSET(Data!H5:H23;MATCH(B32;Data!A5:A23;1)-1;0;2); OFFSET(Data!A5:A23;MATCH(B32;Data!A5:A23;1)-1;0;2))
Convective Heat Transfer Coefficient	
RaL_2	=(9,81*1/T_f_2*(Ts_assumed_2-T_surr_2)*(0,2)^3)*Pr_2/(v_2*10^-6)^2
Nu_2	=0,27*RaL_2^(1/4)
h	=(Nu_2*k_2)/0,2
Surface temperature of cylinder wall	
As	=PI()*0,1025^2
Rcond_2	=1/(2*PI()*B44*L_2)*LN(0,1025/0,1005)
Rconv_2	=1/(B41*B45)
T_s(calc/°C)	=(T_surr_2-273)+((Tin_2-(T_surr_2-273))/(Rcond_2+Rconv_2))*Rconv_2
Ts_calc_K_2	= T_s(calc/°C) +273
Heat loss	
Q	=(Ts_calc_K_2-T_surr_2)/Rconv_2/1000

Bottom Wall Losses

T_f_3	=(Ts_assumed_3+T_surr_3)/2
Geometric properties of air(obtained through interpolation)	
ρ	=FORECAST(B59;OFFSET(Data!B5:B23;MATCH(B59;Data!A5:A23;1)-1;0;2); OFFSET(Data!A5:A23;MATCH(B59;Data!A5:A23;1)-1;0;2))
v	=FORECAST(B59;OFFSET(Data!E5:E23;MATCH(B59;Data!A5:A23;1)-1;0;2); OFFSET(Data!A5:A23;MATCH(B59;Data!A5:A23;1)-1;0;2))
k	=FORECAST(B59;OFFSET(Data!F5:F23;MATCH(B59;Data!A5:A23;1)-1;0;2); OFFSET(Data!A5:A23;MATCH(B59;Data!A5:A23;1)-1;0;2))
Pr	=FORECAST(B59;OFFSET(Data!H5:H23;MATCH(B59;Data!A5:A23;1)-1;0;2); OFFSET(Data!A5:A23;MATCH(B59;Data!A5:A23;1)-1;0;2))
Convective Heat Transfer Coefficient	
RaL_3	=(9,81*1/T_f_3*(Ts_assumed_3-T_surr_3)*(0,2)^3)*B64/(v_3*10^-6)^2
Nu	=0,54*RaL_3^(1/4)
h	=(Nu_3*k_3)/0,2
Surface temperature of cylinder wall	
As	=PI()*0,1025^2
Rcond_3	=1/(2*PI()*B71*L_3)*LN(0,1025/0,1005)
Rconv_3	=1/(h_3*As_3)
T_s(calc/°C)	=(T_surr_3-273)+((Tin_3-(T_surr_3-273))/(Rcond_3+Rconv_3))*Rconv_3
Ts_calc_K_3	= T_s(calc/°C) +273
Heat loss	
Q	=(Ts_calc_K_3-T_surr_3)/Rconv_3/1000

The Geometric properties of air used for interpolation are in APPENDIX E.1.

APPENDIX B: Sizing of Parabolic Trough Collector System for Essential Oil Distillation

APPENDIX B.1: Sizing procedure

The sizing of the solar powered steam distillation system was based on the following equation which defines the aperture area of the PTC needed to meet energy requirements to extract essential oil from essential oil bearing plants (Kültürela and Tarhan, 2016):

$$A_n = \frac{Q_n}{(Q_{sol} \times \eta_s)}$$

Whereby:

An = Aperture area (m^2)

Q_n = Total amount of energy required for essential oil extraction ($KJ.kg^{-1}.°C^{-1}$)

Q_s = Instanteneous Direct Normal Irradiation (W/m^2)

η_o= Overall system efficiency

The Total amount of energy required for distillation, the Instanteneous Direct Normal Irradiation and the overall system efficiency are detailed below:

Total amount of energy required for distillation

$$Q_n = Q_w + Q_s + Q_{st} + Q_o$$

Qw is the energy required to bring 5 kg of water from 20°C to a boiling point at 100°C and is given by the following euqtion:

$$Qw = m_w \times c_w \times \Delta T_w$$

Whereby;

$m_w = \text{mass of water(kg)}$

$C_w = \text{Specific heat capacity of water}(KJ.kg^{-1}.°C^{-1})$

$\Delta T_w = \text{Change in temperature from 20 to 100°C}$

M_w = Mass of water (kg)

c_w = Specific heat capacity of water at constant pressure($KJ.kg^{-1}.°C^{-1}$)

ΔT_w = Change in temperature from 20 to 100°C

Q_w is the amount of energy required to evaporate 5 kg of water at 100°C and is given by the following equation:

$$Q_s = m_w \times L_w$$

Whereby;

m_w = Mass of water (kg)

L_w = Latent heat of vaporization (kJ/kg)

Q_s is the amount of heat that is absorbed by the steel components still, fluid circulation pipes, etc. and is given as follows:

$$Q_s = m_{st} \times c_{st} \times \Delta T_{st}$$

Whereby;

$m_{st} = \text{mass of steel}$

$m_{st} = \text{specific heat capacity of steel}$

$\Delta T_{st} = \text{change in temperature from 20 to 100°C}$

M_{st} = Mass of steel (kg)

M_{st} = Specific heat capacity of steel ($KJ.kg^{-1}.°C^{-1}$)

ΔT_{st} = Change in temperature from 20 to 100°C

Q_o is the the amount of energy required to heat HTF oil from 20 to 100°C and is given by the following formula:

$$Q_{HTF} = m_{HTF} \times c_{HTF} \times \Delta T_{HTF}$$

Whereby:

m_{HTF} = Mass of HTF (kg)

c_{st} = Specific heat capacity of HTF ($KJ.kg^{-1}.°C^{-1}$)

ΔT_{HTF} = Change in temperature from 20 to 100°C

APPENDIX C: Preliminary Assessment of the Solar Resource Potential at a Selected Site for PTC Project

APPENDIX C.1: Estimation of DNI and selection of a suitable PTC

The DNI at the installation site is a crucial factor in evaluating a CST project's solar capacity. DNI and other important information were extracted using an irradiation solar database, namely Global Solar Aklas:

Summary of Data for the CST Installation Site

Project: Pretoria

Location: Cresswell Road, Pretoria, Gauteng 0184, South Africa

Geographical coordinates: -25.729533°, 28.276100° (-25°43'46", 28°16'34")

Time zone: UTC+02, Africa/Johannesburg [SAST]

DNI :2138 kWh/m^2 / year

GHI: 2023 kWh/m^2 / year

DHI: 659 kWh/m^2 / year

The selected site receives a DNI of 2138 kWh/m^2 on a yearly bases as determined from Global Solar Atlas maps (see Figure C1)

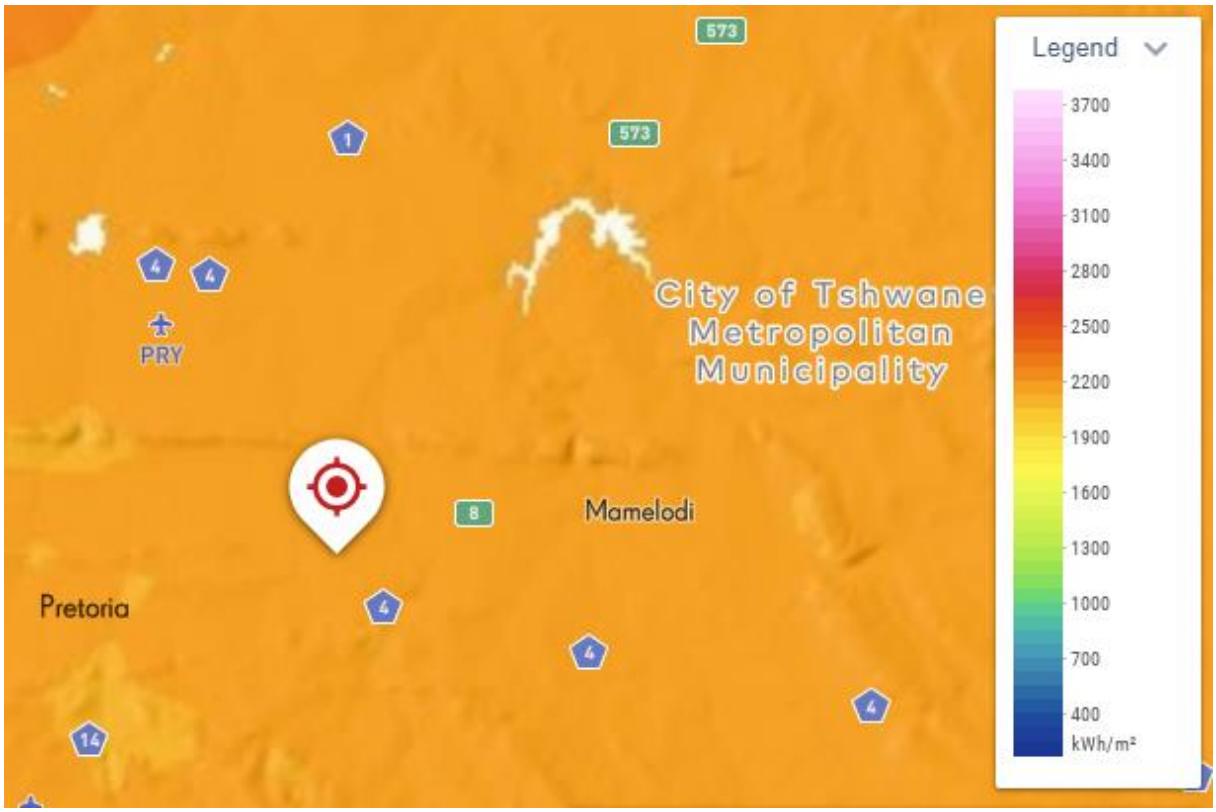


Figure C1 Map of direct normal irradiation for a solar project site monthly averages

For forecasting, monthly average DNI data was generated from Global Solar Atlas. In Figure C2, different colours show the intensities of DNI. It is visible from the figure, that all the months receive adequate irradiations, however, it can be noted that some places, for example January to April, and October to December receive less when compared to the middle section (May to September). This trend can also be demonstrated in Figure C3.

Time	Jan	Feb	Mar	Apr	May	Jun	Jul	Aug	Sep	Oct	Nov	Dec
5 - 6	2									1	11	28
6 - 7	193	105	51	36				3	76	219	284	241
7 - 8	332	320	322	353	351	277	273	328	418	406	399	349
8 - 9	429	422	440	490	600	605	606	575	560	516	490	431
9 - 10	491	498	515	577	701	714	721	687	655	597	560	501
10 - 11	537	542	554	620	749	770	786	753	720	642	595	544
11 - 12	550	561	560	635	756	784	807	789	748	660	607	570
12 - 13	539	550	553	606	737	776	794	790	754	656	594	572
13 - 14	526	534	533	574	708	756	774	767	735	626	570	567
14 - 15	485	483	502	552	660	712	727	723	681	561	513	517
15 - 16	421	417	430	477	588	628	656	648	591	482	437	432
16 - 17	353	351	359	383	318	373	377	498	458	373	353	353
17 - 18	280	277	168	36			3	55	60	133	202	267
18 - 19	22	18										16
Total	5160	5078	4987	5339	6168	6395	6524	6616	6456	5872	5615	5388

Figure C2 Long term average of hourly DNI variation (1994-2015)

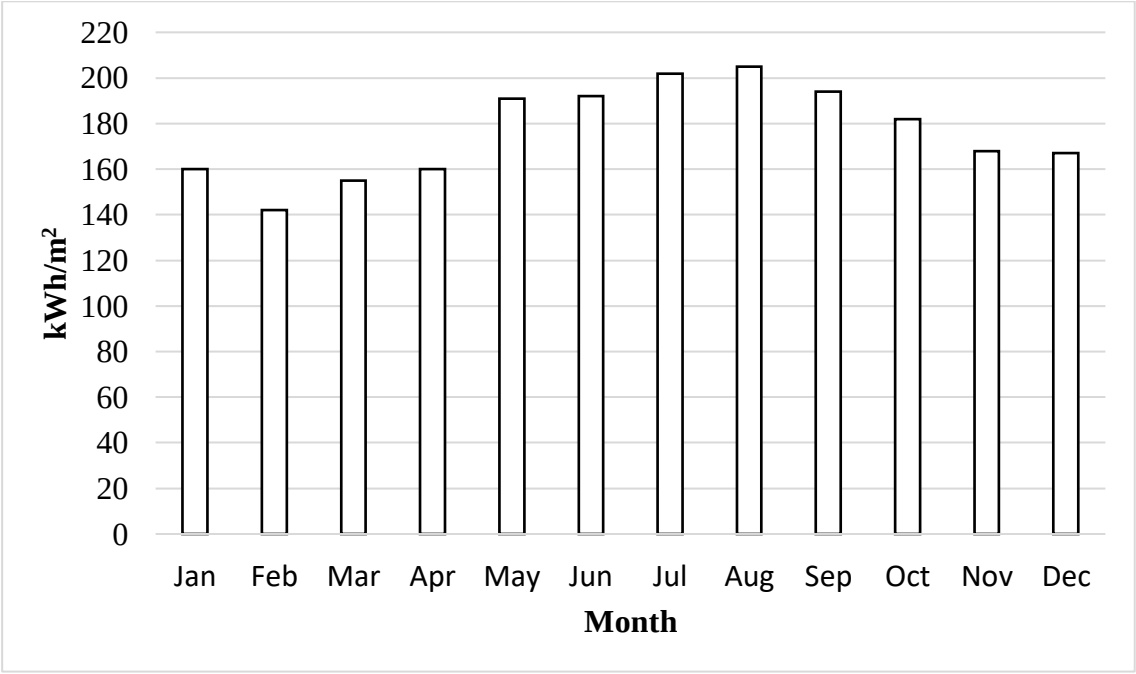


Figure C3 Long term monthly averages of DNI (1994-2015)

Table C1 shows the annual average instantaneous DNI as calculated from long term average DNI of 2138 kWh/m^2

Table C1 Annual average instantaneous DNI (1994-2015)

Month	**Average Sunshine hours Per Day**	**Number of Days per Month**	**Hours in a Month**	**Average Direct Solar Irradiation**
	hours(h)	d/m	h x d/m	kWh/m2/day
Jan	8,4	31	260,4	5,53
Feb	8,4	28	235,2	5,53
Mar	8,2	31	254,2	5,40
Apr	8,2	30	246	5,40
May	9,1	31	282,1	5,99
Jun	9	30	270	5,93
Jul	9,3	31	288,3	6,13
Aug	9,5	31	294,5	6,26
Sep	9,5	30	285	6,26
Oct	8,9	31	275,9	5,86
Nov	8,5	30	255	5,60
Dec	8,8	31	272,8	5,80
Total sunshine hours			3219,4	
Long term average DNI				2138
Annual Average Instantaneous DNI				664,10

The average instantaneous DNI was then estimated to be 659 W/m^2 as seen in the following table:

Overall System Efficiency

The efficiency of the parabolic trough collector system is multiplied by the efficiency of the distillation process to get the total system efficiency. According to Zarza-Moya (2012), the efficiency of industrial process heat systems is generally low, varying between 0.55 and 0.65 at a temperature of 250°C. The low efficiencies of these devices are caused by the poor optical quality of the mirrors used, and the use of non-evacuated tube receivers further decreases their efficiencies. The efficiency for the PTC was set at 65 percent. The distillation unit's efficiency was also selected at 65 percent, taking the total efficiency to 42 percent. The expected thermal energy output was calculated to be 7.5 kW, after all of the main factors of the aperture area equation and thermal energy calculations were understood. The PTC from Dhezhou Gaie Solar Energy had a 15.3 m^2 aperture area and a 9.1 kW rating, which seemed adequate for a 7.5 kW energy requirement.

APPENDIX D: Typical Physical, Chemical and Thermal Properties of Therminol 66

APPENDIX D.1: Data sheet for therminol 66

THERMINOL.66

Therminol 66 is a high performance highly stable synthetic heat transfer fluid offering extended life and very low top-up rates resulting in reduced running costs and minimal downtime for operations at temperatures up to 345°C.

Therminol 66 derives its outstanding performance from the unique stability of the polyphenyl structure.

Intended for use in systems operating at or near atmospheric pressure, Therminol 66 offers potential savings in both capital and operating costs.

Therminol 66 is in use world-wide for many process heating and waste heat recovery applications: resin manufacture, phthalic anhydride distillation, polyester film and fibre production, deodorising fatty acids, phenol production, polyamide polymerisation and extrusion, preheating combustion air in the steel and petrochemical furnaces.

Thermal Stability

The thermal stability of a heat transfer fluid is one of the most important considerations in the selection of a fluid for operation under specific heat transfer conditions. Therminol 66 has made its reputation for its outstanding stability in operation.

Fluid decomposition, both for mineral oil and synthetic hydrocarbon based heat transfer fluids, generally results in the formation of volatile products (low boilers) and polymeric high viscosity fractions (high boilers). The relative proportion of low and high boiler formation and solubility of the high boiling fractions may vary widely, and are critical factors when evaluating fluid performance, predicting top-up costs and the overall risk of deposits or coking.

The chemical composition of Therminol 66 has been carefully selected to minimise the formation of low boilers and eliminate the risk of insoluble high boiler formation and fouling, provided proper attention is given to system design, and operation is within the maximum bulk and film temperatures specified below.

Typical Physical, Chemical and Thermal Properties of Therminol 66

Composition		Hydrogenated terphenyl
Appearance		Clear pale yellow liquid
Max. bulk temperature		345°C
Max. film temperature		375°C
Kinematic viscosity @ 40°C	DIN 51562 - 1	29.64 mm^2/s (cSt)
Density @ 15°C	DIN 51757	1011 kg/m^3
Flash point (Closed cup)	DIN EN 22719	170°C
Fire point	ISO 2592	216°C
Autoignition temperature	DIN 51794	399°C
Pour point	ISO 3016	-32°C
Boiling point @ 1013 mbar		359°C
Coefficient of thermal expansion		0.0009/°C
Moisture content	DIN 51777 - 1	< 150 ppm
Total acidity	DIN 51558 - 1	< 0.02 mg KOH/g
Chlorine content	DIN 51577 - 3	< 10 ppm
Copper corrosion	EN ISO 2160	<< 1a
Average molecular weight		252

Note: Values quoted are typical values obtained in the laboratory from production samples. Other samples might exhibit slightly different data. Specifications are subject to change. Write to Solutia for current sales specifications.

Properties of Therminol®66 vs Temperatures

Temperature °C	Density kg/m³	Thermal Conductivity W/m.K	Heat Capacity kJ/kg.K	Viscosity		Vapour pressure (absolute) kPa*
				Dynamic mPa.s	Kinematic mm²/s**	
0	1021.5	0.118	1.495	1324.87	1297.01	-
10	1014.9	0.118	1.529	344.26	339.20	-
20	1008.4	0.118	1.562	123.47	122.45	-
30	1001.8	0.117	1.596	55.60	55.51	-
40	995.2	0.117	1.630	29.50	29.64	-
50	988.6	0.116	1.665	17.64	17.84	-
60	981.9	0.116	1.699	11.53	11.74	-
70	975.2	0.115	1.733	8.06	8.26	0.01
80	968.5	0.115	1.768	5.93	6.12	0.02
90	961.8	0.114	1.803	4.55	4.73	0.03
100	955.0	0.114	1.837	3.60	3.77	0.05
110	948.2	0.113	1.873	2.92	3.08	0.08
120	941.4	0.112	1.908	2.42	2.58	0.12
130	934.5	0.111	1.943	2.05	2.19	0.18
140	927.6	0.111	1.978	1.75	1.89	0.27
150	920.6	0.110	2.014	1.52	1.65	0.40
160	913.6	0.109	2.050	1.34	1.46	0.58
170	906.6	0.108	2.086	1.18	1.30	0.83
180	899.5	0.107	2.122	1.06	1.17	1.17
190	892.3	0.107	2.158	0.95	1.06	1.62
200	885.1	0.106	2.195	0.86	0.97	2.23
210	877.8	0.105	2.231	0.78	0.89	3.02
220	870.4	0.104	2.268	0.72	0.82	4.06
230	863.0	0.103	2.305	0.66	0.77	5.39
240	855.5	0.102	2.342	0.61	0.71	7.10
250	847.9	0.100	2.379	0.57	0.67	9.25
260	840.3	0.099	2.417	0.53	0.63	11.95
270	832.5	0.098	2.455	0.49	0.59	15.31
280	824.6	0.097	2.492	0.46	0.56	19.46
290	816.6	0.096	2.531	0.44	0.54	24.55
300	808.5	0.095	2.569	0.41	0.51	30.73
310	800.3	0.093	2.608	0.39	0.49	38.22
320	792.0	0.092	2.647	0.37	0.47	47.20
330	783.5	0.091	2.686	0.35	0.45	57.94
340	774.8	0.089	2.726	0.34	0.43	70.68
350	765.9	0.088	2.766	0.32	0.42	85.74
360	756.9	0.086	2.806	0.31	0.41	103.42
370	747.7	0.085	2.847	0.30	0.39	124.09
380	738.2	0.084	2.889	0.28	0.38	148.13

* 1 bar = 100 kPa - ** 1 mm²/s = 1 cSt

Note: Values quoted are typical values obtained in the laboratory from production samples. Other samples might exhibit slightly different data. Specifications are subject to change. Write to Solutia for current sales specifications.

Physical Property Formulae

Density (kg/m³) = $-0.614254 * T(°C) - 0.000321 * T^2(°C) + 1020.62$

Heat capacity (kJ/kg.K) = $0.003313 * T(°C) + 0.0000008970785 * T^2(°C) + 1.496005$

Thermal Conductivity (W/m.K) = $-0.000033 * T(°C) - 0.00000015 * T^2(°C) + 0.118294$

Kinematic Viscosity (mm²/s) = $e^{\left(\frac{586.375}{T(°C)+62.5} - 2.2809\right)}$

Vapour Pressure (kPa) = $e^{\left(\frac{-9094.51}{T(°C)+340} + 17.6371\right)}$

APPENDIX E: Data for Estimation of Grashof Number and the Prandt number

APPENDIX E.1: Geometric properties of air

T (K)	***ρ (kg/m^3)***	**c_p (KJ/Kg.°C)**	***μ (kg/ms)×10^-5)***	***v (m^2/s)×10^-6***	***k (W/m°C)***	**A (m^2/s)×10^-4**	***Pr***
100	3,6010	1,0266	0,692	1,923	0,00925	0,0250	0,770
150	2,3675	1,0099	1,028	4,343	0,01374	0,0575	0,753
200	1,7684	1,0061	1,329	7,490	0,01809	0,1017	0,739
250	1,4128	1,0053	1,488	9,490	0,02227	0,1316	0,722
300	1,1774	1,0057	1,983	16,84	0,02624	0,2216	0,708
350	0,9980	1,0090	2,075	20,76	0,03003	0,2983	0,697
400	0,8826	1,0140	2,286	25,90	0,03365	0,3760	0,689
450	0,7833	1,0207	2,484	31,71	0,03707	0,4222	0,683
500	0,7048	1,0295	2,671	37,90	0,04038	0,5564	0,680
550	0,6423	1,0392	2,848	44,34	0,04360	0,6532	0,680
600	0,5879	1,0551	3,018	51,34	0,04659	0,7512	0,680
650	0,5430	1,0635	3,177	58,51	0,04953	0,8578	0,682
700	0,5030	1,0752	3,332	66,25	0,05230	0,9672	0,684
750	0,4709	1,0856	3,481	73,91	0,05509	1,0774	0,686
800	0,4405	1,0978	3,625	82,29	0,05779	1,1951	0,689
850	0,4149	1,1095	3,765	90,75	0,06028	1,3097	0,692
900	0,3925	1,1212	3,899	99,30	0,06279	1,4271	0,696
950	0,3716	1,1321	4,023	108,2	0,06225	1,5510	0,699
1000	0,3524	1,1417	4,152	117,8	0,06752	1,6779	0,702

Notes: T=temperature, ρ=density, c_p =specific capacity, μ=viscosity, v= μ/ρ=kinetic viscosity, k=thermal conductivity, α= c_p ρ/k=heat(thermal) diffusity, Pr=prandt number

APPENDIX F: Proximate Analysis

APPENDIX F.1: Proximate analysis data

ARC • LNR

ARC-Irene Analytical Services
LNR-Irene Analitiese Dienste

sanas

Private Bag/Privaatsak X2, Irene, 0062 Tel: (012) 672 9294 Fax: (086) 607 7102

Enquiries: Penny Barnes
Tel: 012-672 9292/94

22/09/2020

The Manager
ARC-AE
141 Creswell Road
Silverton
0184

Attention: Dr I Chiyanzu (AE)

Tel: (012) 8424017
E-mail: Chiyanzul@arc.agric.za

TEST REPORT

Date received: 08/09/2020
Date accepted: 08/09/2020
Date completed: 22/09/2020
Test report no: 2020-F-212
Order number:

RESULTS OF BARK

Comment: These are the same samples as 2020-F-213 - the job had to be split as AX R3 cannot generate a journal if there are more than 6 analyses.

Please take note that:

1. Test results relate only to the samples tested.
2. This report may not be reproduced without the written consent of the Quality Manager.
3. The samples received were thoroughly mixed before analysis.
4. Chromatogrammes, if applicable, are available on request.
5. Opinions and interpretations expressed herein are outside the scope of SANAS accreditation.
6. If the condition of the sample could affect the accuracy of analysis, a comment to the effect will be made..

Yours sincerely

P Barnes
Technical Signatory: Chemistry

ARC-IRENE ANALYTICAL SERVICES

Physical Address: ARC-AP, Old Olifantsfontein Road, Irene

Page 1 of 2

TEST REPORT 2020-F-212

This laboratory holds SANAS accreditation for analyses with an ASM number.
Results are expressed on a wet basis, therefore as samples were received.

Analysis	Method Number	Unit	Sample Number 1 : Orange Barks (Fresh Sample)	Sample Number 2 : Lemon Barks (Fresh Sample)	Sample Number 3 : Mandarin Barks (Fresh Sample)	Sample Number 4 : Orange Barks (Distilled Sample)	Sample Number 5 : Lemon Barks (Distilled Sample)	Sample Number 6 : Mandarin Barks (Distilled Sample)
Dry matter	ASM 013	%	86.83	86.92	83.41	86.77	88.12	84.86
Moisture	ASM 013	%	13.17	13.08	16.59	13.23	11.88	15.14
Ash	ASM 048	%	3.41	3.69	2.43	3.48	3.58	2.42
Protein (N x 6.25)	ASM 078	%	10.49	4.88	5.90	5.17	5.64	5.88
Fat (ether extraction)	ASM 044	%	1.42	1.17	1.40	1.39	1.14	1.43
Carbohydrates (calculated)	ASM 075	%	71.51	77.18	73.68	76.73	77.76	75.13

Sample	Sample type	Date analysis commenced
1-6	Bark	14/09/2020

* For the conversion of nitrogen content to protein content the factor 6.25 was used.

ARC-Irene Analytical Services
LNR-Irene Analitiese Dienste

Private Bag/Privaatsak X2, Irene, 0062 Tel: (012) 672 9294 Fax: (086) 607 7102

Enquiries: Penny Barnes
Tel: 012-672 9292/94

23/09/2020

The Manager
ARC-AE
141 Creswell Road
Silverton
0184

Attention: Dr I Chiyanzu (AE)

Tel: (012) 8424017
E-mail: Chiyanzul@arc.agric.za

TEST REPORT

Date received: **08/09/2020**
Date accepted: **08/09/2020**
Date completed: **23/09/2020**
Test report no: **2020-F-213**

RESULTS OF BARK

Comment: These are the same samples as 2020-F-212 - the job had to be split as AX R3 cannot generate a journal if there are more than 6 analyses.
By definition, NDF values must be higher than ADF values as the difference indicates the hemicellulose content. However, when there is no hemicellulose in the product, the ADF values can be slightly higher than NDF values due to the sum of the uncertainties of the two different methods.

Please take note that:

1. Test results relate only to the samples tested.
2. This report may not be reproduced without the written consent of the Quality Manager.
3. The samples received were thoroughly mixed before analysis.
4. Chromatogrammes, if applicable, are available on request.
5. Opinions and interpretations expressed herein are outside the scope of SANAS accreditation.
6. If the condition of the sample could affect the accuracy of analysis, a comment to the effect will be made..

Yours sincerely

PRBarnes

.....

P Barnes
Technical Signatory: Chemistry

ARC-IRENE ANALYTICAL SERVICES

Physical Address: ARC-AP, Old Olifantsfontein Road, Irene

TEST REPORT 2020-F-213

This laboratory holds SANAS accreditation for analyses with an ASM number.
Results are expressed on a wet basis, therefore as samples were received.

Analysis	Method Number	Unit	Sample Number 1 : Orange Barks (Fresh Sample)	Sample Number 2 : Lemon Barks (Fresh Sample)	Sample Number 3 : Mandarin Barks (Fresh Sample)	Sample Number 4 : Orange Barks (Distilled Sample)	Sample Number 5 : Lemon Barks (Distilled Sample)	Sample Number 6 : Mandarin Barks (Distilled Sample)
Total non-structural carbohydrates	ASM 073	%	41.35	33.05	45.07	42.40	30.63	46.93
Fibre (crude)	ASM 059	%	11.57	12.27	8.10	10.62	14.04	8.73
Neutral detergent fibre	ASM 060	%	15.20	18.28	10.37	14.88	18.67	11.92
ADF	Not SANAS accredited	%	16.12	14.94	10.16	15.31	17.93	11.99
ADL	Not SANAS accredited	%	0.71	1.09	0.48	1.54	2.16	2.43

Sample	Sample type	Date analysis commenced
1-6	Bark	09/09/2020

APPENDIX G: Laboratory: Steam Distillation of Orange, Lemon and Mandarin peels

APPENDIX G.1: Laboratory steam distillation of orange samples

Table G1 Orange peels, 250 g samples

Measured parameter	Orange peels , 250 g samples		
	1	2	3
1.1 Butane gas cartridge mass before distillation	315,1392	243,2744	319,7312
1.2 Butane gas cartridge mass after distillation	267,0479	199,3111	279,8223
1.3 Fresh Orange peels sample mass before distillation	250	250	250
1.4 Orange peels mass after distillation	302,8440	273,2100	314,3902
2. Heating time (min)	15	15	13
3.Temperature in the extraction vessel (°C	93,4	91	94,6
4. Quantity of hydrosol (ml)	137	130,5	87,5
5. Quantity of reflux (ml)	14	24,5	10
6. Quantity of essential oil (g)	2,8492	1,4819	1,8861
7. Volume of water in the flask (before steam generation)	880	880	880
8. Volume of water in the flask (After steam generation)	680	650	675

Table G2 Orange peels, 300 g samples

Measured parameter	Orange peels, 300 g samples)		
	1	2	3
1.1 Butane gas cartridge mass before distillation	194,6146	267,1392	317,6452
1.2 Butane gas cartridge mass after distillation	148,7168	223,1704	268,8932
1.3 Fresh Orange peels sample mass before distillation	300	300	300
1.4 Orange peels mass after distillation	496,1871	361,9769	462,7115
2. Heating time (min)	18	15	19
3.Temperature in the extraction vessel (°C	95,5	93,5	87,7
4. Quantity of hydrosol (ml)	151	119	202
5. Quantity of reflux (ml)	14,5	22	34
6. Quantity of essential oil (g)	2,3989	2,5320	2,6039
7. Volume of water in the flask (before steam generation)	880	880	880
8. Volume of water in the flask (After steam generation)	639	673	551

Table G3 Orange peels (350) g samples

Measured parameter	Orange peels (350) g samples)		
	1	2	3
1.1 Butane gas cartridge mass before distillation	317,2343	257,7809	259,1572
1.2 Butane gas cartridge mass after distillation	257,7809	206,5260	194,6146
1.3 Fresh Orange peels sample mass before distillation	350	350	350
1.4 Orange peels mass after distillation	786,7352	571,9128	447,2379
2. Heating time (min)	21	19	24

3.Temperature in the extraction vessel (℃	95,1	94,2	93,2
4. Quantity of hydrosol (ml)	190	165	238
5. Quantity of reflux (ml)	38	25,25	15
6. Quantity of essential oil (g)	2,3965	2,5578	3,8408
7. Volume of water in the flask (before steam generation)	880	880	880
8. Volume of water in the flask (After steam generation)	521	634	475

APPENDIX G.2: Laboratory steam distillation of lemon samples

Table G4 Lemon peels, 250 g samples

Measured parameter	**Lemon peels ,250 g samples)**		
	1	2	3
1.1 Butane gas cartridge mass before distillation	241,3071	186,3522	223,1704
1.2 Butane gas cartridge mass after distillation	186,3071	134,3519	172,3016
1.3 Fresh Orange peels sample mass before distillation	250	250	250
1.4 Orange peels mass after distillation	272,9261	269,1245	267,6962
2. Heating time (min)	19	20	21
3.Temperature in the extraction vessel (℃	95,6	95,6	94,2
4. Quantity of hydrosol (ml)	205	195	177,5
5. Quantity of reflux (ml)	72	72	75
6. Quantity of essential oil (g)	1,4142	1,2452	1,3318
7. Volume of water in the flask (before steam generation)	880	880	880
8. Volume of water in the flask (After steam generation)	560	518	596

Table G5 Lemon peels, 300 g samples

Measured parameter	**Lemon peels , 300 g samples**		
	1	2	3
1.1 Butane gas cartridge mass before distillation	254,3981	194,4146	315,1220
1.2 Butane gas cartridge mass after distillation	194,4146	140,8621	250,2232
1.3 Fresh Orange peels sample mass before distillation	300	300	300
1.4 Orange peels mass after distillation	326,6820	341,4411	327,6624
2. Heating time (min)	22	23	22
3.Temperature in the extraction vessel (℃	95,7	95,7	95,7
4. Quantity of hydrosol (ml)	255	222	302
5. Quantity of reflux (ml)	70	57	61
6. Quantity of essential oil (g)	1,4531	2,3596	1,4461
7. Volume of water in the flask (before steam generation)	880	880	880
8. Volume of water in the flask (After steam generation)	500	539	440

Table G6 Lemon peels, 350 g samples

Measured parameter	Lemon peels ,350 g samples)		
	1	2	3
1.1 Butane gas cartridge mass before distillation	250,2232	193,0395	314,2626
1.2 Butane gas cartridge mass after distillation	193,0395	145,4647	259,1572
1.3 Fresh Orange peels sample mass before distillation	350	350	350
1.4 Orange peels mass after distillation	396,0113	497,4833	376,3327
2. Heating time (min)	23	22	22
3.Temperature in the extraction vessel (°C	50	43,4	64,5
4. Quantity of hydrosol (ml)	180	131	175
5. Quantity of reflux (ml)	63	70	68
6. Quantity of essential oil (g)	2,1195	2,4529	2,2744
7. Volume of water in the flask (before steam generation)	880	880	880
8. Volume of water in the flask (After steam generation)	569	630	565

APPENDIX G.3: Laboratory steam distillation of orange samples

Table G7 Mandarin peels, 250 g samples

Measured parameter	Mandarin peels ,250 g samples		
	1	2	3
1.1 Butane gas cartridge mass before distillation	316,6625	255,9951	203,5003
1.2 Butane gas cartridge mass after distillation	256,0021	203,5003	146,9743
1.3 Fresh Orange peels sample mass before distillation	250	250	250
1.4 Orange peels mass after distillation	282,4446	268,5500	257,2200
2. Heating time (min)	24	19	21
3.Temperature in the extraction vessel (°C	93,7	90,7	90,8
4. Quantity of hydrosol (ml)	255,5	190	225
5. Quantity of reflux (ml)	36	70	75
6. Quantity of essential oil (g)	0,6114	0,4824	0,9130
7. Volume of water in the flask (before steam generation)	880	880	880
8. Volume of water in the flask (After steam generation)	500	573	555

Table G.8 Mandarin peels, 300 g samples

Measured parameter	Mandarin peels ,300 g samples		
	1	2	3
1.1 Butane gas cartridge mass before distillation	250,8612	206,7276	319,6142
1.2 Butane gas cartridge mass after distillation	194,9357	147,3264	253,5915
1.3 Fresh Orange peels sample mass before distillation	300	300	300
1.4 Orange peels mass after distillation	337,5392	326,6600	328,0000
2. Heating time (min)	21	22	20
3.Temperature in the extraction vessel (°C	94,8	93,0	94,2
4. Quantity of hydrosol (ml)	205,0	235	275
5. Quantity of reflux (ml)	70	90	70

6. Quantity of essential oil (g)	0,9296	0,7568	0,5282
7. Volume of water in the flask (before steam generation)	880	880	880
8. Volume of water in the flask (After steam generation)	550	475	490

Table G9 Mandarin peels, 350 g samples

Measured parameter	**Mandarin peels ,350 g samples**		
	1	2	3
1.1 Butane gas cartridge mass before distillation	253,5915	199,1000	315,8861
1.2 Butane gas cartridge mass after distillation	199,1000	134,9303	250,8612
1.3 Fresh Orange peels sample mass before distillation	350	350	350
1.4 Orange peels mass after distillation	379,3408	375,3700	393,4076
2. Heating time (min)	23	23	23
3.Temperature in the extraction vessel (°C	95,0	95,0	94,8
4. Quantity of hydrosol (ml)	210	325	305
5. Quantity of reflux (ml)	70	57,5	79
6. Quantity of essential oil (g)	1,4068	1,0269	1,1272
7. Volume of water in the flask (before steam generation)	880	880	880
8. Volume of water in the flask (After steam generation)	535	390	417

APPENDIX H: Moisture Content Data of Citrus Peels

APPENDIX H.1: Citrus peels's moisture content (laboratory experiments)

Table H1 Moisture content data of orange peels

Weight of pan	Weight of pan + Orange Peels	Weight after 24 hour oven drying at 105 ℃
4,8409	40,0299	14,4747
4,8098	40,0123	14,5078
4,8530	40,0657	14,5534

Table H2 Moisture content data of lemon peels

Weight of pan	Weight of pan + Lemon Peels	Weight after 24 hour oven drying at 105 ℃
4,8695	40,0436	10,7588
4,7726	40,0181	10,6940
4,8247	40,0069	10,7690

Table H3 Moisture content data of mandarin peels

Weight of pan	Weight of pan + Mandarin Peels	Weight after 24 hour oven drying at 105 ℃
4,8682	40,0770	12,3681
4,8206	40,0038	12,1336
4,8723	40,0542	12,5773

APPENDIX H.2: Citrus peels's moisture content (Gas-powered)

Table H4 Moisture content data of orange peels

Weight of pan	Weight of pan + Orange Peels	Weight after 24 hour oven drying at 105 ℃
4,8435	40,0064	11,6767
4,8430	40,0626	11,7953
4,8570	40,0283	11,8809

Table H5 Moisture content data of Lemon Peels

Weight of pan	Weight of pan + Lemon Peels	Weight after 24 hour oven drying at 105 ℃
4,8506	40,0136	11,5253
4,8139	40,0003	11,4566
4,8628	40,0098	11,4560

Table H6 Moisture content data of Mandarin Peels

Weight of pan	Weight of pan + Mandarin Peels	Weight after 24 hour oven drying at 105 ℃
4,8355	40,0085	15,1216
4,8371	40,0181	15,1213
4,8467	40,0330	15,1737

APPENDIX H.3: Citrus peel's moisture content (PTC-powered)

Table H7 Moisture content data of orange peels

Weight of pan	Weight of pan + Orange Peels	Weight after 24 hour oven drying at 105 ℃
4,8501	40,0011	12,6999
4,8480	40,0031	12,7152
4,8560	40,0340	12,7531

Table H8 Moisture content data of Lemon Peels

Weight of pan	Weight of pan + Lemon Peels	Weight after 24 hour oven drying at 105 ℃
4,8505	40,040	10,4961
4,8549	40,0134	10,4850
4,8601	40,0102	10,5705

Table H9 Moisture content data of Mandarin Peels

Weight of pan	Weight of pan + Mandarin Peels	Weight after 24 hour oven drying at 105 °C
4,8440	40,0030	13,2354
4,8580	40,0210	13,2561
4,8461	40,0392	13,2461

APPENDIX I: Gas-Powered Field Experiment

APPENDIX I.1: Gas-powered steam distillation

Table I1 Orange peels experiment

Measured parameter	Orange peels		
	1	2	3
1. LPG + cylinder mass before distillation(kg)	32,9	32,3	30,94
2. LPG +cylinder mass after distillation (kg)	32,62	31,92	30,56
3. Fresh Citrus peels mass (kg	1,3	1,3	1,3
4. Distilled citrus peels mass (kg)	1,8	1,48	1,98
5. Heating time (min)	35	36	39
6. Distillation tank steam inlet temperature (°C	97,9	98	96,5
7. Distillation tank Steam outlet temperature (°C	96	96	95,5
8. Quantity of hydrosol (ml)	2075	2732	3000
9. Quantity of essential oil (g)	8,0675	10,1614	7,0655
10. Quantity of essential oil (ml)	9,9	12	8,9

Table I2 Lemon peels experiment

Measured parameter	Lemon peels		
	1	2	3
1. LPG + cylinder mass before distillation(kg)	31,3	31,72	31,5
2. LPG +cylinder mass after distillation (kg)	30,94	31,5	31,3
3. Fresh Citrus peels mass (kg	1,3	1,3	1,3
4. Distilled citrus peels mass (kg)	1,72	1,94	1,44
5. Heating time (min)	37	36	39
6. Distillation tank steam inlet temperature (°C	98	97	98
7. Distillation tank Steam outlet temperature (°C	96	96	96
8. Quantity of hydrosol (ml)	2600	893,75	1010
9. Quantity of essential oil (g)	4,2690	7,0025	5,6998
10. Quantity of essential oil (ml)	5,25	8,5	6,75

Table I3 Mandarin peels experiment

Measured parameter	Mandarin peels		
	1	2	3
1. LPG + cylinder mass before distillation(kg)	30,56	30,18	29,82
2. LPG +cylinder mass after distillation (kg)	30,18	29,82	29,57
3. Fresh Citrus peels mass (kg	1,3	1,3	1,3
4. Distilled citrus peels mass (kg)	1,54	1,62	1,62
5. Heating time (min)	31	35	30
6. Distillation tank steam inlet temperature (°C	98	97,5	97
7. Distillation tank Steam outlet temperature (°C	96	95,8	95,6
8. Quantity of hydrosol (ml)	2400	2175	1925
9. Quantity of essential oil (g)	15,3426	14,9980	15,0972
10. Quantity of essential oil (ml)	17,5	17	17,75

APPENDIX I.2: Energy consumption (Gas-powered experiments)

Table I4 Citrus peels experiment

Parameter	Gas cylinder weight before distillation (kg)	Gas cylinder weight after (kg)	LPG consumption (g)	Total energy Consumption(KWh)
1,3 kg Orange peel	32,9	32,62	280	3,562
	32,3	31,92	380	4,834
	30,94	30,56	380	4,834
1,3 kg Lemon peel	31,3	30,94	360	4,580
	31,72	31,5	220	2,799
	31,5	31,3	200	2,544
1,3 kg Mandarin peel	30,56	30,18	380	4,834
	30,18	29,82	360	4,580
	29,82	29,57	250	3,181

APPENDIX I.3: Heat losses (Gas-powered experiments)

Table I5 Cylindrical, top and bottom heat losses during the orange experiment

Tin	Heat losses for orange peels (kW)			
	Cylindrical wall heat losses	Top Wall Losses	Bottom Wall Losses	Total heat loss
96,95	0,123958	0,00649	0,01297	0,14342
97	0,125113	0,00655	0,01309	0,14475
96	0,122805	0,00643	0,01286	0,14209

Table I6 **Cylindrical, top and bottom heat losses during the lemon experiment**

Tin	Heat losses for lemon peels (kW)			
	Cylindrical wall heat losses	Top Wall Losses	Bottom Wall Losses	Total heat loss
97	0,12511	0,00655	0,01309	0,14475

96,5	0,12396	0,00649	0,01297	0,14342
97	0,12511	0,00655	0,01309	0,14475

Table I7 Cylindrical, top and bottom heat losses during the lemon experiment

Tin	Heat losses for mandarin peels (kW)			
	Cylindrical wall heat losses	Top Wall Losses	Bottom Wall Losses	Total heat loss
97	0,12511	0,00655	0,01309	0,14475
96,5	0,12396	0,00649	0,01297	0,14342
96,3	0,1235	0,00646	0,01293	0,14289

APPENDIX J: PTC-Powered Field Experiment

APPENDIX J.1: PTC-powered Steam distillation

Table J1 Orange peels experiment

Measured parameter	Orange peels		
	1	2	3
1. Fresh Citrus peels mass (kg)	1,3	1,3	1,3
2. Distilled citrus peels mass (kg)	1,56	1,9	1,75
3. Heating time (min)	35	37	37
4. Distillation tank steam inlet temperature (℃	98	97	98
5. Distillation tank Steam outlet temperature (℃	95	95	97
6. Quantity of hydrosol (ml)	2642	2990	2115
7. Quantity of essential oil (g)	9,7515	8,3251	7,9995
8. Quantity of essential oil (ml)	11,8	10	9,7

Table J2 Lemon peels experiment

Measured parameter	Lemon peels		
	1	2	3
1. Fresh Citrus peels mass (kg	1,3	1,3	1,3
2. Distilled citrus peels mass (kg)	1,490	1,84	1,86
3. Heating time (min)	37	38	37
4. Distillation tank steam inlet temperature (℃	97	98	98
5. Distillation tank Steam outlet temperature (℃	96	96	97
6. Quantity of hydrosol (ml)	970	2500	963,75
7. Quantity of essential oil (g)	6,5522	6,9991	7,0055
8. Quantity of essential oil (ml)	8,7	7,9	8,1

Table J3 Mandarin peels experiment

Measured parameter	Mandarin peels		
	1	2	3
1. Fresh Citrus peels mass (kg	1,3	1,3	1,3
2. Distilled citrus peels mass (kg)	1,69	1,58	1,60
3. Heating time (min)	35	36	35
4. Distillation tank steam inlet temperature (℃	98	97	98
5. Distillation tank Steam outlet temperature (℃	96	95	97
6. Quantity of hydrosol (ml)	2095	2015	2300
7. Quantity of essential oil (g)	14,1991	14,4111	13,9111
8. Quantity of essential oil (ml)	15,3	15,7	15,9

APPENDIX J.2: Energy consumption (PTC-powered experiment)

Table J4 Energy consumption in orange experiments

Parameter	Orange experiments		
	1	2	3
Ti(inlet)(℃)	26,8	26,9	26,9
Tf(inlet)(℃)	98	97	98
Tf(outlet)(℃)	95	95	97
Mp(%)	77,61	77,61	77,61
mp(kg)	1,3	1,3	1,3
cw(J/(kg.℃)	4213,637	4213,27	4214,357
md(kg)	10	10	10
cs(J/(kg.℃)	885	885	885
cf(J/(kg.℃)	3347	3347	3347
hw(J.kg)	2260000	2260000	2260000
Et(J)	2958061	2952200	2966866
t(m)	21	20	21
t(s)	1260	1200	1260
Et(kW)	2,35	2,46	2,35
Quantity of essential oil (g)	9,7515	8,3251	7,9995

Table J5 Energy consumption in lemon experiments

Parameter	Lemon experiments		
	1	2	3
Ti(inlet)(℃)	28	28	28
Tf(inlet)(℃)	97	98	98
Tf(outlet)(℃)	96	96	97
Mp(%)	83,89	83,89	83,89
mp(kg)	1,3	1,3	1,3
cw(J/(kg.℃)	4213,637	4213,999	4214,357
md(kg)	10	10	10
cs(J/(kg.℃)	885	885	885
cf(J/(kg.℃)	3347	3347	3347
hw(J.kg)	2260000	2260000	2260000
Et(J)	3135744	3140669	3145595
t(m)	22	22	21
t(s)	1320	1320	1260
Et(kW)	2,38	2,38	2,50
Quantity of essential oil (g)	6,5522	6,9991	7,0055

Table J6 Energy consumption in mandarin experiments

Parameter	Mandarin experiments		
	1	2	3
Ti(inlet)(℃)	27,8	28	28
Tf(inlet)(℃)	98	97	98
Tf(outlet)(℃)	96	95	97
Mp(%)	76,12	76,12	76,12
mp(kg)	1,3	1,3	1,3
cw(J/(kg.℃)	4213,999	4213,27	4214,357
md(kg)	10	10	10
cs(J/(kg.℃)	885	885	885
cf(J/(kg.℃)	3347	3347	3347
hw(J.kg)	2260000	2260000	2260000
Et(J)	2908286	2896585	2911223
t(m)	20	19	19
t(s)	1200	1140	1140
Et(kW)	2,42	2,54	2,55
Quantity of essential oil (g)	14,1991	14,4111	13,9111

Table J7 Thermal energy output from PTC

	Thermal energy output during orange experiments					
Parameter	1	2	3	4	5	6
ti(℃)	45,6	47,3	44,6	47	48,9	46,9
to(℃)	281	279	289,7	290	289,5	285
Tav(℃)	163,3	163,15	167,15	168,5	169,2	165,95
V(ℓ/h)	100	100	100	100	100	100
p(kg/m3)	911,7523	911,8601	908,979	908,0043	907,4984	909,8444
m(kg/s)	0,025326	0,025329	0,025249	0,025222	0,025208	0,025273
Cp(KJ/kg℃)	2,06094	2,060399	2,074837	2,079716	2,082247	2,070502
Q(kW)	12,28701	12,09214	12,8404	12,74664	12,62906	12,45948

Table J8 Thermal energy output from PTC

	Thermal energy output during lemon experiments					
Parameter	1	2	3	4	5	6
ti(℃)	50,4	53,3	45,2	47,5	49,5	48,3

to(℃)	292,5	296	292,5	294	295,8	299
Tav(℃)	171,45	174,65	168,85	170,75	172,65	173,65
V(ℓ/h)	100	100	100	100	100	100
p(kg/m3)	905,8703	903,5492	907,7514	906,3772	905,0007	904,2753
m(kg/s)	0,025163	0,025099	0,025215	0,025177	0,025139	0,025119
Cp(KJ/kg℃)	2,090389	2,101984	2,080981	2,087855	2,094735	2,098358
Q(kW)	12,7346	12,80408	12,97647	12,95757	12,97	13,21393

Table **J9 Thermal energy output from PTC**

	Thermal energy output during mandarin experiments					
Parameter	1	2	3	4	5	6
ti(℃)	47,1	43,9	48,3	48,3	49,6	48,9
to(℃)	289	280	289,8	290	295	295
Tav(℃)	168,05	161,95	169,05	169,15	172,3	171,95
V(ℓ/h)	100	100	100	100	100	100
p(kg/m3)	908,3293	912,7224	907,6069	907,5346	905,2544	905,5081
m(kg/s)	0,025231	0,025353	0,025211	0,025209	0,025146	0,025153
Cp(KJ/kg℃)	2,078089	2,056074	2,081704	2,082066	2,093467	2,092199
Q(kW)	12,68355	12,30753	12,67452	12,68621	12,9184	12,95103

APPENDIX J.3: Heat losses (PTC-powered experiment)

Table J11 Cylindrical, top and bottom heat losses during the orange experiment

Tin	Heat losses for orange peels (kW)			
	Cylindrical wall heat losses	Top Wall Losses	Bottom Wall Losses	Total heat loss
96,5	0,123958	0,00649	0,01297	0,14342
96	0,122805	0,00643	0,01286	0,14209
97,5	0,12627	0,00661	0,01321	0,14609

Table J12 Cylindrical, top and bottom heat losses during the lemon experiment

Tin	Heat losses for lemon peels (kW)			
	Cylindrical wall heat losses	Top Wall Losses	Bottom Wall Losses	Total heat loss

96,5	0,12396	0,00649	0,01297	0,14342
97	0,12511	0,00655	0,01309	0,14475
97,5	0,12627	0,00661	0,01321	0,14609

Table J 13 Cylindrical, top and bottom heat losses during the mandarin experiment

Tin	Heat losses for mandarin peels (kW)			
	Cylindrical wall heat losses	Top Wall Losses	Bottom Wall Losses	Total heat loss
97	0,12511	0,00655	0,01309	0,14475
96	0,12281	0,00643	0,01286	0,14209
97,5	0,12627	0,00661	0,01321	0,14609